A Thermosensitive and Photocrosslinkable Composite Polymer study for 3-D Soft Tissue Scaffold Printing

A Thesis

Submitted to the Faculty

of

Drexel University

by

Christopher Gerald Geisler

in partial fulfillment of the

requirements for the degree

of

Doctor of Philosophy

July 2011

Dedications

To my parents,

Gerald and Linda Geisler,

And to my sister and brother,

Susan and Daniel Geisler

Acknowledgments

I am very grateful for the support, advice, and assistance that I have received from so many people. I could not have performed this challenging research without their help. I would like to especially thank my advisor and mentor Dr. Jack G. Zhou for his patience, support and excellent guidance throughout my undergraduate career, doctoral studies, and research work. Under his guidance, I gained an invaluable amount of knowledge and experience on how to do research. I would also like to express my thanks to Drs. David Wootton and Peter Lelkes for all the time, effort and patience they gave to me on this research. I am grateful for their ideas and valuable suggestions over the years. I appreciate the National Science Foundation for their support (CMMI–0700139: Electrowetting Micro Array Printing System for Bioactive Tissue Construct Manufacturing) as well as the Mechanical Engineering and Mechanics Department for their teaching assistance support.

I would like to thank the thesis committee members, Drs. Antonios Kontsos, Young Cho and John Lacontora for their time and helpful suggestions on this project inspiring me to always discover more. I am also very appreciative of Dr. Anthony Lowman, Dr. Ying Sun, Dr. Yasha Kresh and Dr. Giuseppe Palmese for allowing me to use their laboratory and equipment.

I would like to make a special thanks to Dr. Ho-lung Li for allowing me to use his 3-D printer and helping me to print my material. I'd like to thank my lab partners: Dr. Qingwei Zhang, Dr. Lin Lu, Jepthe Augustin, Haibo Gong, Sean Devlin, Xiang Ren, and

Steven Leist as well as my colleagues in Dr. Lowmans' lab: Jason Coleman, Erik Brewer, Valerie Binetti, Michael Marks, and a special thank you to Dr. Kara Spiller for her help and discussions on my research during my studies.

Many thanks to the faculty and staff in the Department of Mechanical Engineering and Mechanics, including Kathie Donahue and Mark Shiber, for their constant support during my studies here at Drexel.

Thank you all for your wonderful support and generous help. You all have been a great contribution to the success of this project.

Table of Contents

List of Tables ..... **viii**

List of Figures ..... **ix**

Abstract ..... **xii**

Chapter 1 : Introduction **1**

Chapter 2 : Background **3**
2.1 Tissue Engineering 3
2.2 Hydrogels 5
2.3 3-D Printing Methods 5
2.3.1 Non-automated Methods 6
2.3.2 Solid Freeform Fabrication 7
2.3.3 Types of 3-D Printers 8
2.4 Photocrosslinkable Materials 9
2.5 Thermosensitive Materials 12
2.6 Rheology 13

Chapter 3 : Research Goals **24**

Chapter 4 : Develop a biomaterial that is compatible with solid freeform fabrication printers **25**
4.1 Introduction 25
4.1.1 Covalently Crosslinked Hydrogels 26
4.1.2 Physically Crosslinked Hydrogels 27
4.1.3 Ionically Crosslinked Hydrogels 28
4.1.4 Chitosan 29
4.1.5 Photocrosslinkable Material 30
4.1.6 Thermosensitive Material 32
4.1.6.1 PNIPAAm 32
4.1.6.2 PEG-PLGA-PEG 33
4.1.7 Degradation 34
4.2 Materials and Methods 35
4.2.1 Materials 35
4.2.1.1 Ionic / Covalent Crosslinking 35
4.2.1.2 Photocrosslinkable 35
4.2.1.3 Thermosensitive 35
4.2.2 Chitosan and Tripolyphosaphate 36
4.2.3 Photocrosslinkable Hydrogels 37
4.2.4 Thermosensitive Hydrogels 38
4.2.5 Rheology 38
4.3 Results and Discussion 40
4.3.1 Chitosan and Tripolyphosphate 40

4.3.2 Photocrosslinkable Hydrogels 41
4.3.3 Thermosensitive Hydrogels 41
4.4 Conclusion 43

Chapter 5 : Characterize the physical, chemical and thermal properties of the biomaterial 56
5.1 Introduction 56
5.2 Materials and Methods 57
5.2.1 Synthesis of PEG-PLGA-PEG Polymer 57
5.2.2 Molecular Weight of PEG 59
5.2.3 Molecular Weight of PLGA 59
5.2.4 Spectroscopy 60
5.2.5 Rheology 60
5.2.5.1 Viscosity 60
5.2.5.2 Dynamic Mechanical Analysis 60
5.3 Results & Discussion 61
5.3.1 Material Gelation 61
5.3.2 Molecular Weight of PEG 62
5.3.3 Molecular Weight of PLGA 62
5.3.4 Spectroscopy 63
5.3.4.1 Purification of PEG-PLGA-PEG 63
5.3.4.2 Gel pH 63
5.3.4.3 Polymer Verification 64
5.3.5 Rheology 65
5.3.5.1 Viscosity 65
5.3.5.2 Dynamic Mechanical Analysis 66
5.4 Conclusions 67

Chapter 6 : Increase mechanical properties and long-term stability of the gels using permanent crosslinks 86
6.1 Introduction 86
6.2 Materials and Methods 88
6.2.1 Materials 88
6.2.2 Synthesis of PEGma-PLGA-PEGma Polymer 88
6.2.3 Molecular Weight of PLGA 89
6.2.4 Molecular Weight of PEGma 89
6.2.5 Rheology 90
6.2.5.1 Viscosity 90
6.2.5.2 Dynamic Mechanical Analysis 90
6.2.6 Photosensitivity 90
6.3 Results & Discussion 91
6.3.1 PEGma-PLGA-PEGma (526-2810-526) 91
6.3.2 PEGma-PLGA-PEGma with varied PLGA Mw 92
6.3.2.1 PEGma-PLGA-PEGma (526-5620-526) 92
6.3.2.2 PEGma-PLGA-PEGma (526-1404-526) 93
6.3.3 Blend of PEG-PLGA-PEG and PEGma-PLGA-PEGma (550-2810-550/526-2810-526) 94

6.3.3.1 50/50 Mix Ratio 95
6.3.3.2 35/65 Mix Ratio 96
6.3.3.3 20/80 Mix Ratio 96
6.3.3.4 10/90 Mix Ratio 97
6.4 Conclusions 98

Chapter 7 : Assess the feasibility of the biomaterial for 3-Dimensional tissue scaffold printing 126
7.1 Introduction 126
7.2 Methods and Materials 127
7.2.1 Material Printing 127
7.2.1.1 2-D Printing 127
7.2.1.2 3-D Printing 128
7.2.2 Software 128
7.2.3 Hardware 129
7.3 Results & Discussion 131
7.3.4 2-D Printing 131
7.3.5 3-D Printing 133
7.4 Conclusions 134

Chapter 8 : Conclusions and Recommendations for Future Work 147
8.1 Conclusions 147
8.2 Recommendations 152

References 155

List of Tables

Table 2.1 - Commercial and Research SFF Bio-printers 17
Table 2.2 - Material Design Criteria for Solid Freeform Fabrication Printing 18
Table 2.3 - Viscosity comparison 23
Table 4.1 - PNIPAAm gelation characteristics 54
Table 4.2 - Gel characteristics of 550-2810-550 triblock material 55
Table 5.1 - Effect of PEG molecular weight on viscosity 73
Table 5.2 - Effect of PLGA molecular weight on viscosity 73
Table 5.3 - Maximum and minimum viscosity of 550-2810-550 85
Table 5.4 – Maximum elastic modulus and corresponding temperature of 550-2810-550 85
Table 6.1 - Comparison of maximum elastic modulus 101
Table 6.2 - Comparison of maximum viscosities 101
Table 6.3 - Comparison of mixed polymers - (PEG-PLGA-PEG/PEGma-PLGA-PEGma) 103
Table 6.4 - Elastic modulus comparison to measured liver tissue 125
Table 7.1 - SFF printer variables tested and final values 143

List of Figures

Figure 2.1 - Conversion of unit layers into scaffold layers [65] 15
Figure 2.2 – A & B: 3D robotic industrial bioprinter - 'BioAssembly Tool' (designed by Sciperio/nScript, Orlando, USA), C: Rapid Prototype Robotic Dispensing System (RPBOD) with dual dispensing nozzles [66]. 16
Figure 2.3 - Irgacure 2959 breaking into free radicals due to UV irradiation 19
Figure 2.4 - Effect of UV light exposure on SMCs [42] 20
Figure 2.5 - Effect of Irgacure 2959 on SMCs [42] 21
Figure 2.6 - Effect of Irgacure 2959 concentration and UV exposure on SMCs [42] 22
Figure 4.1 - Chemical structure of PEG-PLGA-PEG 45
Figure 4.2 - Phase diagram of PEG-PLGA-PEG [58] 46
Figure 4.3 - Brookfield DV-II+Pro Viscometer 47
Figure 4.4 - Texas Instrument AR 2000ex Rheometer 48
Figure 4.5 - Close-up of Texas Instrument AR 2000ex Rheometer Testing Plate 49
Figure 4.6 - % Chitosan (Low and High Molecular Weight) vs. Viscosity 50
Figure 4.7 - Shear rate vs. instantaneous viscosity of high molecular weight chitosan 51
Figure 4.8 - Shear rate vs. instantaneous viscosity of low molecular weight chitosan 52
Figure 4.9 - PEG-DA gelation time under UV light 53
Figure 5.1 - Ring opening polymerization of glycolide and DLLA to form PEG-PLGA diblock 69
Figure 5.2 - Chemical Structure and polarity of PEG-PLGA-PEG 70
Figure 5.3 - Chemical structure representation of PEG-PLGA-PEG 71
Figure 5.4 - PEG-PLGA-PEG formation of a micelle 71
Figure 5.5 - Micelle properties due to PEG-PLGA-PEG concentration 72
Figure 5.6 - NMR showing residual DCM, toluene, and diethyl ether 74
Figure 5.7 - NMR of 550-2810-550 triblock material with corresponding example types of bonds with no extra residual material 75
Figure 5.8 - H-NMR spectra of PEG-PLGA-PEG triblock copolymers in CDCl3. The molecular weight of PLGA is 2810 (a) and 5000 (b) 76
Figure 5.9 - Viscosity of 25% 550-2810-550 triblock material 77
Figure 5.10 - Viscosity of 35% 550-2810-550 triblock material 78
Figure 5.11 - Viscosity of 45% 550-2810-550 triblock material 79
Figure 5.12 – Comparison of viscosity of 25%, 35%^, and 45% 550-2810-550 triblock material 80
Figure 5.13 - Elastic and viscous modulus of 25% 550-2810-550 triblock material 81
Figure 5.14 - Elastic and viscous modulus of 35% 550-2810-550 triblock material 82
Figure 5.15 - Elastic and viscous modulus of 45% 550-2810-550 triblock material 83
Figure 5.16 - Gelation point for 25%, 35%, and 45% 550-2810-550 triblock material 84
Figure 6.1 - Various chemical structure of PEG 100

Figure 6.2 - Chemical structure of PEGma-PLGA-PEGma 100
Figure 6.3 - UV Light set-up..... 102
Figure 6.4 - Elastic and viscous modulus of 35% 526-2810-526 triblock material 104
Figure 6.5 - Elastic and viscous modulus of 45% 526-2810-526 triblock material 105
Figure 6.6 - Viscosity of 45% 526-2810-526 triblock material..... 106
Figure 6.7 - Viscosity of 25% 526-1405-526 triblock material..... 107
Figure 6.8 - Viscosity of 35% 526-1405-526 triblock material..... 108
Figure 6.9 - Viscosity of 45% 526-1405-526 triblock material..... 109
Figure 6.10 - Elastic and viscous modulus of 25% 526-1404-526 triblock material 110
Figure 6.11 - Elastic and viscous modulus of 35% 526-1404-526 triblock material 111
Figure 6.12 - Elastic and viscous modulus of 45% 526-1404-526 triblock material 112
Figure 6.13 - Viscosity of 45% concentration of 50/50 mix of 550-2810-550 and 526-1404-526 triblock material with and without 0.03% Irgacure..... 113
Figure 6.14 - Elastic and viscous modulus of 45% concentration of 50/50 mix of 550-2810-550 and 526-1404-526 triblock material with and without 0.03% Irgacure 114
Figure 6.15 - Viscosity of 45% concentration of 35/65 mix of 550-2810-550 and 526-1404-526 triblock material with 0.03% Irgacure..... 115
Figure 6.16 - Elastic and viscous modulus of 45% concentration of 35/65 mix of 550-2810-550 and 526-1404-526 triblock material with 0.03% Irgacure 116
Figure 6.17 - Viscosity of 45% concentration of 20/80 mix of 550-2810-550 and 526-1404-526 triblock material with 0.03% Irgacure..... 117
Figure 6.18 - Elastic and viscous modulus of 45% concentration of 20/80 mix of 550-2810-550 and 526-1404-526 triblock material with 0.03% Irgacure 118
Figure 6.19 - Comparison of 20/80 mix to 35/65 mix triblock copolymer material 119
Figure 6.20 - 20/80 mix triblock copolymer material gelation..... 120
Figure 6.21 - Viscosity of 45% concentration of 10/90 mix of 550-2810-550 and 526-1404-526 triblock material with 0.03% Irgacure..... 121
Figure 6.22 - Elastic and viscous modulus of 45% concentration of 10/90 mix of 550-2810-550 and 526-1404-526 triblock material with 0.03% Irgacure 122
Figure 6.23 - Comparison of viscosity for all mixes of 550-2810-550 and 526-2810-526 123
Figure 6.24 - Comparison of gelation characteristics for all mixes of 550-2810-550 and 526-2810-526..... 124
Figure 7.1 - Schematic of 3-D Printer..... 136
Figure 7.2 - Actual 3-D Printer Set-up..... 137
Figure 7.3 - Extrusion method deposition modes: A) droplet mode, B) continuous mode, and C) contact mode 138
Figure 7.4 - 3-D structure designs: A) Drexel D, B) 3 tiered birthday cake..... 139
Figure 7.5 - Schematic of the Software Printing Process 140
Figure 7.6 - Integrated Software for 3-D Printing Preparation..... 141

Figure 7.7 - Schematic of 741MD-SS Needle Microvalve [123] 142
Figure 7.8 - Custom Copper Needle Tips of Inner Diameters (a) 250 µm and (b) 500 µm 143
Figure 7.9 - 2-D printed circles: (a) Continuous and (b) Contact. Width of line = 1mm 144
Figure 7.10 - Final printing variables confirmed. ID =19mm OD = 21mm 144
Figure 7.11 - 3-D Drexel D structure (10 layers)..... 145
Figure 7.12 - 3-D Three tiered birthday cake: A) program dimensions, B)side view of printed structure, C) isometric view of printed structure, and D) time duration spread effect during printing..... 146
Figure 8.1 - Schematic of how PEG and PLGA molecular weight (MW) affect solution viscosity 154

Abstract

A Thermosensitive and Photocrosslinkable Composite
Polymer study for 3-D Soft Tissue Scaffold Printing

Christopher Gerald Geisler
Jack G. Zhou, Ph.D.

A novel biocompatible and biodegradable thermosensitive and photocrosslinkable material has been designed for use with solid freeform fabrication (SFF) printers. The blend of a thermosensitive poly (ethylene glycol-b-(DL-lactic acid-co-glycolic acid)-b-ethylene glycol), PEG-PLGA-PEG, triblock and photocrosslinkable PEG methacrylate-PLGA-PEG methacrylate, PEGma-PLGA-PEGma, allow for a material that is well suited for the fabrication of 3-D soft tissue scaffold printing. It is a solution of low viscosity at low temperature and becomes a highly viscous material with increase in temperature. Additional strength and irreversibility of the gel is gained with UV light irradiation.

Other types of natural and synthesized materials were studied for use with SFF printers but none were capable of general use with a multiple number of printers because of specialized gelation steps or long solidification times. Thermosensitive and photocrosslinkable materials were also studied because of their simplicity allowing for the elimination of additional crosslinking material. Alone, each material is not able to build 3-D structures due to its mechanical abilities, but combined, the advantages of each material create a material that is ideal for soft tissue scaffold printing. This type of material allows for the integration of cell printing so that precise complex architecture can be accomplished with the incorporation of cells where needed in the scaffold.

Chapter 1 : Introduction

In the US alone, around eight million surgical procedures are performed every year to treat maladies related to damaged tissue; over 70,000 patients are waiting for organ transplants, and more than 100,000 people die each year with tissue related disorders [1]. The current demands for replacement organs and tissues far exceed the supply, and research indicates that this gap will continue to widen [2]. The history of reconstructive surgery began with ablative surgery, followed by tissue and organ transplantation, leading to contemporary tissue reconstruction [3]. In recent years, the main focus of tissue engineering has been on the culture of cells. In general, tissues are 3-D structures composed of living cells and a support structure. Therefore, the generation of functional implants from living cells relies heavily on the fabrication of the 3-D structure. Tissue engineering has been successfully used to replace skin, blood vessels, and cardiac tissue [4]. For the generation of complex 3-D implants, more sophisticated technology is required. Complex shapes and structures can be created from special biodegradable and biocompatible polymers so that a tissue's natural support structure replaces the synthetic scaffold as it degrades. The materials should therefore be considered only as a temporary support for cell growth and cell adhesion [5]. For engineering soft tissues, ideal scaffolds are made of synthetic or natural biopolymers providing porous (up to 90%) support structure, thus mimicking the natural extracellular matrix environment in which cells attach, multiply, migrate and function [1, 6]. The pores in the scaffold must be interconnected to allow efficient nutrient transfer and waste exchange to permit survival of any cells cultured on the scaffold. The pores should typically be 100–300 μm, around 5–10 times a cell's diameter [5]. Porous scaffolds facilitate tissue formation while

providing adequate mechanical strength to withstand implantation and permit normal physiological function in the human body [5]. In this project, a novel material that is thermoresponsive and photocrosslinkable has been designed and fabricated to be used in many different applications of solid freeform fabrication. This material has been used to print detailed microstructures utilizing an innovative 3-D printer built by the Biomedical Design and Manufacturing Lab at Drexel University. This system can fabricate scaffolds from a variety of polymers and solutions and can include sensitive materials such as cells and growth factors.

Chapter 2 : Background

2.1 Tissue Engineering

Tissue engineering (TE) is a promising approach to create artificial constructs for repairing or replacing parts of or whole diseased tissues [7]. In TE, a highly porous artificial extracellular matrix or scaffold is required to accommodate cell growth and tissue regeneration in three dimensions (3-D). However, most existing 3-D TE scaffolds are far from ideal for practical application, not only because of inappropriate mechanical properties, but also because of a lack of interconnected channels [8-9]. There are four general requirements for soft tissue scaffolds [1, 7]:

- Highly porous 3-D interconnected structure for cell growth and flow transportation of nutrients and metabolic waste;
- Biocompatible and bioresorbable with a controllable degradation rate to match new tissue growth;
- Suitable surface chemistry for cell attachment, proliferation, and differentiation;
- Sufficient mechanical properties to match those of the tissues at the site of implantation.

Currently, most TE constructs do not include vascular networks and thus vascular ingrowth can only occur after implantation, which drastically limits the size and cellular content of the implants, and delays integration with the body [10]. Scaffolds that provide a conducive environment for normal cellular growth and differentiation are important components of tissue engineered grafts because the rapid integration with the host is essential for long-term graft viability [11]. Scaffolds should also safely degrade in the

body as cells produce their own natural extra cellular matrix (ECM). They must also provide certain mechanical support during the construction process to maintain the fabricated 3-D structure and resist deformation during implantation. The porous structure must be interconnected to allow the ingrowth of cells and transport of nutrients [12]. For a scaffold to serve as a synthetic tissue construct, it should not only be biocompatible and have appropriate mechanical properties, but it should also be bioactive, containing growth factors that enhance new tissue growth and cells that secrete new ECM. The scaffold must be manufactured to a specific, complex 3-D shape and size that exactly matches the tissue to be replaced at both the microscopic and macroscopic levels. Thus, three challenges currently face tissue engineers: Specific manufacturing techniques for mimicking tissue and ECM architecture are needed to produce scaffolds with high resolution (less than 10 μm) for tissues reconstruction such as myocardium (heart muscle), blood vessels, bone or nerves; Innovative multiple jet printing methods are needed for controlled delivery of cells and growth factors into scaffolds [6]; Manufacturing techniques for vascular structures within the tissue construct are needed to circumvent limits on the size and cellular content [10].

Computer-aided tissue engineering (CATE) is the partnership of computer-aided design, modeling, simulation, and manufacturing technologies combined with the engineering and biological principles to derive systematic solutions for tissue engineering problems [13]. Advances in computer-aided tissue engineering and the use of biomimetic design approaches enable the introduction of biological and biophysical requirements into the scaffold design process [14].

2.2 Hydrogels

Hydrogels have been widely used in various biomedical applications including TE due to their biocompatibility, low toxicity and low cost. Hydrogels are hydrophilic polymer networks that can absorb up to a thousand times their dry weight in water. Their high water contents make them more similar to native tissues than dry porous polymer scaffolds. Hydrogels can either be chemically stable or degradable which eventually disintegrate and dissolve [15]. They are called 'physical' gels when the networks are held together by molecular entanglements and/or secondary forces including ionic, hydrogen-bonding or hydrophobic forces [16-17]. Physical hydrogels are not homogeneous, since clusters of molecular entanglements, or hydrophobically- or ionically-associated domains, can create inhomogeneities. Free chain ends or chain loops also represent transient network defects in physical gels [15]. The polymer chains can be easily modified to vary the resultant hydrogel properties to fit the application. For TE purposes, hydrogels may be functionalized to promote cell proliferation, migration and adhesion. In addition, hydrogels are highly permeable, which facilitates exchange of oxygen, nutrients, and other water soluble metabolites, making them ideal for cell encapsulation. The hydrophilicity inhibits protein adsorption thereby minimizing the foreign body responses when implanted *in vivo* [18].

2.3 3-D Printing Methods

One of the main key criteria for manufacturing tissue engineered scaffolds is a high degree of pore interconnectivity. Pore sizes that are 5-10 times as large as the cell diameter promote cellular mobilization and cell viability, as well as waste removal [5]. A

wide variety of methods have been developed for manufacturing 3-D scaffolds with embedded cells and growth factors for soft tissue engineering. They can be generally classified into two categories: Non-automated and Solid Freeform Fabrication. Non-automation methods are often used for basic research purposes, while computer aided solid freeform fabrication has been developed to better control scaffold architecture and cell/growth factor incorporation.

2.3.1 Non-automated Methods

Non-automated methods have the advantages of simplicity and low cost, however, control of the microarchitecture and pore size is limited to approximate control of the cast hydrogels. Control of seeding is limited to cell density control, and heterogeneous cell patterning cannot be achieved.

Decellularized and denatured tissue constructs are a means of not having to seed cells in the scaffold. The process of decellularizing has the potential for tissue swelling or damage to the tissue but usually is capable of replicating the mechanical properties of the normal tissue it is replacing [19-20]. It is difficult to completely decellularize a construct and continue to maintain the biochemical and biomechanical properties but the process is promising and indicate the potential of decellularized tissue constructs that could be used to treat damaged tissue without eliciting an immune response [20].

In most non-automated methods, an internal porous structure is generated by randomly packed porogens that are later removed by particulate leaching and cannot be controlled

precisely. The biggest limitation with this class of methods is its incapability of making complex 3-D multicellular constructs and incorporating a vascular network where the pore size and porosity can be guaranteed every time [12]. Major disadvantages of this method include the possibility of toxic residual organic solvent from the fabrication of the scaffold and that the addition of cells to the scaffold cannot occur until after fabrication. The distribution of cells and proteins within a tissue is not random and homogenous but is highly organized and varies depending on the location in the tissue. Manufacturing methods that do not allow precise control over the scaffold architecture can never reach the level of complexity that is found in native tissues.

2.3.2 Solid Freeform Fabrication

Solid Freeform Fabrication (SFF) is a relatively new manufacturing technology involving a group of rapid prototyping technologies that are capable of producing complex freeform parts directly from a computer aided design (CAD) model of an object without part-specific tooling or fixture.

Rapid prototyping is a system for fabricating structures with defined internal and external architectures. Rapid prototyping for tissue engineering applications begins with information from 3-D CAD software or obtained through reverse engineering from the data of computed tomography, magnetic resonance imaging (MRI), confocal microscopy, serial sectioning histology, or a 3-D Coordinate Measuring Machine. Figure 2.1 demonstrates the different types of unit layers that are converged into scaffold layers.

The CAD model is transposed into sliced layers and based on this, numerical control codes are generated to control the machine in building the part. SFF technology makes parts in an additive fashion through layer-by-layer process. In each layer, materials can be added line by line, even dot by dot, so the internal structure of the porous scaffold can be controlled directly and precisely to meet any special requirements including relatively complex and curved shapes such as myocardial microvascular networks [12]. For a typical SFF printer, a computer controls the movement of the printing substrate in the X and Y axis as well as the Z axis for 3-D printing. The computer can also control the printing nozzles, whether it is an array of nozzles or only one nozzle printing at a time (Figure 2.2). Today's printers can print a variety of material including cells and growth factor and for some types of materials to gel, a catalyst or crosslinker is also needed to be printed as well. Prices of the printers range from a homemade printer costing around $2000 to higher resolution printers costing $700,000. Commercial and research printers also range in printing resolution from 100-500μm (Table 2.1).

2.3.3 Types of 3-D Printers

All of the SFF methods for soft TE are still in their early stages of development and face many limitations (Table 2.2). The inkjet printing method depends on commercial inkjets designed to dispense ink. These systems can only function in a narrow low viscosity range, which limits the type and strength of solutions that can be printed. In addition, inkjets are not well suited to dispense cells. A 25% cell death has been reported along with clogging of the jets with cells [21]. Inkjet printing also only has a resolution limit of around 200μm. Extrusion-based SFF methods produce a limited range of scaffold

architectures with parallel linear elements stacked in layers at a resolution of around 100μm but do not enable heterogeneous cell patterning (precise arrangement of multiple cell types). Laser-based SFF methods expose cells to high stress, ultra-violet (UV) light, and heat which must be carefully controlled to avoid damaging cells. This method does not scale up easily to 3-D manufacturing because cells are delivered from 2-D arrays [22].

Various methods for the manufacturing of 3-D scaffolds have been developed: microfabrication, fiber bonding, solvent casting or salt leaching, phase separation, high-pressure gas expansion, and emulsion freeze-drying [23-24]. These methods do not allow for the precise control to create porous structures or porous gradients to exactly replicate the architecture of human soft tissue. More recently, SFF technology has shown great potential in tissue engineering to build biomimetic tissues and organs for replacing or improving damaged or injured tissues [7, 25-27]. The first biomedical structures made directly by SFF were reported in the early 1990's using a custom-built three dimensional printing machine [28-30]. Since then, numerous already existing commercial and experimental SFF printing systems, such as fused deposition modeling, 3D printing, selective laser sintering, and stereolithography have been utilized to make scaffolds for biopolymer deposition.

2.4 Photocrosslinkable Materials

In recent years, photopolymerization to form gels has gained considerable interest in the field of tissue engineering because of its ability to rapidly convert a liquid to a gel under

physiological conditions. Photopolymerization, the ability of a material to change state due to its sensitivity to UV light, creates a gel that has similar water contents to the ECM which allows for efficient nutrient movement for cell viability [31]. Photopolymerization uses UV light to dissociate photoinitiator molecules into free radicals (Figure 2.3). During UV irradiation, the photoinitiator free radicals break apart the associated polymer macromolecules for that photoinitiator, creating a link between different broken polymer macromolecules [32]. Irgacure 2959 is a type of photoinitiator that breaks into free radicals during UV irradiation. Irgacure 2959 works best using a UV wavelength of 365nm [32-33]. As free radicals, Irgacure 2959 attacks carbon double bonds because they are less stable than the free radicals. One electron pair in a material that is compatible with Irgacure 2959 (posses a carbon double bond) is secured between two carbons while the other electron in the bond is loosely held. The Irgacure free radicals use the loose electron to form a stable bond with one of the carbon atom. This event turns the original double carbon bond material into another radical, similar to the Irgacure free radicals, allowing it to continue to repeat to create stable bonds with other carbon double bonds until the radical becomes less stable than any of the remaining carbon double bonds [32]. This domino effect creates extensive crosslinks between polymer chains.

Photocrosslinkable materials are being used in applications such as glass [34], paint, resin [35], solder [36], dyes and pigments [37], and in TE applications like wound healing hydrogel [38-39], clay nanocomposite material [40], 2-D biomaterial [31-32, 41-43], bio-degradable gel beads [44], photo-patterned hydrogels [45], and biological adhesive [46]. In TE applications, photocrosslinkable material can be used that allows for cell

attachment and proliferation and drug delivery [31]. It also has the ability to gel *in situ* as a minimally invasive technique [32]. Poly (ethylene glycol) diacrylate (PEG-DA) is increasingly being used for TE hydrogels due to its biocompatibility and high water content which is similar to native tissue. PEG-DA hydrogel has already been used in cartilage and bone tissue engineering [47-48]. PEG-based hydrogels utilizing a photocrosslinking mechanism are currently in clinical trials in Europe for cartilage repair [49]. An advantage of PEG-DA hydrogel is its moldability into any necessary shape and dimensions. However, it is difficult to decrease the extended degradation rate with PEG-DA hydrogel [41]. Polymers can be rendered photocrosslinkable through the addition of a methacrylate group because it contains the necessary double carbon bond. Naturally-derived polymers such as hyaluronan, gellan gum, and chondroitin sulfate, have also been prepared as photocrosslinkable polymers for hydrogel formation [50-51].

Cell encapsulation in a photocrosslinkable material can lead to interactions between cells and free radicals thus raising a concern of cell viability and proliferation. Bryant and Anseth have studied numerous types of photoinitiators and showed that Irgacure 2959 has the least detrimental effects on cells of all the photoinitiators they studied [32]. Sabnis et al studied how the concentration of Irgacure 2959 and amount of UV light affects cells; UV exposure at 365 nm and an intensity of 10mW/cm^2 on human aortic smooth muscle cells (SMC) under a time period of 5 minutes does not greatly affect the cells, there is no significant difference between the cell survival in UV exposure after 5 minutes and without any UV exposure (Figure 2.4) [42]. The less exposure a cell has to UV light, the better chance of survival. According to Sabnis' research, a total of 5 minutes of UV

irradiation should not greatly affect cell survival but should also not be surpassed. Greater than or equal to a 0.04% concentration of photoinitiator has a large affect on the survival of SMCs (Figure 2.5) [42]. To ensure cell survival, very small amounts of photoinitiators should be utilized. Finally, the combined effect of photoinitiator and UV light exposure was studied by Sabnis et al. and found that, like the individual studies, the greater the photoinitiator concentration and the greater the UV exposure time, the greater the number of cells that will not survive (Figure 2.6) [42].

2.5 Thermosensitive Materials

Thermosensitive hydrogels, also referred to as thermoreversible hydrogels, made with natural and synthesized materials are very popular in the field of tissue engineering and drug delivery [6, 52-59]. Examples of synthesized thermosensitive materials include poly(ethylene glycol)/poly(propylene glycol) block copolymers (poloxamers), poly(ethylene glycol)/ poly(butylenes glycol) block copolymers, poloxamer-g-poly(acrylic acid) and copolymers of N-isopropylacrylamide [52]. These materials show a solution to gel phase transition temperature when in an aqueous solutions [15]. Most of these materials are not biodegradable, which limits their use in TE. Diblock and triblock copolymers which are incorporated with other types of materials including synthesized materials become somewhat biodegradeable and therefore work well as an injectable drug-delivery system [54-55, 57-59]. There are also naturally derived materials that can create thermosensitive polymers. Some examples of these biocompatible natural materials are gelatin, agarose, amylase, amylopectin, and gellan [60-61]. These materials transition from solution to gel because they are physical gels; they take up a random coil

shape at high temperature and are in a solution phase but as temperature decreases, the material forms entangles double helices and becomes a gel [60].

2.6 Rheology

Rheology deals with the deformation and flow of matter, or the ability of a material to flow or be deformed [62]. A rheometer is able to conduct a detailed analysis of almost any type of fluid depending on the viscosity maximum of the machine. Viscosity is the measure of the internal friction of a fluid [63]. The greater the friction between the fluid and surface material, the greater the amount of force, shear, that is required. Higher viscous fluids require more force to move or be moved than a less viscous material. Examples of materials and their corresponding viscosities are shown in Table 2.3 [64]. The knowledge of this type of rheological behavior is important when designing a printer or piping system to deliver fluid.

Rheological measurements allow for the study of chemical, mechanical, and thermal properties of materials as well as any type of reaction that can take place. Rheology is the most sensitive method for material characterization because flow behavior is responsive to properties such as molecular weight and molecular weight distribution [63]. Measurements can be used as a quality check to monitor the manufacturing of a material. A heated substrate can be used to find the change in a material when temperature is increased or decreased. A plate/plate set-up, where a top flat rotating plate and a flat stagnant substrate bound a material produces accurate and reproducible viscosity measurements for most fluids while a cone/plate set-up, where the top plate is cone

shaped, offers absolute viscosity measurements with precise shear rate and shear stress readings. Both set-ups require extremely small samples ranging from 1-3ml and allows for simple temperature control.

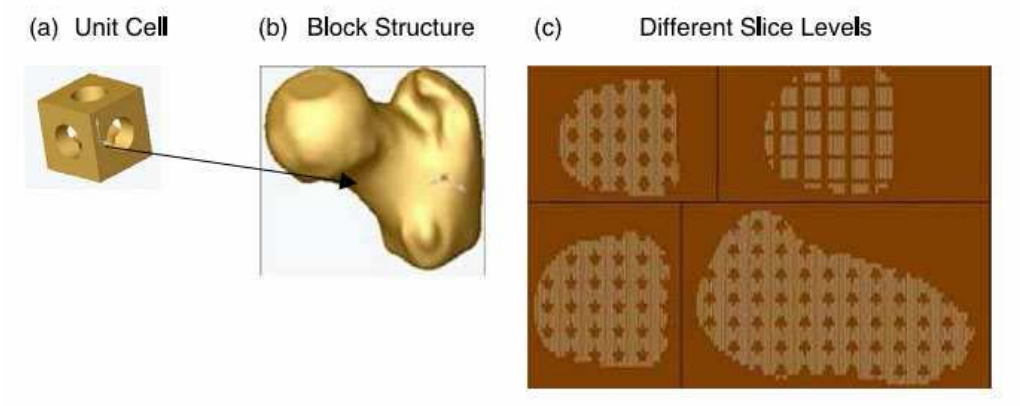

Figure 2.1 - Conversion of unit layers into scaffold layers [65]

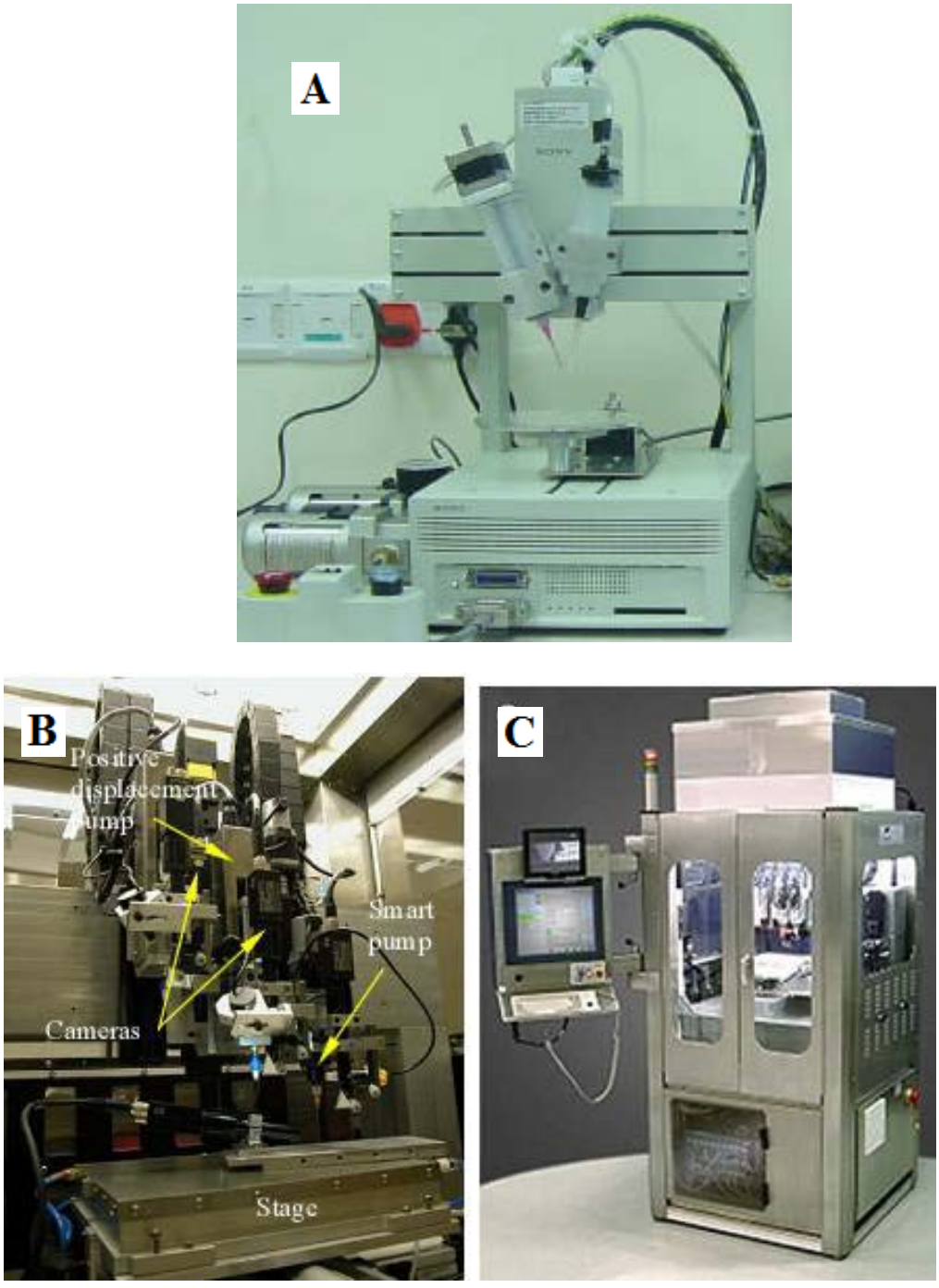

Figure 2.2 – A & B: 3D robotic industrial bioprinter - 'BioAssembly Tool' (designed by Sciperio/nScript, Orlando, USA), C: Rapid Prototype Robotic Dispensing System (RPBOD) with dual dispensing nozzles [66].

Table 2.1 - Commercial and Research SFF Bio-printers

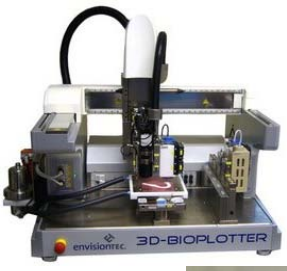

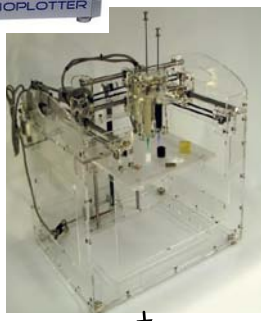

Company	Organovo (San Diego, CA, USA)	Neatco (Carlisle, Canada)	Sciperio (Orlando, FL, USA)	RPBOD (Ang et al., Singapore)	3D-Bioplotter (envisionTEC, Inc. Germany)	Fab@Home Model 2 (USA)
Price	$200,000	$?	$700,000	$?	>$50,000	<$2000
Nozzles	2	1	2	2	1 with 5 different cartridges	2
Printing resolution	500µm	300µm	100µm	100 µm	250 µm	500 µm

Table 2.2 - Material Design Criteria for Solid Freeform Fabrication Printing

Method	Advantages	Disadvantages	Minimum & Maximum Solution Viscosity
Print head (Thermal bubble)	Good droplet controllability	High power consumption, heating of liquid, rapid evaporation, slow speed, 25% cell death, low resolution (200um) [67]	10 - 20 cP
Pressurized mini-extruder	Fast solidification, no solvents, strong structure	Heating material to melting, low resolution (usually ~200mm)	200 - 500 cP
Solenoid micro-nozzle	No heating involved	Only for low viscosity, Poor droplet controllability [68]	60 - 100 cP
Piezoelectric micro-nozzle	No heating involved, good droplet controllability, high-speed delivery	Only for low viscosity, not continuous deposition	10 - 40 cP
Pneumatic micro-nozzle	Can handle high viscosity materials	Poor droplet controllability, low precision deposition [69]	160 - 600 cP
Electrowetting on Dielectric	Low power consumption, no heating involved, configurable, good droplet controllability, fine resolution (~1μm), fast	Liquid used should be conductive or at least should be polar	120 - 300 cP

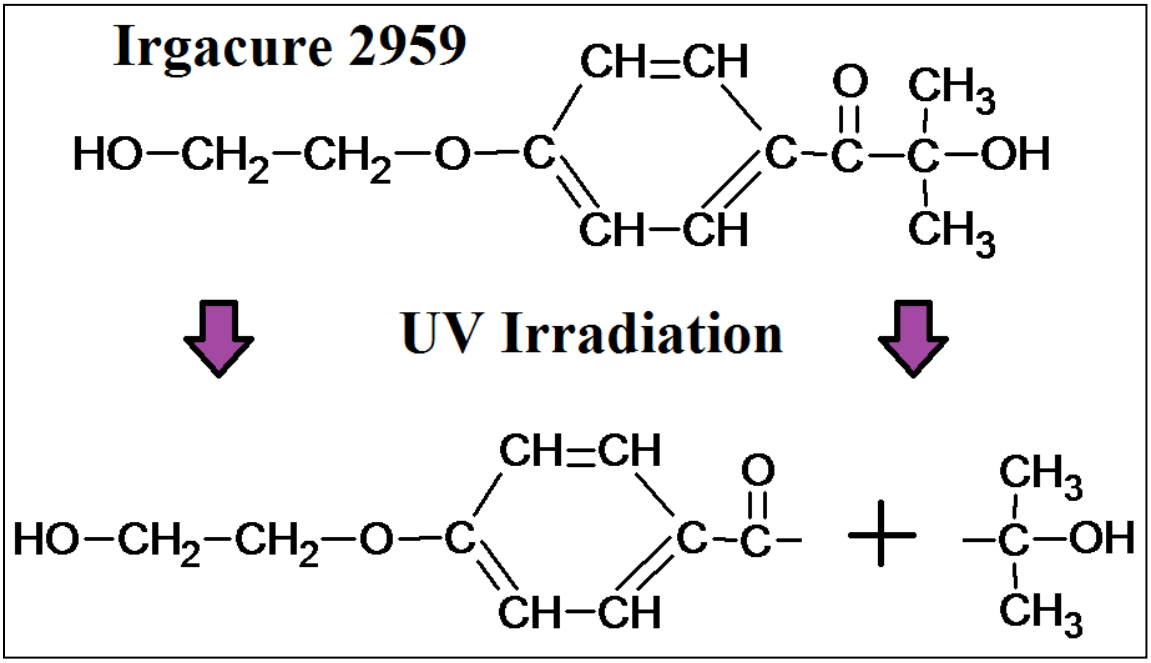

Figure 2.3 - Irgacure 2959 breaking into free radicals due to UV irradiation

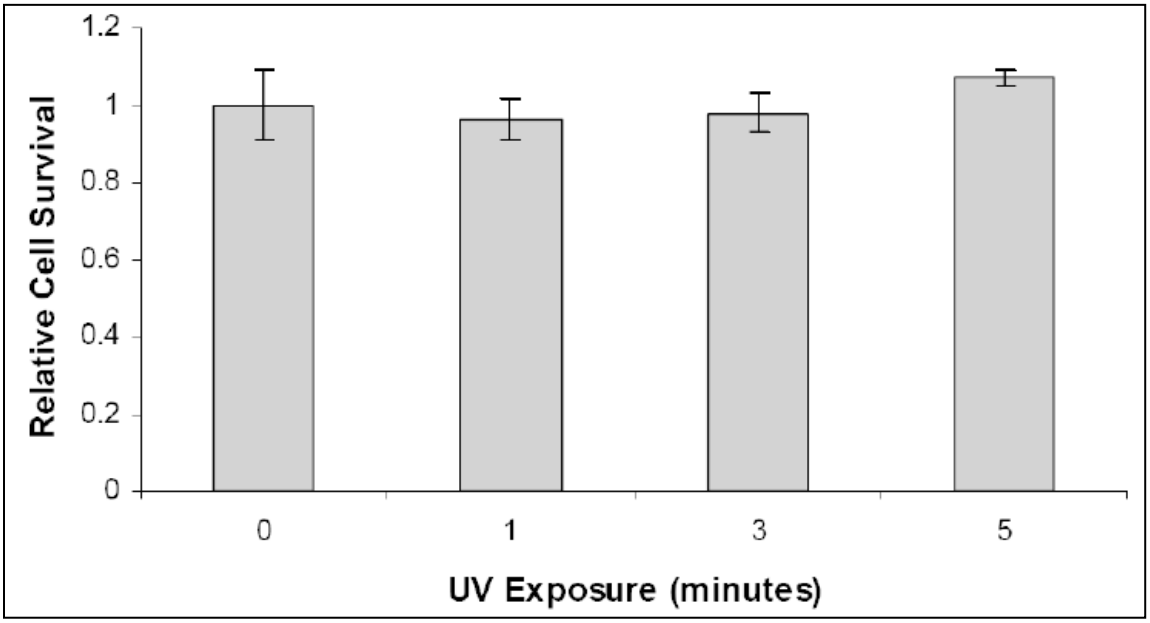

Figure 2.4 - Effect of UV light exposure on SMCs [42]

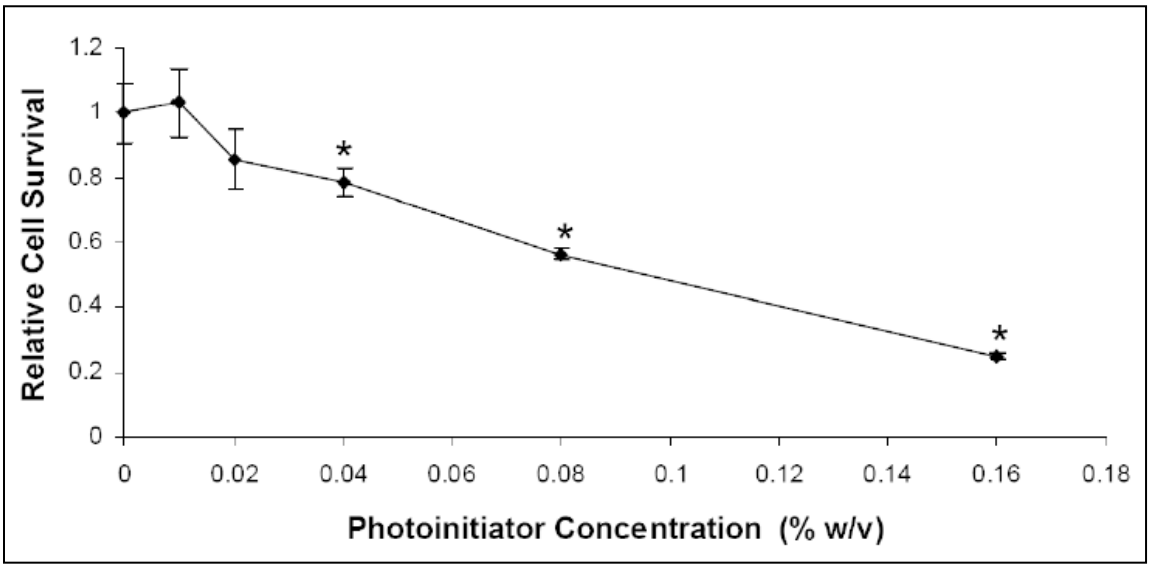

Figure 2.5 - Effect of Irgacure 2959 on SMCs [42]

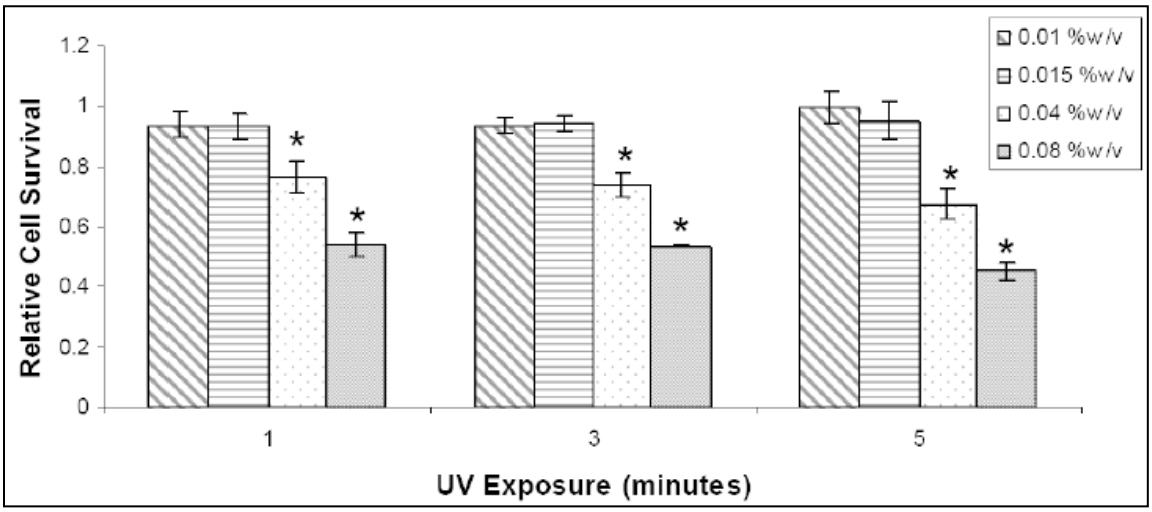

Figure 2.6 - Effect of Irgacure 2959 concentration and UV exposure on SMCs [42]

Table 2.3 - Viscosity comparison

Material @ 20°C	Viscosity (cP = mPa*s)
Petroleum	0.65
Water	1
Ethanol	1.19
Milk	3
Motor Oil SAE 10	65
Motor Oil SAE 30	200
Conformal Coating	50-5000
Varnish	250-1100
Castor Oil	240-1000
Maple Syrup	500
Honey	3,000
Chocolate Syrup	10,000
Ketchup	50,000
Mustard	70,000
Sour Cream	100,000
Peanut Butter	150,000-200,000
Shortening	1,200,000

Chapter 3 : Research Goals

The specific aims of this work are to:

1. Develop a biomaterial that is compatible with solid freeform fabrication printers.
2. Characterize the physical, chemical, and thermal properties of the biomaterial.
3. Increase mechanical properties and long-term stability of the gels using permanent crosslinks.
4. Assess the feasibility of the biomaterial for 3-D tissue scaffold printing.

Chapter 4 : Develop a biomaterial that is compatible with solid freeform fabrication printers

The aim of the work described in this chapter is to research materials that would be suitable for use in solid freeform fabrication printers to create 3-D scaffolds for soft tissue. Various types of materials were researched and materials that seemed capable of use in a 3-D printer were further tested to verify that they met every requirement and if they could be fully utilized for SFF 3-D printing.

4.1 Introduction

Physically linked gels have connected networks that are held together by molecular entanglements, and/or secondary forces including ionic, H-bonding or hydrophobic forces [70]. Physical gels are not homogeneous since groups of entanglements can create inhomogeneities. Free polymer chain ends that are not crosslinked also represent network defects in physical gels. All of these interactions are reversible, and can be disrupted by changes in physical conditions such as ionic strength, pH, temperature, application of stress, or addition of specific solutes [70]. Physical gels are formed by reversible links while chemical gels are formed by irreversible covalent or ionic links [71]. A covalent bond is a chemical bond that shares a pair of electrons between atoms. The pull and push of the forces between these atoms when they share electrons is known as covalent bonding. An ionic bond, or noncovalent bond, is a chemical bond formed through the attraction between two oppositely charged ions. Ionic bonds are usually formed between a metal and a nonmetal. There are many different macromolecular structures and forms

that are possible for physical and chemical hydrogels including: (a) solid molded forms, (b) pressed powder matrices, (c) microparticles, (d) coatings, (e) membranes or sheets, (f) encapsulated solids, and (g) liquids [70].

Naturally derived hydrogel forming polymers such as chitosan and alginate have frequently been used in tissue engineering applications because they have macromolecular properties similar to the natural material they are being substituted for, are biocompatible, and can be degraded by cell-secreted enzymes [18]. Comparatively, synthetic hydrogels such as PEG and PLGA are appealing for use in tissue engineering because their properties are controllable and reproducible. Synthetic polymers can be produced with specific molecular weights, degradable linkages, and crosslinking modes. These properties help to determine gel formation dynamics, crosslinking density, material mechanical properties, and degradation properties [18].

4.1.1 Covalently Crosslinked Hydrogels

Chen et al. has crosslinked genipin with alginate-chitosan to form microcapsules [72]. Due to its nonhomogeneity, this type of hydrogel is unlikely to build free standing 3-D structures. Kim et al. has developed chitosan/gelatin-based films covalently crosslinked by proanthocyanidin forming the final gel by mixing in dry power [73]. Many different types of printers do not have the capabilities for movement of dry material so this type of gelation would not work for our type of printer. Jin's addition of poly(ethylene oxide) (PEO) to the genipin/chitosan hydrogel increased the complete gelation time to 1 day [74]. Mi et al. claims a period of at least 24 hours is needed before full gelation of his

combination of chitosan and genipin [43]. Tripolyphosphate (TPP) was then added to the genipin to crosslink with chitosan. A sitting time of 24 hours plus a drying time of another 24 hours was needed for this gel to be complete [44]. The gelation time of our hydrogel has to be as short as possible to allow for the printing of additional layers on top of the current layer. Rapid printing of layers is needed to ensure adhesion from one layer to the next. For these reasons, genipin was eliminated as a possible material for our printing material.

4.1.2 Physically Crosslinked Hydrogels

Hydrogels can be physically crosslinked through the formation of hydrogen bonds between polymer chains. Methods of producing these physical bonds are typically not suitable for 3-D printing methods. For example, Patel and Amiji have created chitosan-poly(ethylene oxide) hydrogels that require the material be dried either by freeze-drying or air-drying technique for approximately 48 hours [75]. The process of freeze-drying layers of gel between the printing of the subsequent layer would increase total print time so this type of step is not applicable for our process. Koyano et al. and Berger et al. demonstrated that chitosan/ poly(vinyl alcohol) hydrogels can either be prepared by the autoclaving method, where the solution is autoclaved under nitrogen and then dried at room temperature for 24 hours [76], or by the freeze-thaw method [77]. Due to the limitation of the processes of autoclaving and freeze-thaw with our rapid printing requirement, physically crosslinked hydrogels will not fit our design.

4.1.3 Ionically Crosslinked Hydrogels

Ionic crosslinking is a simple and mild procedure. In contrast to covalent crosslinking, no auxiliary molecules such as catalysts are required, which is of great interest for medical or pharmaceutical applications [71]. Qu et al. confirmed that chitosan powder dispersed in deionized (DI) water dissolved by adding lactic and/or glycolic acid and needs to be dried at 80°C followed by extraction with methanol for 24 hours [78]. Gang et al. has shown that a nano-hydroxyapatite/konjac glucomannan/chitosan composite has to be stirred for 24h, aged for 24h, and finally dried in a vacuum oven at 80°C [79]. The drying of the hydrogel cannot take more than a minute, vertical printing of layers needs to continue without much waiting time. So, the polymerization of solution to gel of N-vinyl pyrrolidone and polyethylene glycol diacrylate with an aqueous acetic acid solution of chitosan that needs to dry at 37°C for a period of 3 hours would also not work [80]. Another requirement necessary for building a free standing 3-D scaffold is that a homogenous gel is needed. Chen, Wu et al. and Lin, Liang et al. validated that alginate blended with a DI water-soluble chitosan (N,O-carboxymethyl chitosan, NOCC) was prepared to form microencapsulated beads [81-82]. Eiselt et al. confirmed that beads are also formed when alginate is dropped into a calcium chloride/acetic acid solution [83]. Kuo and Ma mixed sodium alginate dissolved in DI water with either calcium sulfate or calcium carbonate in combination with glucono-δ-lactone and vortexed it for 1 minute to initiate gelation and then stored for 48 hours of gelation [84]. Vortexing of the solution after printing would destroy the architecture of the scaffold that was printed. Ionic crosslinking methods of hydrogel formation typically result in hydrogels that are not

stable in physiologically conditions, as the exchange of ions with those in the body would cause gel dissolution [85].

4.1.4 Chitosan

Chitosan hydrogel was originally selected as our pioneer scaffold material because of its biocompatibility properties. Chitosan, a deacetylated derivative of chitin commonly found in the shells of crustaceans, was an attractive candidate as a natural biopolymer hydrogel. Chitosan has been extensively used in drug delivery and tissue engineering because of its biocompatibility, biodegradability, antibacterial properties, bioadhesion and low cost [73, 86-91]. Chitosan is conveniently degraded by lysozyme, an enzyme present naturally in the human body, allowing resorption of the material during subsequent tissue replacement. Chitosan has been combined with several additive biomaterials such as alginate, collagen [86], gelatin [73], chitin [88], hydroxyapatite [87, 89], PMMA [87], calcium phosphate cement [87], β-tricalcium phosphate [90], poly-lactic-co-glycolic acid (PLGA) [91], and a variety of growth factors.

Csaba and Alonso show that ionically crosslinked particles are formed with the combination of high or low chitosan with TPP [92]. The mechanical properties of a chitosan and TPP hydrogel can be varied with the ratio of each in their characterization studies [93]. Hwang and Shin proved that the rheological properties of chitosan solution can differ according to its concentration [94]. Kumbar et al. have shown that polyacrylamide-grafted-chitosan crosslinked with glutaraldehyde forms microspheres [95]. The difficulty of working with glutaraldehyde is that that the crosslinking between

a cell-containing solution and glutaraldehyde is very complicated to achieve because it will prefer to crosslink with the cell membranes rather than the hydrogel and thus will kill cells [96].

In our multi-jet printing process, hydrogel solution is solidified (gelled) by adding crosslinkers after hydrogel solution is deposited. Chitosan can be crosslinked by covalent or ionic crosslinkers. Covalently crosslinked hydrogels are bound by irreversible chemical links and tend to have better mechanical properties [71, 97-99]. Hydrogels are often formed by the covalent cross-linking of hydrophilic polymers, and is often achieved with glutaraldehyde, glyoxal or other reactive cross-linking agents. Most of the crosslinkers used to perform covalent crosslinking may induce toxicity even in trace amounts, reducing the hydrogel's biocompatibility [100]. A method to overcome this problem is to prepare hydrogels by reversible ionic crosslinking so that no toxic crosslinking agent is required [71]. Another advantage of ionically crosslinking hydrogels is the low viscosity of the individual solutions before mixing. Genipin, a naturally occurring covalent crosslinking agent which has been used in herbal medicine and food dyes, has recently been used as a crosslinker on chitosan with no cytotoxic effect [101-102]. Other possible crosslinkers are ionic in nature and include tripolyphosphate, which has been used for simulation of permeability of drugs through skin [103].

4.1.5 Photocrosslinkable Material

The advantages associated with UV-curing technology are a solvent-free solution transformed rapidly at ambient temperature into a solid material, with a minimum

consumption of energy [40]. By adding a photoinitiator, chitosan solutions can be made photocrosslinkable so that application of UV light results in an insoluble, flexible hydrogel like soft rubber within 60 seconds [39, 46]. However, solutions of photocrosslinkable chitosan are generally too viscous for use in electrowetting or the amount of time required for complete gelation during UV irradiation is not feasible for 3-D building [38-39, 46, 104]. Ono, Saito et al. found that Az-CH-LA (photocrosslinkable chitosan to which both azide and lactose moieties are introduced) aqueous solutions that are gelatinized by UV irradiation are very viscous in their solution phase [46]. The viscous Az-CH-LA aqueous solution is too viscous to work with most SFF printers since it has to be moved from a reservoir to a nozzle and deposited accurately and precisely according to the microarchitecture of the tissue.

Poly (ethylene glycol) diacrylate (PEGDA) hydrogels are increasingly used for tissue engineering because of their high biocompatibility, tissue-like water content and 3-D network structure. For instance, PEGDA hydrogels have been used in cartilage, bone and adipose tissue engineering [41]. Dikovsky and Seliktar created a unique biosynthetic hybrid scaffold comprised of synthetic polyethylene glycol (PEG) and endogenous fibrinogen precursor molecules. The PEGylated fibrinogen was cross-linked using photoinitation in the presence of cells to form a dense cellularized hydrogel network. The fibrin-like scaffold material maintained its biofunctionality through the fibrinogen backbone, while changes in the molecular architecture altered the structural properties of the scaffold, including mesh size and permeability [33].

4.1.6 Thermosensitive Material

In situ gel formation can also be achieved using a thermoresponsive polymer that is a free flowing solution in DI water at ambient temperatures and undergoes gelation upon rising above a certain temperature. With the use of a thermosensitive hydrogel, a more simplistic printing nozzle array can be used since only one material has to be printed instead of a material and a crosslinker. One such polymer is poly(N-isopropylacrylamide) (PNIPAAm) [105].

4.1.6.1 PNIPAAm

PNIPAAm hydrogel has been researched extensively as a drug delivery material because of its phase transition behavior due to temperature changes [53, 105]. PNIPAAm hydrogels have a phase separation and exhibit a sudden shrinking in volume near their phase transition temperature [106]. These reactions are due to the quick changes in hydrophilicity and hydrophobicity among the hydrogel sub-groups [53, 106]. A limitation of PNIPAAm is that it is non-biodegradable which would require additional surgery for remove after tissue regrowth and it posses low mechanical properties when swollen [105]. Aqueous solutions of PNIPAAm undergo a phase transformation at a low critical solution temperature (LCST) around 32°C, making it ideal as an injectable material that gels at body temperature [107]. Below the LCST, the polymer is hydrophilic while above the LCST, the polymer becomes hydrophobic so that the polymer and DI water separate to form a compact gel [108]. Copolymers of N-isopropylacrylamide and poly(ethylene oxide)–poly(propylene oxide)–poly(ethylene oxide) are typical examples of thermosensitive polymers, but their use in drug delivery is limited because they are

toxic and non-biodegradable. Although it may be somewhat toxic and non-biodegradable, PNIPAAm has been used in many *in vitro* and *in vivo* experiments and show the capability of cell adhesion and proliferation [53, 105, 107-109].

4.1.6.2 PEG-PLGA-PEG

Aqueous solutions of new biodegradable triblock copolymers, poly(ethylene glycol-b-(DL-lactic acid-co-glycolic acid)-b-ethylene glycol) (PEG-PLGA-PEG) (Figure 4.1), have shown to have solution-to-gel (lower transition) and gel-to-solution (upper transition) transitions as temperature increases (Figure 4.2). The lower transition is important for scaffold fabrication because the solution flows freely at room temperature and becomes a gel at body temperature [54]. The transition temperatures depend on the concentration of polymers. With increasing temperature, an aqueous solution of PEG-PLGA-PEG triblock copolymer with molecular weights of 550-2810-55 undergoes a solution to gel transition in the range of 30-35°C and a gel to solution transition in the range of 40-70°C. In between the two transitions, a gel phase exists. Testing was needed to verify PEG-PLGA-PEG gels were stable at body temperature over long periods of time. PEG-PLGA-PEG triblock copolymers are amphiphilic in nature because DI water is a poor solvent for the hydrophobic PLGA block while it is a good solvent for the hydrophilic PEG blocks [57]. It is reported that the viscosity of PEG-PLGA-PEG triblock copolymer aqueous solution with 33 wt % concentration at room temperature is 10 cP and that the viscosity abruptly increases at the sol-to-gel transition temperature of 34°C [54].

4.1.7 Degradation

Degradation is important in tissue engineering materials to allow for encapsulated cells and growth of surrounding tissue into the scaffold. Another advantage of degradation is to allow for drug delivery at the repaired site [54, 110]. The drug release of spironolactone in PBS was studied from a PEG-PLGA-PEG (550-2810-550) triblock material and was found to fully release after 58 days [59]. The benefit of using a PEG-PLGA-PEG material is that the PLGA is biodegradeable, unlike PNIPAAm, which permits the release of drugs and the growth of cells [55-58]. The degradation rate of PLGA has been researched and found to depend on several factors including DLLA:GA ratio, molecular weight, and water content [9, 59, 110-111].

Three different types of crosslinking methods were found that required further research to discover if they are viable for use in 3-D scaffold printing: physical, covalent, and ionically crosslinked hydrogels. Chitosan, a natural biocompatible, biodegradable, antibacterial, bioadhesive and inexpensive material can be physically, covalently or ionically crosslinked. Photocrosslinkable and thermosensitive hydrogels require less material to be printed but require additional steps for gelation, UV light irradiation and temperature change respectively. All materials had interesting aspects that made them probable for SFF printing but an in-depth look into the gelation mechanism and material properties such as viscosity and gel mechanical strength would be needed in order to proceed with any option.

4.2 Materials and Methods

4.2.1 Materials

4.2.1.1 Ionic / Covalent Crosslinking

Chitosan (Low Mn = 50,000 - 190,000 , High Mn = 310,000 - 375,000) (Aldrich), sodium tripolyphosphate - technical grade, 85% (Sigma-Aldrich), and acetic acid ACS reagent, ≥99.7 % (Sigma-Aldrich) were all used as received. All solvents and other chemicals are of analytical grade.

4.2.1.2 Photocrosslinkable

1 Propane-2hydroxy-1-[4-(2-hydroxyethoxy)-phenyl]-2-methyl (Irgacure®2959) was generously provided by BASF Corporatio, Vandalia, IL and polyethylene glycol - diacrylate (PEG-DA) and polyethylene glycol - fibrinogen (PEG-Fb) were generously provided by Dr. Dror Seliktar, from Technion, Israel Institute of Technology; all were used as received. All solvents and other chemicals are of analytical grade.

4.2.1.3 Thermosensitive

Polyethylene glycol (PEG) diol (Mn = 2000, 4600, 8000, and 10,000 g/mol) (Sigma–Aldrich), initiator 2,20-azobisisobutyronitrile (AIBN), 98% (Sigma–Aldrich), poly(ethylene glycol) dimethacrylate (PEGDM) (Mn = 1000) (Polysciences), DL-lactide (DLLA) (Aldrich), glycolide (GA) (Aldrich), monomethoxy poly(ethylene glycol) (PEG) (Mw = 550, Aldrich), anhydrous toluene (Sigma), and hexamethylene diisocynate

(HMDI) (Sigma) were all used as received. All solvents and other chemicals are of analytical grade.

4.2.2 Chitosan and Tripolyphosaphate

Solutions of chitosan and tripolyphosaphate were examined in terms of their rheological properties and their abilities to form homogenous gels. Various concentrations of chitosan were prepared in either 1% or 2% acetic acid. Higher percentages of acetic acid were too acidic (too low pH value) for gelation to occur when mixed with tripolyphosphate [112]. The viscosities of the chitosan solutions were then measured based on shear rate using a rheometer. According to Shu and Desai, only 1% of total weight of TPP should be added to the chitosan solution to prevent an overly acidic environment which would damage cells in tissues [113-114]. Increments of 0.25 from 0.5% to 2% of TPP were added to all samples. In every sample of 0.2% to 2% chitosan solution mixed with TPP, non-homogenous gelation occurred. Gelation was determined by visual observations. Large pieces of gels were suspended in solution, and the consistencies of the gel pieces were slightly more viscous than the original chitosan solution. The only gel that formed from chitosan solution that had a low enough viscosity for use with most SFF printing formed gels that were too weak to its shape. Because of the many disadvantages associated with the crosslinking of chitosan, it was concluded that chitosan was not a feasible material for general SFF 3-D printing of scaffolds.

4.2.3 Photocrosslinkable Hydrogels

A modified protocol of Dikovsky's was obtained from Seliktar that was used in his lab to create scaffolds for cell culture. It involved the use of PEG-Fibrinogen, PEG-DA, and the photoinitiator Irgacure®2959. Fibrinogen is very expensive so initial testing was conducted using PEG-DA, which has similar functional groups for crosslinking and gelation properties to PEG-Fibrinogen [33]. Once a concentration was found that would be suitable for SFF, characterization tests were performed on the gel using PEG-Fib. A maximum concentration of the photoinitiator of 0.04% was used because any higher of a percentage could interfere with the viability of cells in future scaffolds [33].

A 4% w/v photoinitiator stock solution to be later mixed with a PEG solution was created using Irgacure 2959 and 70% ethanol. A 10% w/v PEG-DA solution was also created from PEG-DA powder in phosphate buffered saline, PBS (pH 7.4). 1% v/v of the photoinitiator stock was then added to the PEG-DA solution by aspiration of the stock into the solution. The final photoinitiator concentration in the solution was 0.04% w/v.

A total of 1mL of the PEG-DA solution and photoinitiator stock were placed in a clear tube with an inner diameter of 10mm on top of a substrate that allowed UV light to enter from only the bottom. Each layer had a height of about 3mm. After the droplets were placed in the tube, the tube was tilted slowly back and forth and the solution was touched every 5 seconds to test for gelation. When the recently deposited layer no longer shifted in the tube while being tilted and there was no residue when the top of the layer was touched, the layer was considered fully gelled.

4.2.4 Thermosensitive Hydrogels

The properties of thermosensitive polymer solutions prior to gelation and its mechanical strength as a gel make these materials ideal for SFF systems. PNIPAAm and PEG-PLGA-PEG were tested to find solution viscosity before gelation to qualify them for use with SFF. A low solution viscosity and short gelation time of less than 1 minute would provide a material that would work with SFF printers. The only trouble with these materials would be the fact that they are reversible. Further modification to their molecular structure by adding additional crosslinking were necessary in order to prevent printed gel from reverting back to a liquid. The molar ratio of NIPAAm:PEG and the final concentration of the polymer in water were varied to find material property trends. The trends were analyzed to find a suitable material for SFF printing. The molar ratios of NIPAAm to PEG tested for viscosity and gelation time were 700:1, 1600:1, and 2000:1. All molar ratios were tried at three different concentrations of the polymer in water, 70%, 80%, and 90%. Three concentrations of PEG-PLGA-PEG material were created, 25%, 35%, and 45% and also tested. The viscosity as well as the rheology properties of these materials were tested and compared to the needs of SFF printers to find a viable material solution.

4.2.5 Rheology

A rheometer and viscometer were used for material testing. A viscometer is similar to a rheometer in that the mechanics are similar but a viscometer is only capable of measuring viscosity. A Brookfield DV-II+Pro Viscometer that is a stand-alone unit was used; it is

not connected to a computer so readings were recorded manually (Figure 4.3). It has a display that presents the viscosity in real time. The advantage to using this viscometer is that the sample is enclosed in a sealed environment during testing.

The solution to gel transition as well as the elastic and viscous modulus of PEG-PLGA-PEG was investigated using a Texas Instrument AR 2000ex rheometer (Figure 4.4). This rheometer was used for some viscosity readings due to its capability to automatically record data as tests are being completed. Due to the fact that the testing surface is exposed to the atmosphere, there was a possibility for evaporation of the material being tested (Figure 4.5). The material was heated from 20°C to 75°C at a rate of 5°C per minute. Parallel plates having a diameter of 40 mm were used with a gap distance of 1 mm. The data was collected under controlled angular frequency (6.283 rad/s), oscillation stress (σ=0.7956 Pa), and strain (γ=0.216). G' is the elastic storage shear modulus; it is a materials tendency to deform elastically. G" is the loss, or viscous, shear modulus; it is due to loss of energy and is directly related to the viscous properties of a material. The temperature at which the storage modulus, G', equals the loss modulus, G", (G'=G") is considered the gel point temperature. At the gel point, the material exhibits visco-elastic behavior. When the storage modulus is less than the loss modulus (G">G'), the material displays more of a viscous, liquid-like behavior while an elastic solid-like behavior is shown when the storage modulus is greater than the loss modulus (G'>G") [115].

4.3 Results and Discussion

4.3.1 Chitosan and Tripolyphosphate

For a material to be suitable for use with SFF printer, it has to be a non-viscous solution to allow for easy transport of the material to the print head. The average viscosity of samples of high and low molecular weight chitosan in an acetic acid solution compared to each other is shown in Figure 4.6. The high molecular weight chitosan solution was found to be a non-Newtonian fluid (Figure 4.7) while the low molecular chitosan solution acted like a Newtonian fluid (Figure 4.8). This behavior of the solution helps to predict how it will act in SFF printers; as a Newtonian fluid, the viscosity is not affected by the shear rate. Newtonian material will not increase viscosity whether it is moving slow or fast along a tube or another material where additional stresses could be incurred. TPP was then added to the chitosan solutions to test for gelation. The addition of TPP resulted in rapid gelation of the chitosan solutions. The gelation occurred only at a 1:1 ratio with the TPP to the chitosan solution. To be able to form a homogenous batch of gel with the use of TPP as a crosslinker, a large and therefore toxic amount would be needed. Such a large quantity of TPP would not allow for the proliferation of cells. A different material with different gelation properties would be needed for the scaffolding. The type of material that requires the use of additional crosslinking material causes the need for specialized gelation techniques that would hinder the construction of 3-D scaffolds.

4.3.2 Photocrosslinkable Hydrogels

The benefit of using photocrosslinkable material is quick gelation of a material with the use of only UV light; no additional crosslinking material is needed. This allows for simplification of printing, using one print head instead of two. The protocol provided by Seliktar for creating scaffolds for cell culture in smooth muscle was used for our testing purposes; the component weights and volumes were also used since smooth muscle is a soft tissue [116]. The protocol concentrations of 9.9% w/v PEG-DA and 0.04% w/v photoinitiator were tested to find readings of below 20 cP for both. The gelation of the hydrogel using PEG-DA occurred, on average, after 10 seconds of 365nm UV light exposure, for all concentrations tested. Droplet size was directly dependent on gelation time. This correlation of droplet size with gelation time was confirmed using PEG-Fib.

For the purpose of accuracy and precision, most SFF printers have a very small gap, smaller than 2mm, between the print nozzles and the substrate unless a complex fiber optic system was integrated into the nozzle array. This allows UV light to only enter from the underside of the printing substrate. Placing a UV flood light beneath the printing substrate showed that as the thickness of layers increases, the gelation time increases exponentially (Figure 4.9). Given that the gelation time would be too high for a thick gel, this type of hydrogel was not viable for our application.

4.3.3 Thermosensitive Hydrogels

Thermosensitive gels, like photocrosslinkable gels, have the advantage of not having to use an additional crosslinking material. PNIPAAm hydrogel was prepared as given by

Vernengo [105] using PEG of molecular numbers: 2000, 4600, 800, and 10,000 g/mol. Molar ratios of NIPAAm monomer units to PEG branches of 700:1, 1600:1 and 2000:1 were used [105]. A direct relationship existed between the viscosity of the initial solution and the consistency of the gel and its capability to hold its shape as a gel (Table 4.1). In order to form a gel that is stiff enough to manage 3-D construction, the initial solution would be too viscous for most SFF printer nozzles to handle. Another type of material that has similar final gel qualities as PNIPAAm but a less viscous material as a solution would work better.

PEG-PLGA-PEG, a thermosensitive triblock, was stated to be a low viscous solution at low temperatures and gel rapidly as temperature is increased [54]. The ability of PEG-PLGA-PEG to become a stiff gel is not directly related to the viscosity of the initial solution like PNIPAAm. To verify that solution viscosity does not linearly relate to gel stiffness, the concentration of PEG-PLGA-PEG polymer in DI water was varied and the viscosity was measured. Lactic acid and glycolic acid were mixed using a molar ratio of 78/22 [54-55, 57] to create a PLGA material of molecular number 1405. A PEG of molecular number 550 was also used. Concentrations of 20%, 30% and 40% triblock to DI water were tested and each mixture's solution viscosities were found to be below 300 cP and gelation was found to happen instantaneously as the solution encountered a warm atmosphere or warm substrate (Table 4.2). The stiffer material that was formed after the temperature was increased was not always classifies as a gel though. A material is considered a gel when it elastic modulus is greater than its viscous modulus. Table 4.2 shows that not all of the concentrations became gels. The 25% concentration of PEG-

PLGA-PEG became stiffer than it was as a solution but not fully a gel. It is possible to alter the properties of PEG-PLGA-PEG with simple changes to the molecular weights of the components and concentration of the polymer in water. It was thus determined that this material had potential with minor alteration to work for our purposes. Modifications such as the gel's mechanical strength and irreversibility were required for full use in our SFF printer.

4.4 Conclusion

For a material to best suit solid freeform fabrication and rapid prototyping, it must: 1) be a low-viscous solution before being printed, 2) involve easily joined on-substrate mixing to form a homogenous gel, 3) have a short solution to gel transition time, 4) be a mechanically strong material to allow vertical building, and 5) be an irreversible gel to prevent deformation of the printed structure. There are no readily available materials that are capable of printing 3-D tissue scaffolds using SFF printers. Gelation techniques, drying time, printer set-up, or final material properties are problems with current materials that prevent their use with most SFF 3-D printers.

Chitosan was originally considered as the scaffold material for 3-D printing due to its biocompatibility and appropriate strength however, it is not suitable for this work because of its non-homogenous gelation. The natural and synthetic materials that were investigated require an additional crosslinking material and need steps like long drying time, freeze/thaw, drying in an oven, and other intensive steps that SFF printers are unable to accommodate. Photoinitiators are somewhat toxic but can still function in

biomaterial in small quantities. Irgacure 2959, one of the least toxic photoinitiator to cells, was found to crosslink PEG-DA as well as PEG-Fib. A hydrogel that is only photocrosslinkable would not work due to one of our printer limitations, that a UV light cannot be shined from a fixed position above due to nozzle positioning,. The thermosensitive material, PNIPAAm, was found to gel as temperature increases. Unfortunately with PNIPAAm, to acquire a gel that was capable of 3-D building, such a high concentration of polymer would be needed that the initial viscosity of the solution would be too high for SFF printing nozzles to handle. PEG-PLGA-PEG triblock polymer mixed with DI water possesses low viscosity as a solution even at high concentrations. It gels rapidly at the corresponding concentration's sol-to-gel temperature and ultimately transitions to liquid like qualities at its gel-to-sol transition temperature. Thermosensitive materials posses the most similar qualities to what is needed for SFF printing. A thermosensitive material that has the ability to hold its shape to allow for 3-D building is the optimum material for a SFF 3-D printer.

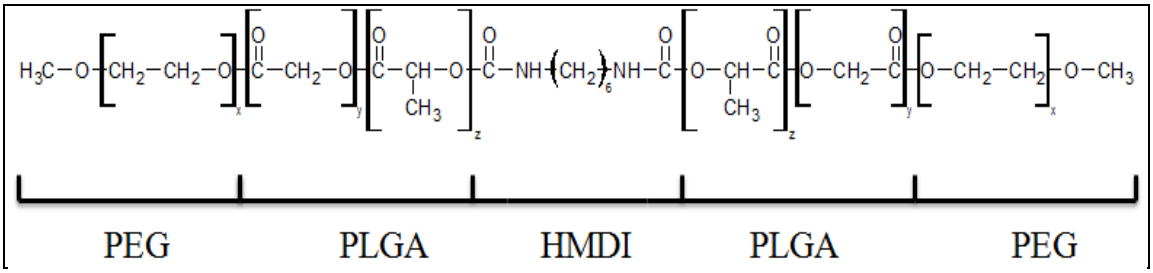

Figure 4.1 - Chemical structure of PEG-PLGA-PEG

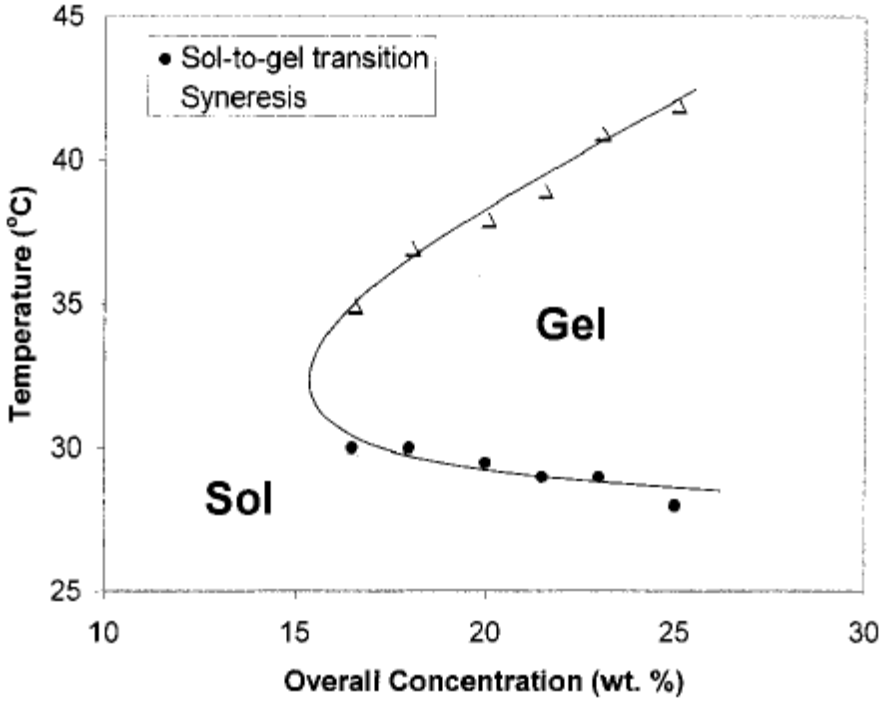

Figure 4.2 - Phase diagram of PEG-PLGA-PEG [58]

- • : sol-to-gel transition

Δ : gel-to-sol transition

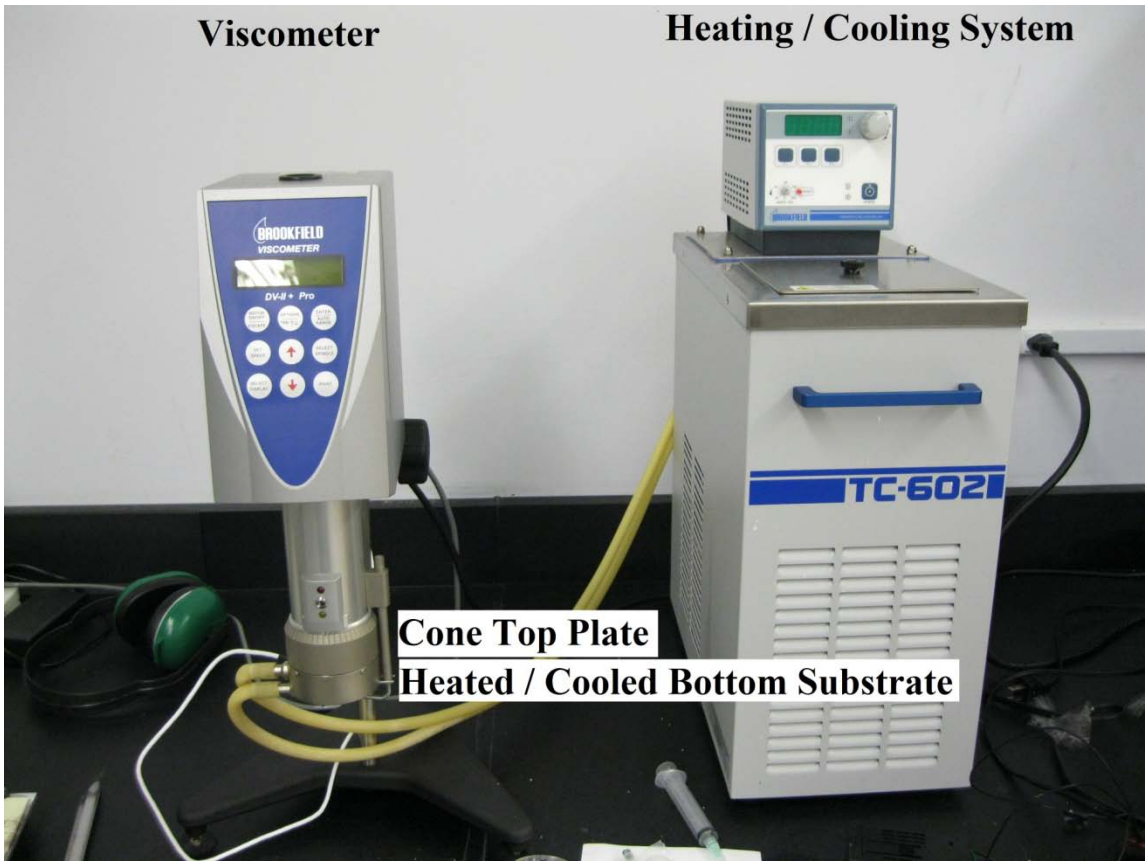

Figure 4.3 - Brookfield DV-II+Pro Viscometer

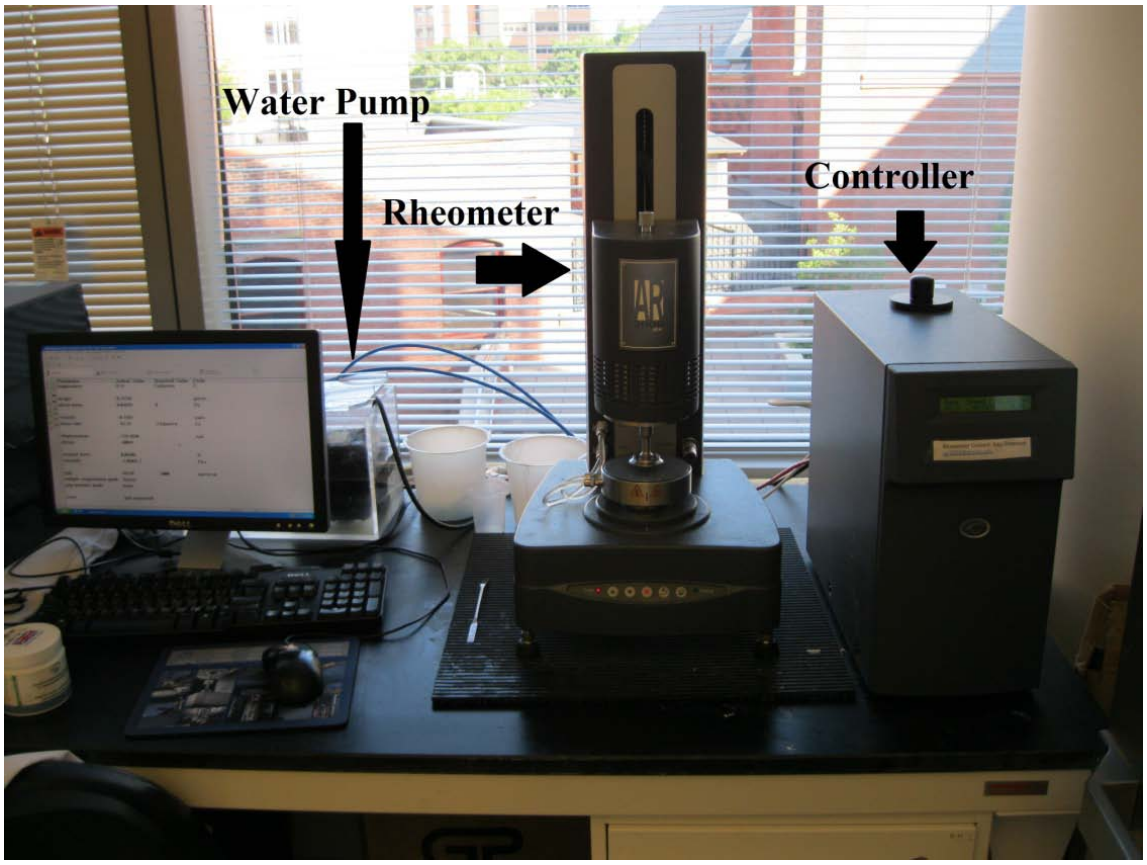

Figure 4.4 - Texas Instrument AR 2000ex Rheometer

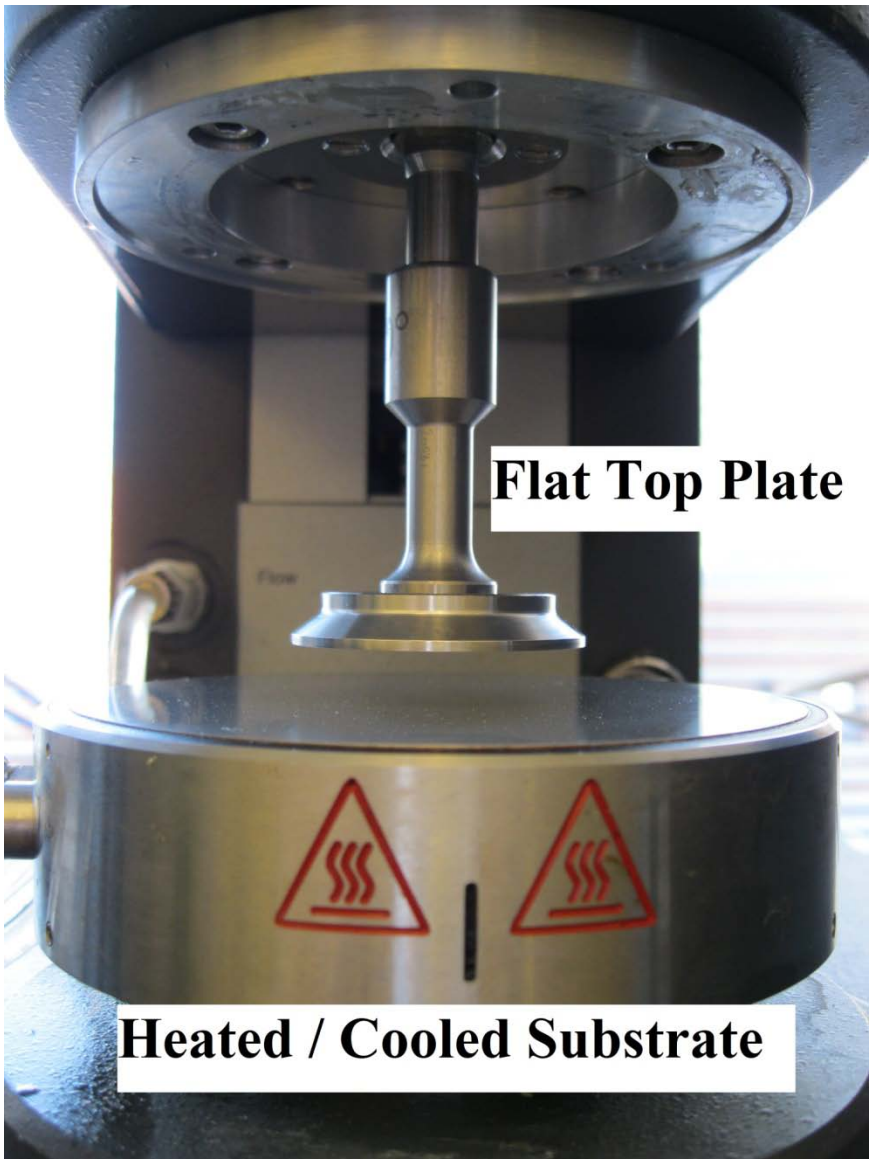

Figure 4.5 - Close-up of Texas Instrument AR 2000ex Rheometer Testing Plate

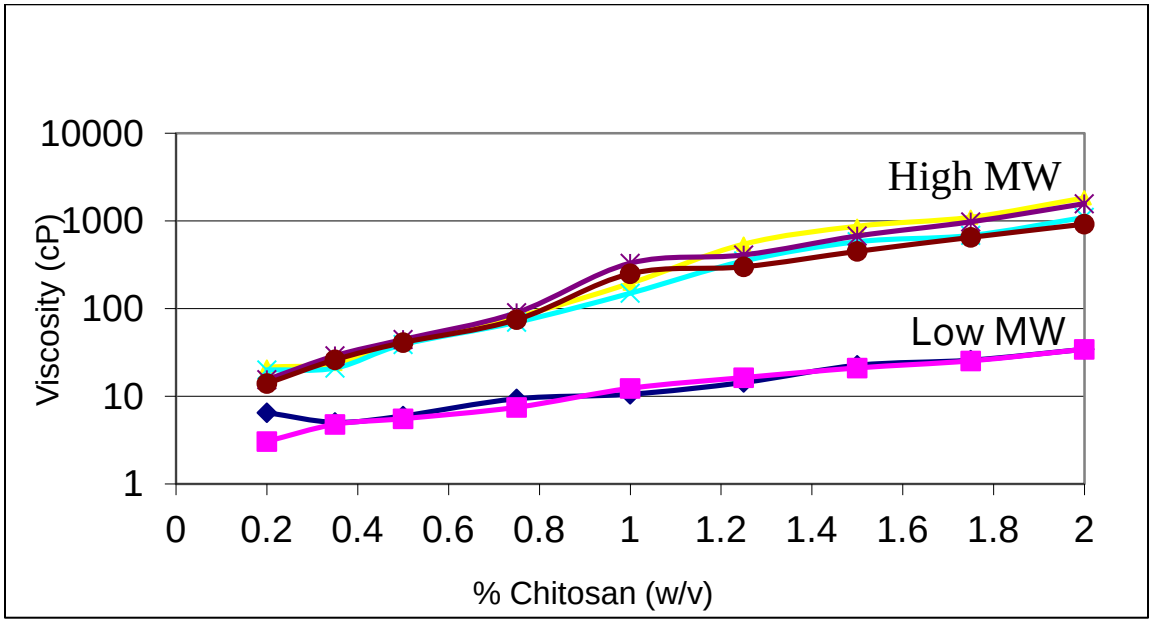

Figure 4.6 - % Chitosan (Low and High Molecular Weight) vs. Viscosity

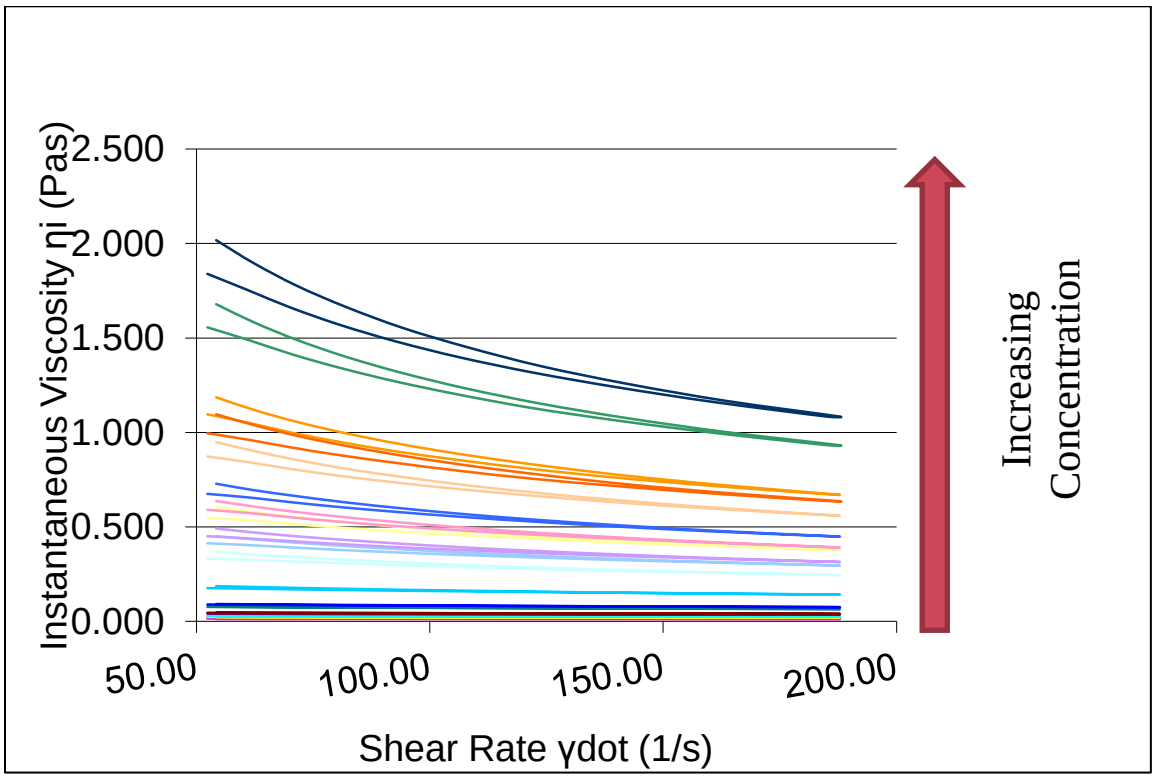

Figure 4.7 - Shear rate vs. instantaneous viscosity of high molecular weight chitosan

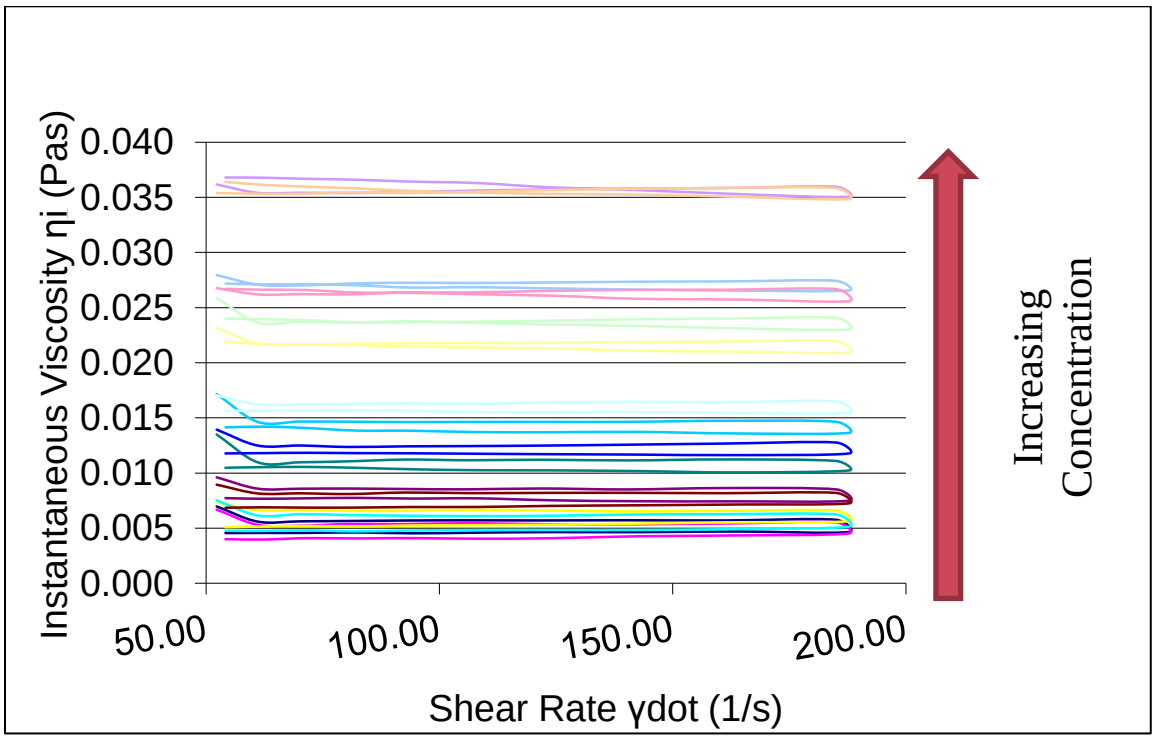

Figure 4.8 - Shear rate vs. instantaneous viscosity of low molecular weight chitosan

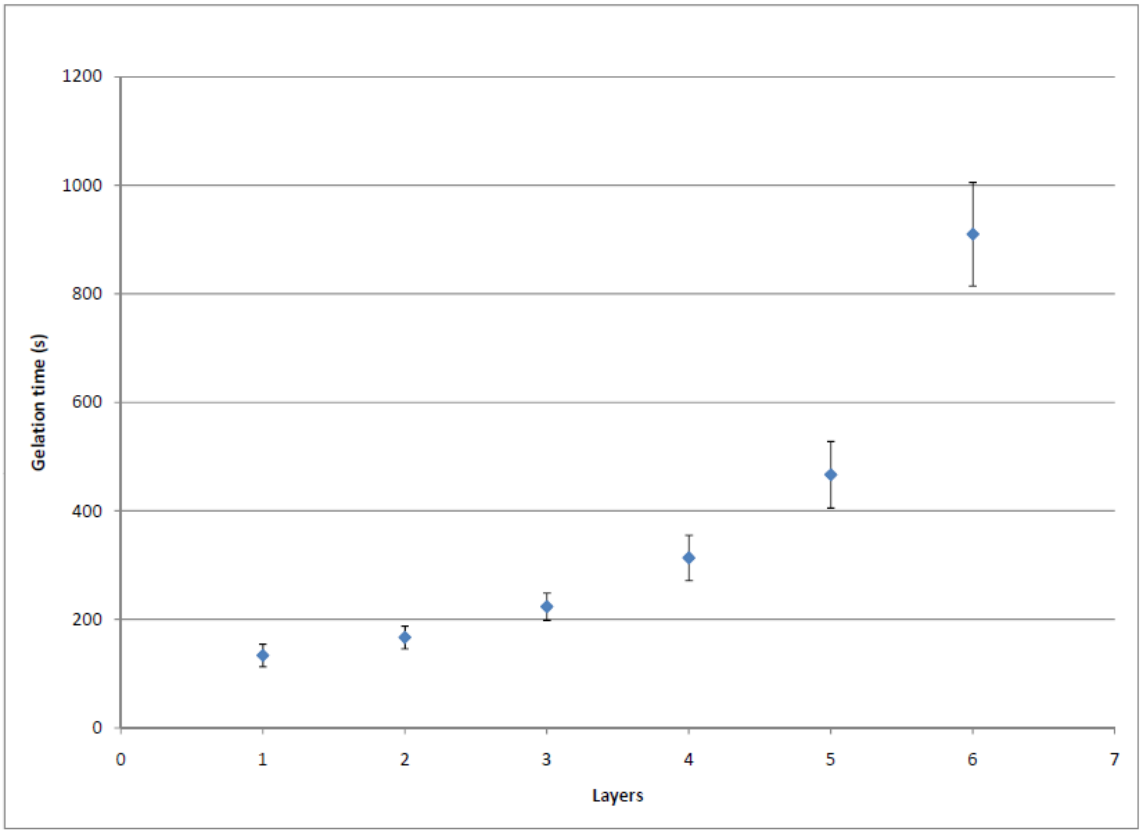

Figure 4.9 - PEG-DA gelation time under UV light

Gelation time increases exponentially with every additional layer when UV light irradiated from below the printing substrate.

Table 4.1 - PNIPAAm gelation characteristics

% DI water: PNIPAAm/PEG	Molar Ratio NIPAAm:PEG	Solution Viscosity (cP)	Ability to Vertically Build
90	700:1	176	No
	1600:1	296	No
	2000:1	421	No
80	700:1	982	No
	1600:1	2245	Yes
	2000:1	3402	Yes
70	700:1	5682	Yes
	1600:1	7005	Yes
	2000:1	8226	Yes

Table 4.2 - Gel characteristics of 550-2810-550 triblock material

Concentration (%)	Solution Viscosity (cP)	Gelation Temperature (°C)	Gel Viscosity (cP)	Max G' (Pa)	Max G" (Pa)	Classified as a Gel (G'>G")?
25	26.97	49.5	494.7	104.75	146.65	No
35	96.85	43.8	1,067	159.6	108.3	Yes
45	212.04	27.8	14,780	179.45	136.85	Yes

As concentration increases, solution viscosity and G' increase while gelation temperature decreases.

G': elastic storage shear modulus

G": loss, or viscous, shear modulus

G'=G": gel point

G">G': liquid-like behavior

G'>G": elastic solid-like behavior

Chapter 5 : Characterize the physical, chemical and thermal properties of the biomaterial

The aim of the work described in this chapter is to further explore the possibility of PEG-PLGA-PEG as a general material for use in SFF 3-D printing of soft tissue scaffolds. The optimal material needs to be able to meet every requirement: Low viscosity as a solution, simple gelation process, short solution to gel time, ability to support additional layers for vertical building, and irreversible gelation. PEG-PLGA-PEG is tested to discover if it can meet every requirement.

5.1 Introduction

To build a 3-D scaffold structure, a material needs to be capable of supporting additional layers on top of it. Any excess DI water after gelation will hinder subsequent layer gelation. The smaller the amount of excess water after gelation, the better the ability of the material to be build vertically. For use in the body to replace soft tissue, a biomaterial that can degrade to allow for growth of cells and transport of nutrients throughout the scaffold must be used. By using a material with DI water-rich hydrogel properties, it should not induce tissue irritation during degradation.

The focus of this work is to characterize the physical, chemical and thermal properties of PEG-PLGA-PEG gels in order to determine the important properties that affect its ability to build 3-D scaffold structures. An understanding of the relationship between change in

certain properties and its resultant mechanical properties will allow this material to be tailored to match various types of soft tissue material.

The synthesis of the polymer, mechanism of gelation, molecular weight of each component, material solution viscosity before gelation, and gel mechanical properties are explained and measured.

5.2 Materials and Methods

5.2.1 Synthesis of PEG-PLGA-PEG Polymer

Polyethylene glycol (PEG) methyl ether (Mn = 550, 750, and 1,000 g/mol) (Sigma–Aldrich), DL-lactide (DLLA) (Aldrich), glycolide (GA) (Aldrich), anhydrous toluene (Sigma), and hexamethylene diisocynate (HMDI) (Sigma) were all used as received. All solvents and other chemicals are of analytical grade.

PEG is typically terminated with hydroxyl groups which can serve as a point of synthetic modification. The free hydroxyl groups of PEG are ring-opening initiators for lactide and glycolide [117]. Lactide and glycolide in the molar ratio of 78/22 were used to create a PLGA material of molecular number 1405. Ring opening polymerization of lactide and glycolide onto monomethoxypoly(ethylene glycol), molecular weight of 550, using stannous octoate (tin(II) 2-ethylhexanoate) (SnOct) as the catalyst was performed to synthesize PEG-PLGA diblock copolymers (Figure 5.1). In ring opening polymerization, the terminal end of the of a polymer, the hydroxyl end group (-OH) of the PEG, acts as a

reactor and breaks apart a cyclic monomer, Glycolide and DLLA, to form a large polymer chain. The polymer chain that is formed is the diblock polymer PEG-PLGA . Anhydrous toluene was added as a solvent in the reaction. The materials were mixed in a covered, but not sealed, ball flask at 130°C in an oil bath for 24 hours. Ester bonds form in the reaction between PLGA and PEG while the byproduct of H_2O was evaporated off during the reaction. The copolymer was then coupled by adding HMDI and was mixed in an oil bath at 60°C for 12 hours (Figure 5.2). The final product was two PEG-PLGA diblocks coupled in the middle with HMDI to form a PEG-PLGA-HMDI-PLGA-PEG polymer chain. Because the HMDI coupler of the two PLGA chains is somewhat insignificant compared to the high molecular weight PLGA and PEG, the product is considered a triblock copolymer, PEG-PLGA-PEG with a large PLGA chain between two PEG components. HMDI was added in a 0.5 molar equivalence to the mass of the PEG. A reflux was then performed at 110°C , the boiling temperature of toluene, for 12 hours. Afterward, the material was precipitated in cold diethyl ether, dissolved in dichloromethane (DCM), and then re-precipitated in cold diethyl ether to remove any impurities. Finally, the PEG-PLGA-PEG triblock copolymer was placed in a vacuum oven overnight to remove any residual solvents. The material was then stored at -20°C to prevent any degradation of the PLGA.

Additional steps involving rotoevaporation were added later to help guarantee the absence of unwanted solvents, including toluene, diethyl ether, and dichloromethane. Rotoevaporating, or rotary evaporator, entails using a device to efficiently and gently remove solvents from samples by evaporation. The sample is places in a ball flask and

rotated while in a hot bath of water or oil. The contents are put under vacuum to help assist in quickly evaporating any excess solvents. The rotary motion allows for more surface area for solvents to evaporate quicker. These two additional rotoevaporation steps were added after the reflux and after the copolymer was re-precipitated in dichloromethane. The rotoevaporation was conducted at 80°C and under vacuum.

To prepare the triblock copolymer for printing, DI water was added and the solution was stirred at 4°C for 24 hours with constant inspection to ensure homogeneity. The product was then characterized by spectroscopy and rheology to determine its molecular composition, viscosity, and elastic and viscous moduli.

5.2.2 Molecular Weight of PEG

In order to determine the proper type of PEG to use in this work, viscosity tests were performed on different molecular weight of PEG methyl ether. The molecular weight of the PEG used was varied to determine how it would affect the viscosity of the material before gelation. Using a molar ratio of 78:22 for DLLA to GA and a projected molecular weight of 2810 for the PLGA, molecular weights of 550, 750, and 1000 were used for the PEG.

5.2.3 Molecular Weight of PLGA

The molecular weight of the PLGA was varied as well to verify if it would affect the viscosity and the material properties. PEG methyl ether (550) and a molar ratio of 78:22

for DLLA to GA was used along with PLGA of molecular weights: 1000, 2810, and 5000.

5.2.4 Spectroscopy

A Varian 500 MHz super-conducting FT-NMR spectrometer was used for H-NMR, Hydroge - Nuclear Magnetic Resonance, to determine the composition of the triblock copolymer.

5.2.5 Rheology

5.2.5.1 Viscosity

The viscosities of PEG-PLGA-PEG aqueous solutions were measured as a function of temperature using a Brookfield DV-II+Pro Viscometer. The material was heated from 20°C to 75°C at a rate of 5°C per minute. A cone/plate set-up was used with a cone angle of 0.8° and gap distance of 0.013 mm.

5.2.5.2 Dynamic Mechanical Analysis

The solution to gel transition of PEG-PLGA-PEG was investigated using a Texas Instrument AR 2000ex rheometer. The material was heated from 20°C to 75°C at a rate of 5°C per minute. Parallel plates having a diameter of 40 mm were used with a gap distance of 1 mm. The data was collected under controlled angular frequency (6.283 rad/s), oscillation stress (σ=0.7956 Pa), and strain (γ=0.216).

5.3 Results & Discussion

5.3.1 Material Gelation

Poly(ethylene glycol-b-(DL-lactic acid-co-glycolic acid)-b-ethylene glycol), PEG-PLGA-PEG, is a polymer made up of hydrophobic and hydrophilic blocks. PLGA is hydrophobic while PEG is hydrophilic (Figure 5.2). In an aqueous solution, PEG-PLGA-PEG is a free-flowing solution at room temperature and becomes a gel as temperature is increased to around body temperature, 37°C. The polymer forms a micellar structure around body temperature with PLGA as its core and PEG as the corona [54]. A chemical structure representation of PEG-PLGA-PEG in shown in Figure 5.3 and a schematic of micelle formation is shown in Figure 5.4. The micellar diameter can be as big as nine nanometers [58]. As temperature increases, the sizes of the micelles grow. Above a critical gel concentration, micelles pack together to occupy the entire volume, resulting in gel formation (Figure 5.5). Because of this, formed gel is subject to dissolution upon dilution. When diluted, the interaction forces between packed micelles are not strong enough to stay tightly packed together and result in dissociation [54]. With temperature continuing to increase, the miscibility between the two blocks increase even in the gel phase, leading to unusual turbidity changes and an eventual phase transition back to liquid. At elevated temperatures above body temperature, PEG becomes more hydrophobic resulting in phase mixing with PLGA. PEG segments interact with the PLGA core, forming an intermixed phase between core and shell of the micelle and the material reverts back to a liquid form [54].

5.3.2 Molecular Weight of PEG

The viscosity of the triblock using PEG molecular weights of 550, 750, and 1000 were used and as expected, the viscosity increased as the molecular weight of the PEG was increased (Table 5.1). The lower the solution viscosity of a material, the greater the number of printers that can use it. To expand the use of our material for multiple printers, a PEG of molecular weight 550 was used in all further tests.

5.3.3 Molecular Weight of PLGA

The PEG-PLGA-PEG copolymer with a PLGA molecular weight of 1000 was mixed with water at concentrations of 25, 35, and 45% and none of the samples changed viscosity. The copolymer can dissolve in water after numerous hours of mixing but upon increase in temperature, the material does not gel (Table 5.2). Hydrophobic interactions are what drive micelle formation and aggregation so a copolymer with a low molecular weight PLGA block is not hydrophobic enough to form micelles and so cannot form a gel. A copolymer with a corresponding PLGA molecular weight of 5000 is not capable of fully dissolving in water. The increased molecular weight of PLGA creates a copolymer that is too hydrophobic and is insoluble in water. To continue with our tests, a PLGA made to a molecular weight of 2810 was used.

5.3.4 Spectroscopy

5.3.4.1 Purification of PEG-PLGA-PEG

Original H-NMR scans of the final PEG-PLGA-PEG material show additional additives in the final material. It was found that dichloromethane (DCM), diethyl ether, and toluene were still present after the material was placed in the vacuum oven overnight before being prepared (Figure 5.6). To help rid the final polymer of any excess materials, additional steps of rotoevaporating was added after reflux and after purification in DCM and diethyl ether (Figure 5.7). The purity of the product was confirmed by H-NMR; there are no trace amounts of toluene, DCM or diethyl ether in the final product (Figure 5.5 and 5.6).

5.3.4.2 Gel pH

The human body can only handle material with a pH between 7 and 8 [118]. The addition of the rotoevaporate procedures also assisted in optimizing the final pH of the material. Prior to the addition of the rotoevaporate steps, the pH of the final material ranged from 2 to 4. To increase the pH of a non-rotoevaporated material, 1M and 5M sodium hydroxide (NaOH) solutions were made to attempt to increase the pH of the solution to an acceptable level. An average of 3.24 mL of 1M NaOH material or 871µL of 5M NaOH material was needed to increase the pH of a non- rotoevaporated material of 25% concentration to an acceptable level. Adding the NaOH solutions while stirring and allowing time for the pH to settle before adding more material created a non-homogenous material with lumps of material in the solution.

By adding rotoevaporate steps, it eliminated the need to add NaOH solution to correct for low pH. Following the purification steps according to the new protocol involving rotoevaporation, the pH of the material reached, on average, a value of 7.

5.3.4.3 Polymer Verification

Figure 5.6 shows the H-NMR spectra of a PEG-PLGA-PEG copolymer with corresponding molecular weights of 550-2810-550 (a) and 550-5000-550 (b). According to general NMR reference standards, the peaks at 5.20 ppm correlate to the CH bonds of the DLLA, 4.80ppm to CH_2 of GA, 3.65 ppm to CH_2 of PEG, 3.38 ppm to CH_3 of methyl ether end groups of PEG, and 1.55 ppm to CH_3 of DLLA (Figure 5.8) [57]. The peaks that include bonds that are present in PLGA, including DLLA and GA, are larger in the 550-5000-550 material than in the 550-2810-550 material. Balancing of the two samples to account for intensity of the readings and integration of the DLLA peaks confirm a ratio similar to the molecular weights for PLGA, 2810:5000 and 7.99:14.58. DLLA is only a component of PLGA so a comparison of the total amount of CH bonds found in DLLA is a direct comparison to the molecular weight ratio. H-NMR verified that the final products were made up of only the materials we wanted and the molecular weights were exactly what we wanted.

5.3.5 Rheology

5.3.5.1 Viscosity

The results show that as the concentration of 550-2810-550 PEG-PLGA-PEG increases, the solution minimum viscosity decreases, material maximum viscosity increases, and the temperature where maximum viscosity occurs decreases (Table 5.3). A 25% concentration of 550-2810-550 had a viscosity of 2.825cP around 20°C and increased dramatically to 423cP at 42 °C (Figure 5.9). The viscosity then decreased and leveled off at a higher viscosity than what it started at as a liquid. The same general trend is observed with 35% concentration of material except it possesses a starting solution viscosity of 8.908cP around 20°C and a maximum viscosity of 8,299cP at 33.7°C (Figure 5.10). The 45% concentration of material has a solution minimum viscosity of 141cP and maximum viscosity of 15,829.5cP at a temperature of 24.5°C. The viscosity of the 45% concentration, though, remains high during the 10 degree increase in temperature after initial sol-to-gel transition and then finally decreases before leveling off at a steady viscosity (Figure 5.11).

The reason for the sharp increase in viscosity at the sol-to-gel transition temperature is because the micelles have reached their maximum size. If temperature continues to increase, with the micelles at their maximum size, the PEG begins to becomes hydrophobic and the micelles break apart quickly. As the temperature continues to increase, the micelles break apart and the material returns to a lower viscosity, higher than the original viscosity though due to water evaporation.

When comparing the 25%, 35%, and 45% concentrations of material, it is simple to see that the 25% has the lowest initial viscosity and forms tightly packed micelles at the highest temperature (Figure 5.12). The 45% concentration of material forms micelles at the lowest temperature and becomes the most viscous. For a printer to use this type of material, it would be best to keep the temperature of nozzles and material reservoirs at 20°C and then increase the temperature of the printing substrate to the corresponding maximum viscosity temperature.

5.3.5.2 Dynamic Mechanical Analysis

Using the oscillation program of the rheometer allows a material's elastic and viscous modulus to be found as a function of temperature. For the 25% concentration, the maximum elastic and viscous moduli both reach close to their maximum at a temperature close to their maximum viscosity reading (Figure 5.13). Unlike the 25% concentration, the 35% concentration of material reaches it elastic and viscous maximum after their maximum viscosity temperature (Figure 5.14). Both the 25% and 35% materials have such high percentages of water that the material does not form a gel at maximum micelle concentration and viscosity. The elastic modulus does not become greater than the viscous modulus until a higher temperature. This is due to the evaporation of water in the material. The elastic modulus corresponds directly to the gelation of a material. The maximum point of the elastic modulus shows the temperature at which a material is at its most stiff point. The 45% concentration of material becomes gel while the material is at

its greatest viscosity. At this point, G' is greater than G" starting at 40°C signifying characteristics of a gel (Figure 5.15). As the temperature increases, the water in the material continues to evaporate and becomes a gel for a short amount of time before breaking apart and returning to a liquid.

The reason for only the 45% material sharing its maximum viscosity temperature and gelation temperature is because at this concentration, there is only enough water needed for micelle formation and gelation. The 25% and 35% concentrations have excess water that only hinder formation of a stiff gel, helping to decrease viscosity during maximum micelle formation. Interestingly, all concentrations of PEG-PLGA-PEG have similar elastic and viscous modulus near a temperature of 50°C (Figure 5.16). As the excess water is evaporated from the lower concentrations, all of the materials become similar. As temperature continues to increase, the differences in polymer concentration affect the elastic and viscous properties. The elastic modulus of each material is compared to the temperature that it is reached at in Table 5.4. An optimum material would have the greatest elastic modulus at the lowest temperature. This requires less heating and allows for less time for water in the solution to evaporate.

5.4 Conclusions

To create a material that posses a high viscosity after reaching its sol-to-gel transition temperature that allows for vertical building, the concentrations and molecular weights of polymer as well as the pH of PEG-PLGA-PEG were altered. 25% and 35%

concentrations of PEG-PLGA-PEG polymer in water form micelles and become increasingly viscous as temperature increases. But they do not form a gel at the maximum micelle formation temperature, they form gels as temperature continues to increase and excess water evaporates. A 45% concentration becomes more viscous and possesses higher elastic and viscous modulus than the 25% and 35% material closer to its most viscous point (Table 5.4). The 45% concentration is the only material that technically gels while it is at its most viscous stage. It stays close to its most viscous point from 22°C to 32°C and reaches its maximum elastic modulus around 31°C.

The optimal concentration of triblock copolymer to use for a printer would be a 45% concentration because it has the highest possible viscosity of the three tested concentrations, 15,830cP. It also forms a gel when it is at its most viscous stage, G'= 179.45>G"=136.85. But, even at a viscosity of just about 10,000cP, which is similar to chocolate syrup, it is unable to build 3-D structures. This assessment was made after trying to layer droplets on top of each other and not being successful; after a droplet was placed on a heated substrate and allowed to transition from liquid to gel for 30 seconds, another droplet was placed on top and proceeded to combine with the previous droplet, expanding the contact area on the substrate, but not building vertically. A material that encompasses the qualities of a non-viscous solution, the irreversible mechanically strong properties of a photocrosslinkable material, and the rapid gelation of a thermosensitive material is needed for use in SFF printers.

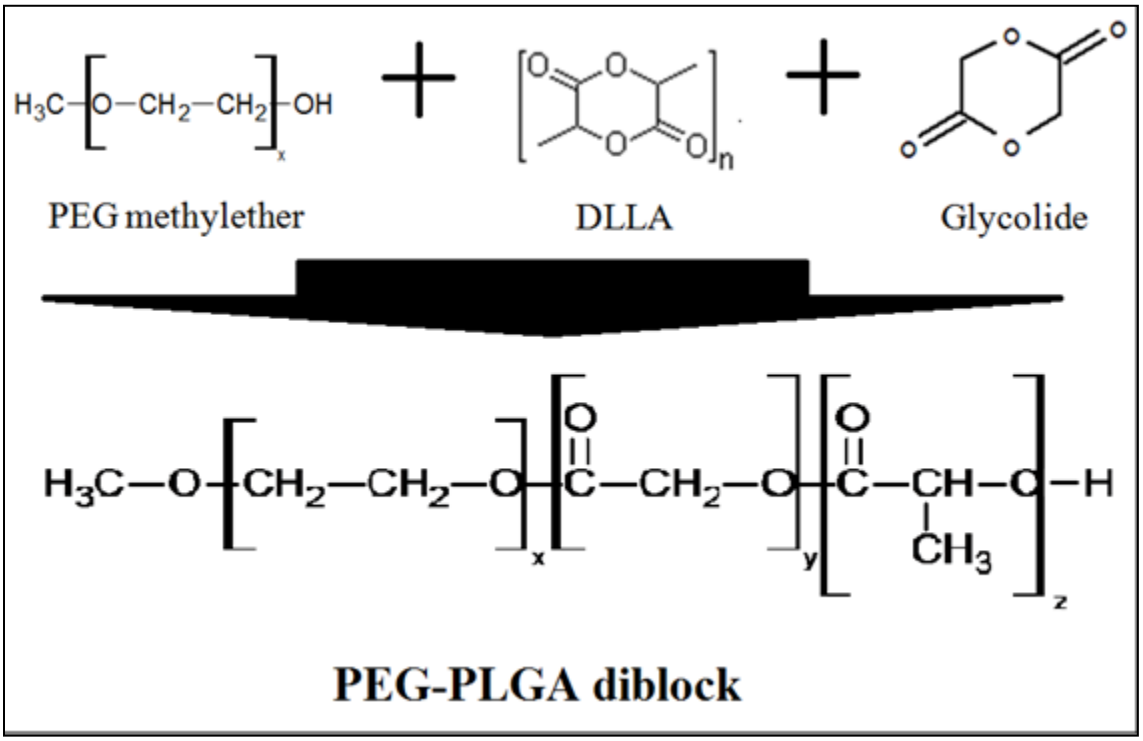

Figure 5.1 - Ring opening polymerization of glycolide and DLLA to form PEG-PLGA diblock

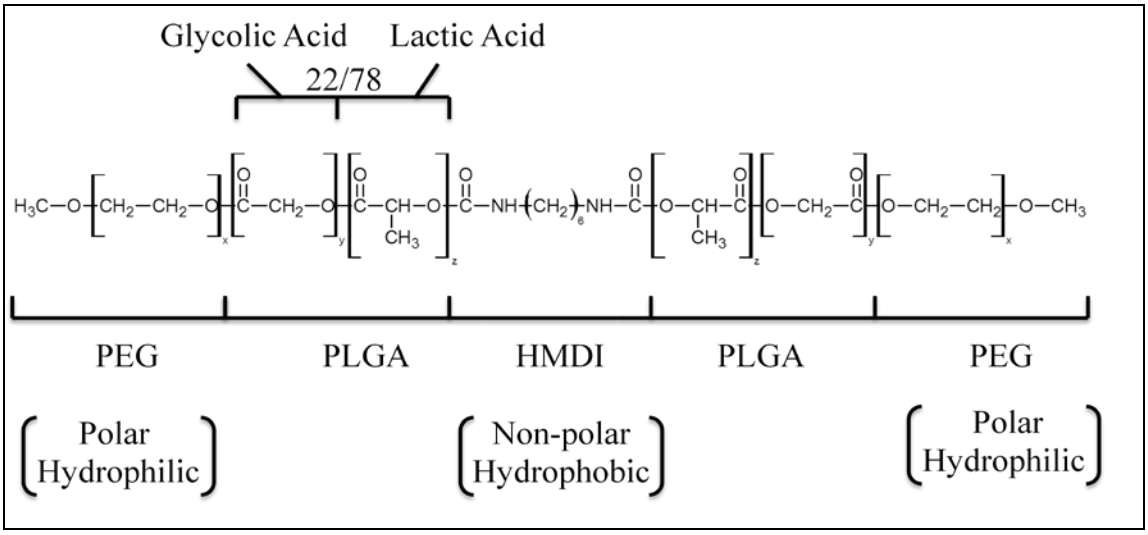

Figure 5.2 - Chemical Structure and polarity of PEG-PLGA-PEG

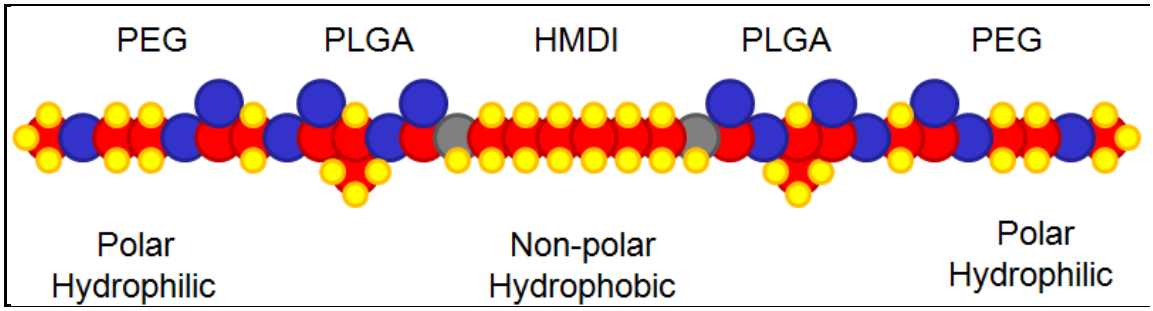

Figure 5.3 - Chemical structure representation of PEG-PLGA-PEG

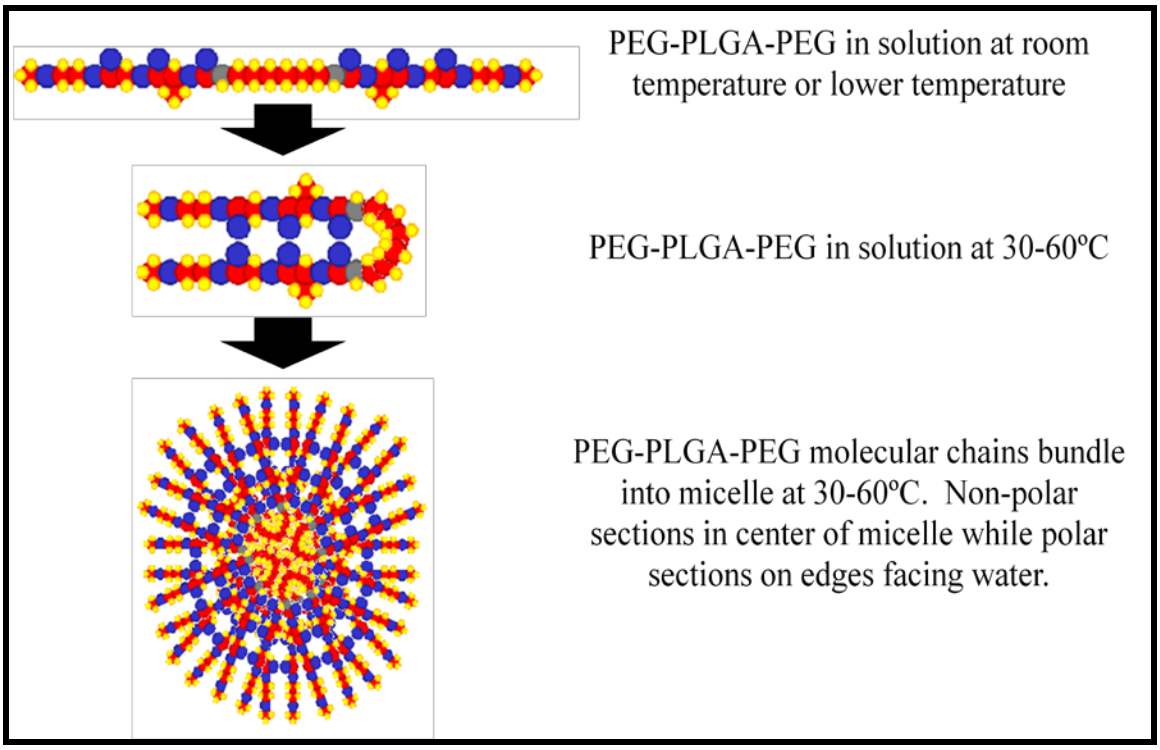

Figure 5.4 - PEG-PLGA-PEG formation of a micelle

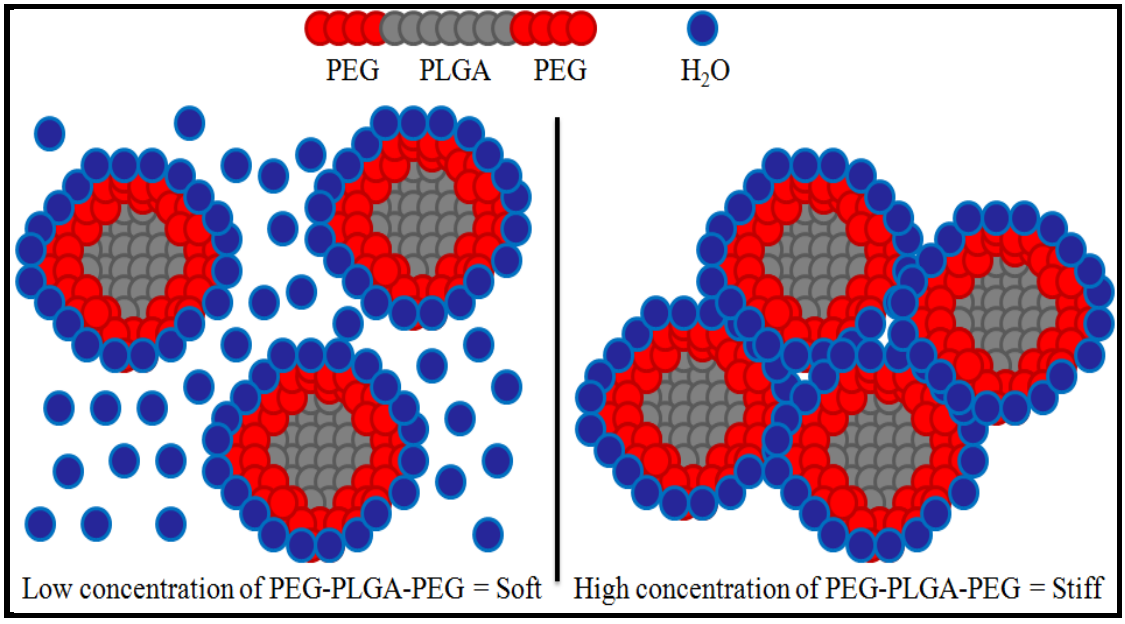

Figure 5.5 - Micelle properties due to PEG-PLGA-PEG concentration

Table 5.1 - Effect of PEG molecular weight on viscosity

PEG MW	Polymer Consistency	Viscosity @ 25 °C (cP)	
		25%	35%
550	Liquid	25.5	96.85
750	Liquid	121.1	229.7
1000	Powder	300.4	Does not dissolve

Table 5.2 - Effect of PLGA molecular weight on viscosity

PLGA MW	35 % PEG-PLGA-PEG viscosity (cP)	
	@ 25 °C	@ 37 °C
1000	38.46	40.02
2810	96.85	1,067
5000	Nonhomogenous material	Nonhomogenous material

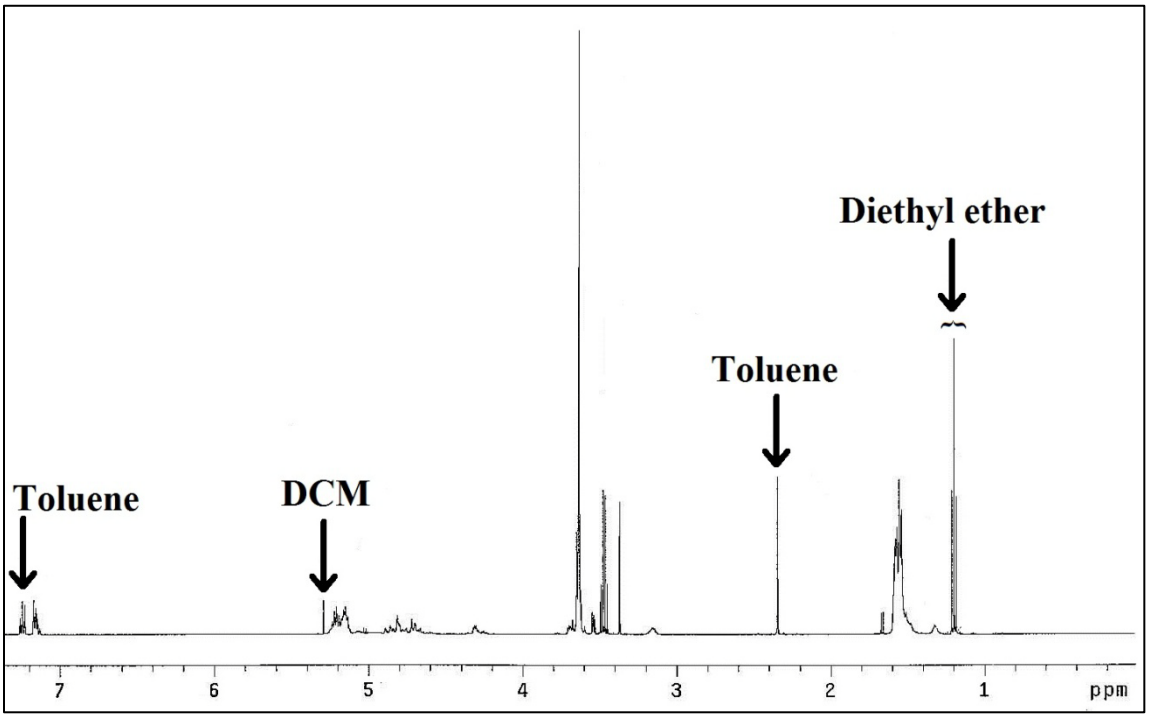

Figure 5.6 - NMR showing residual DCM, toluene, and diethyl ether

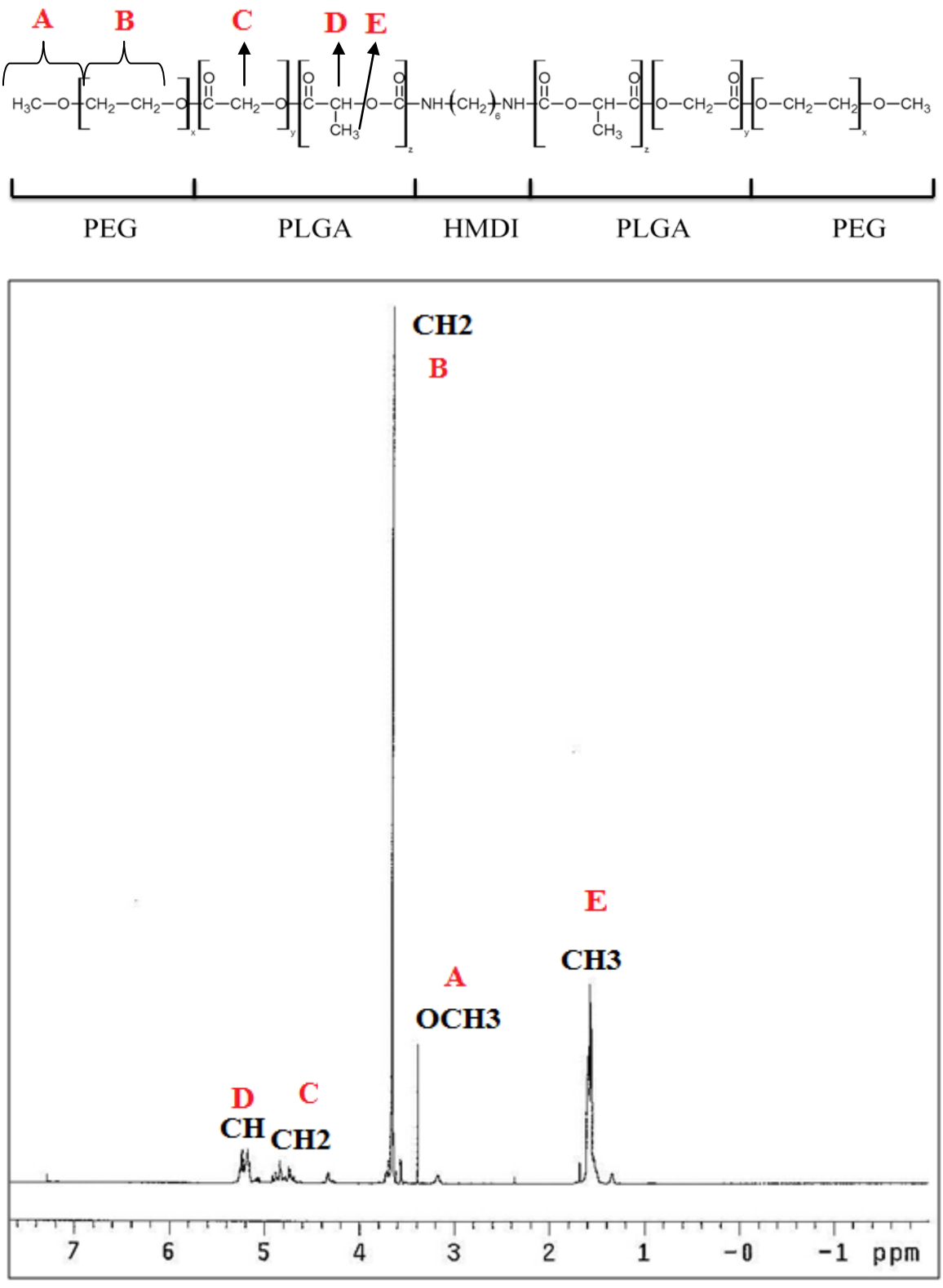

Figure 5.7 - NMR of 550-2810-550 triblock material with corresponding example types of bonds with no extra residual material

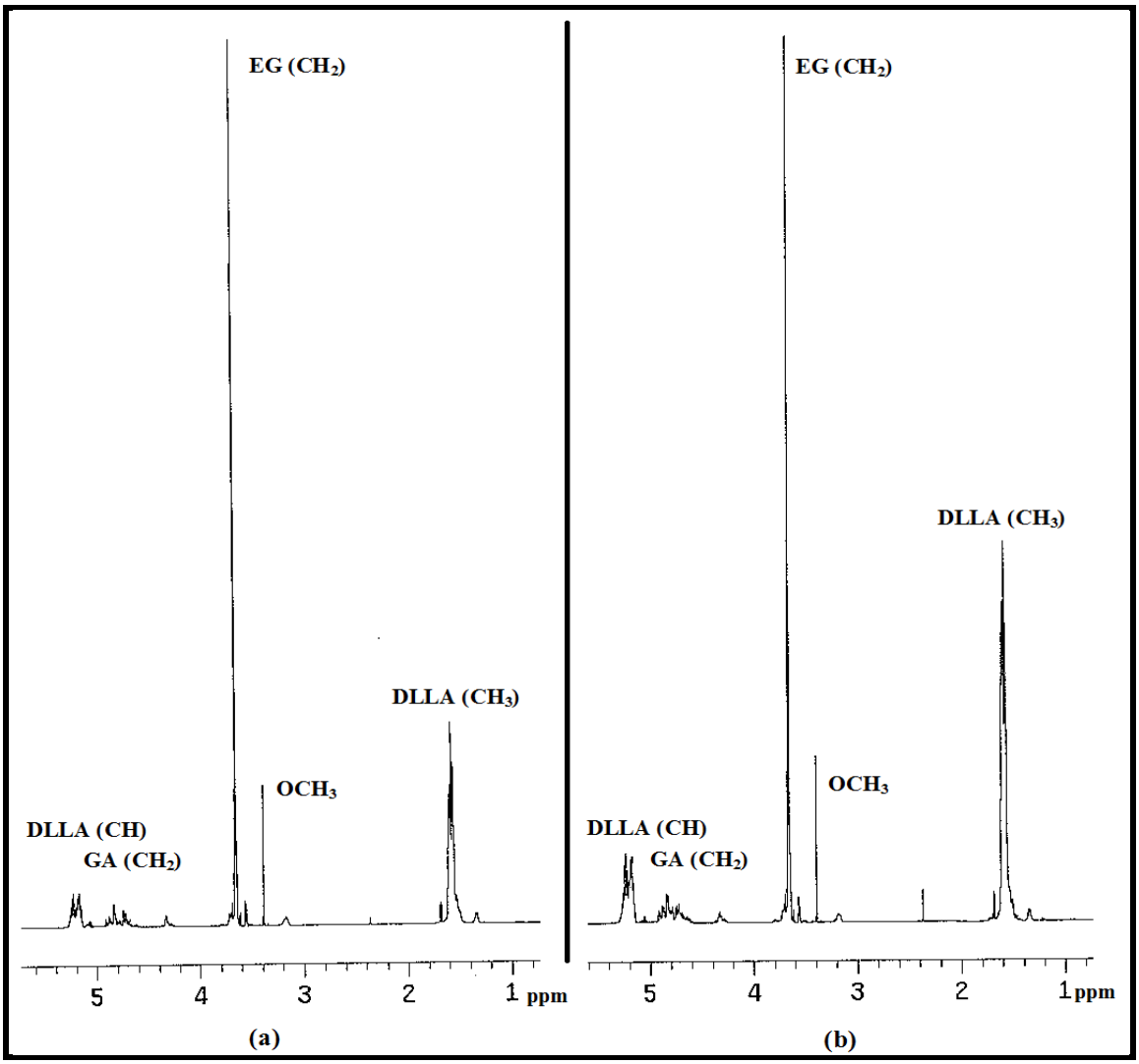

Figure 5.8 - H-NMR spectra of PEG-PLGA-PEG triblock copolymers in CDCl3. The molecular weight of PLGA is 2810 (a) and 5000 (b)

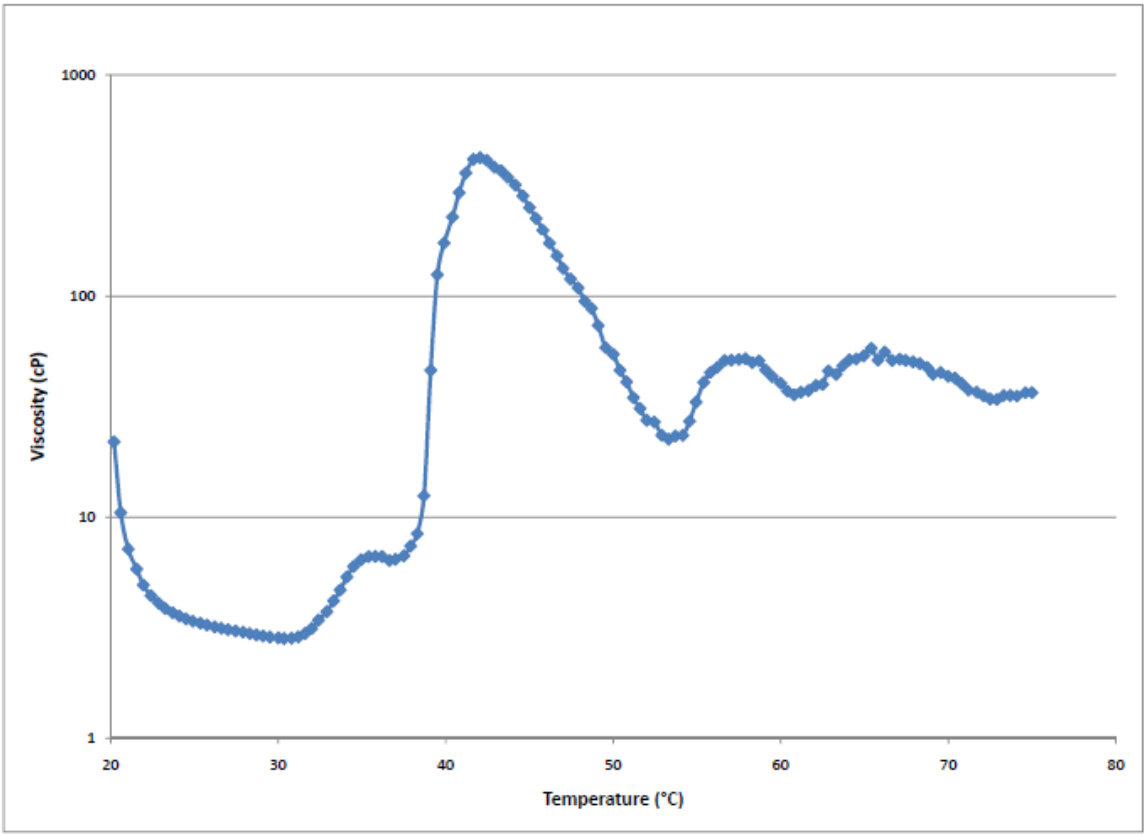

Figure 5.9 - Viscosity of 25% 550-2810-550 triblock material

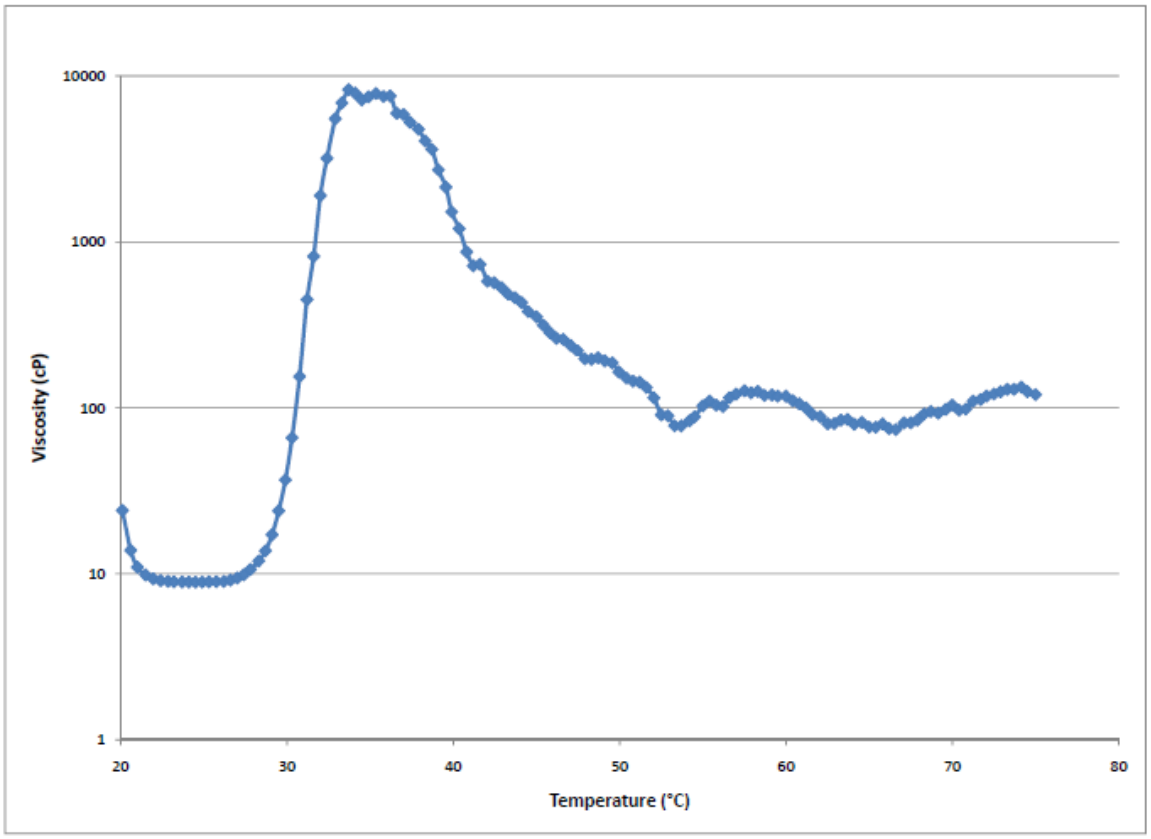

Figure 5.10 - Viscosity of 35% 550-2810-550 triblock material

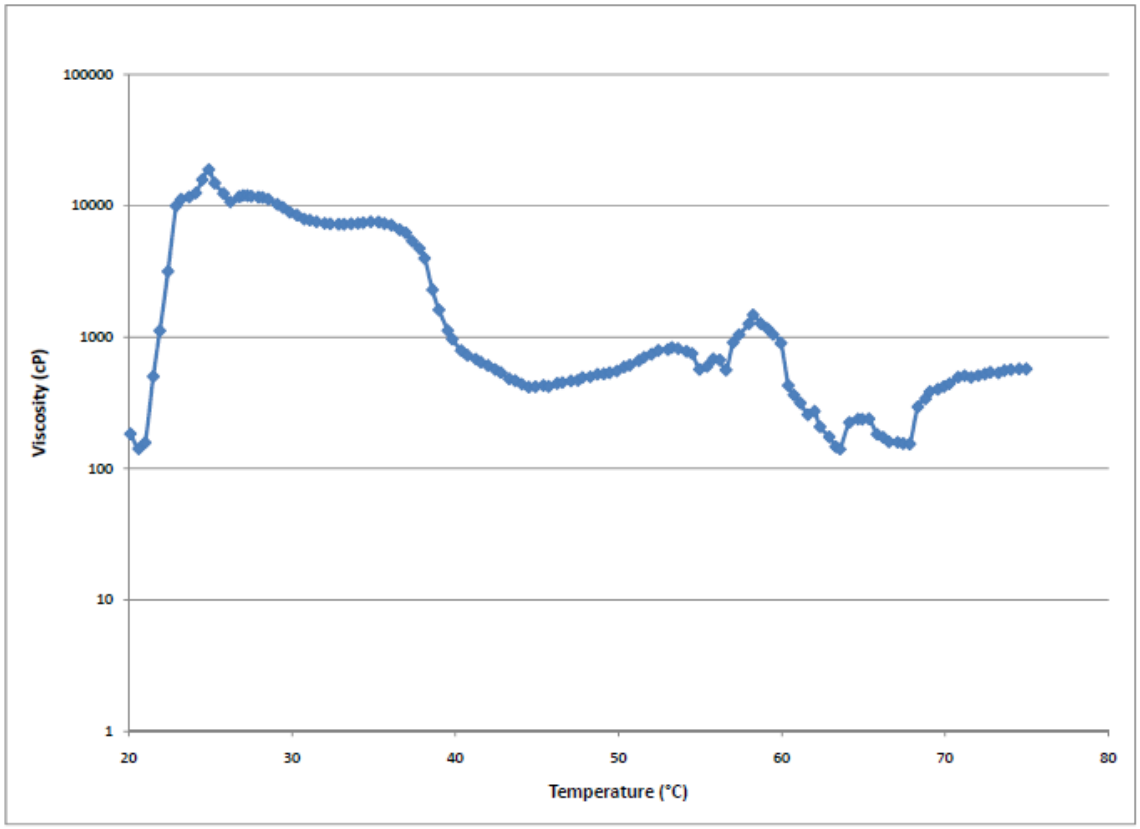

Figure 5.11 - Viscosity of 45% 550-2810-550 triblock material

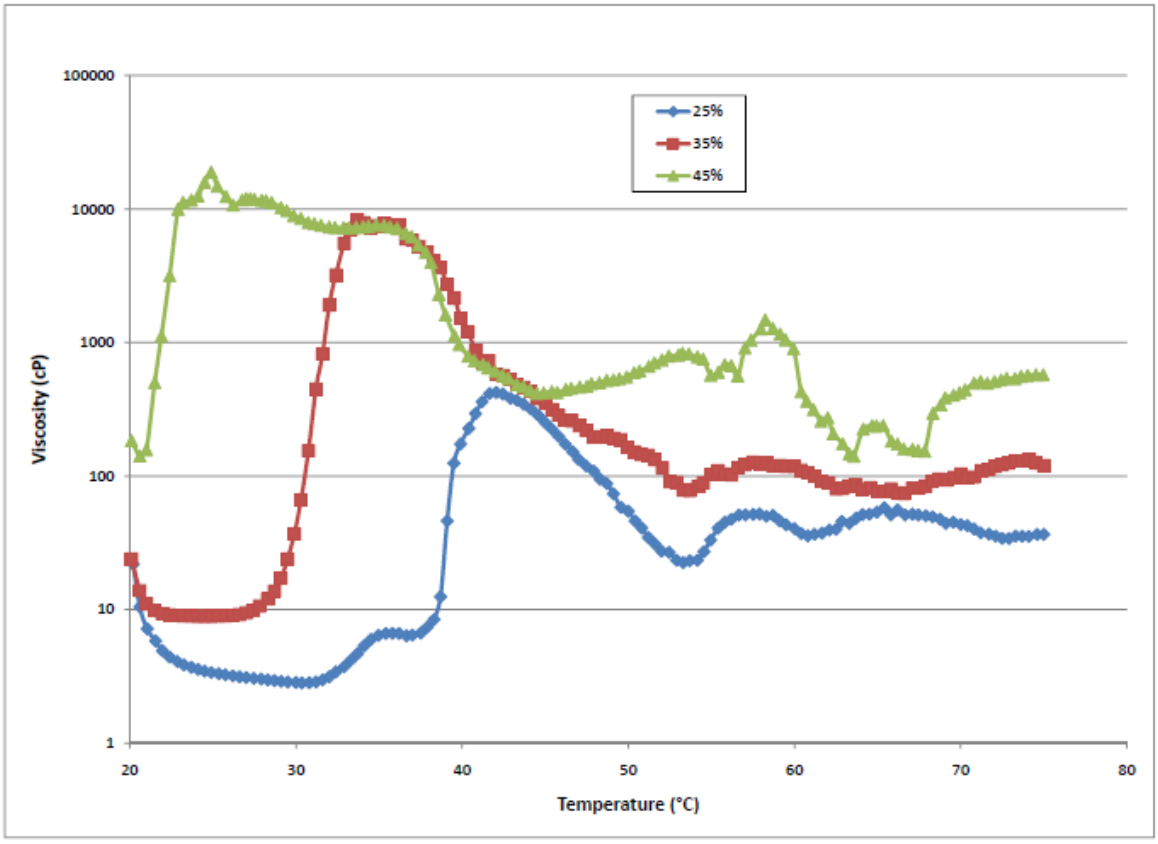

Figure 5.12 – Comparison of viscosity of 25%, 35%^, and 45% 550-2810-550 triblock material

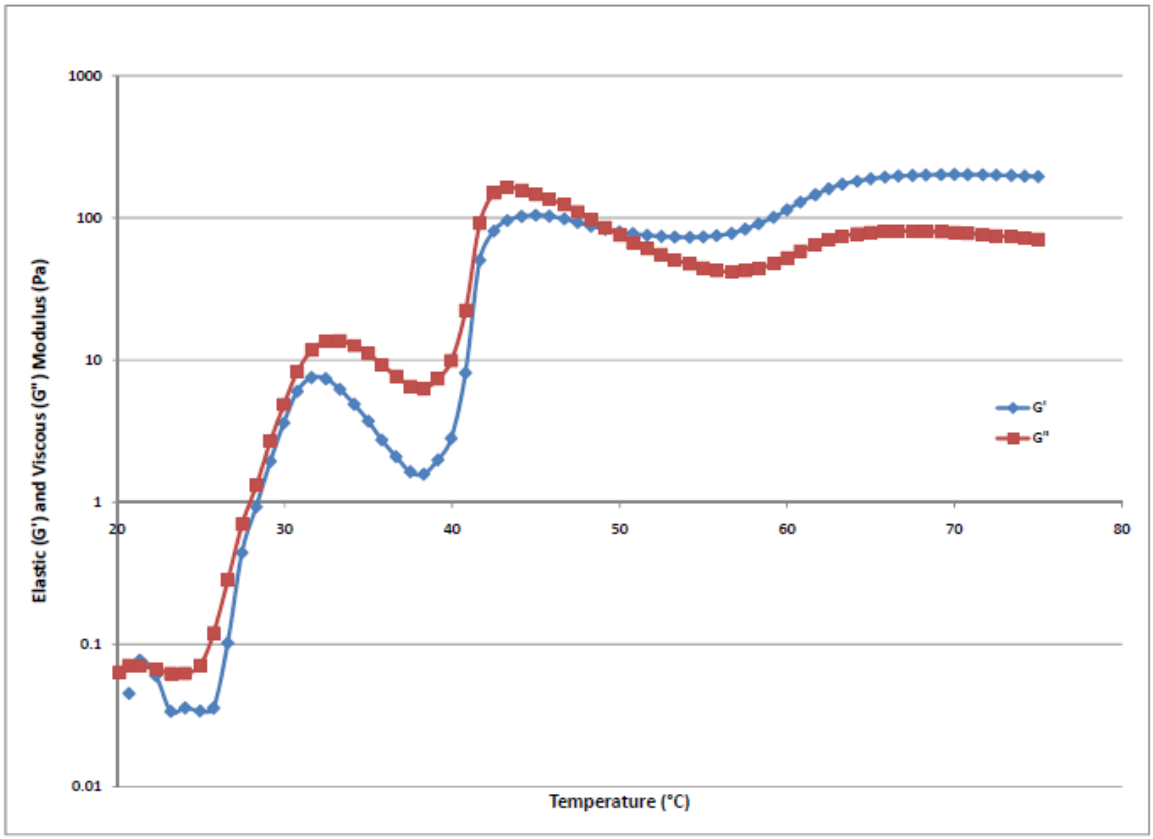

Figure 5.13 - Elastic and viscous modulus of 25% 550-2810-550 triblock material

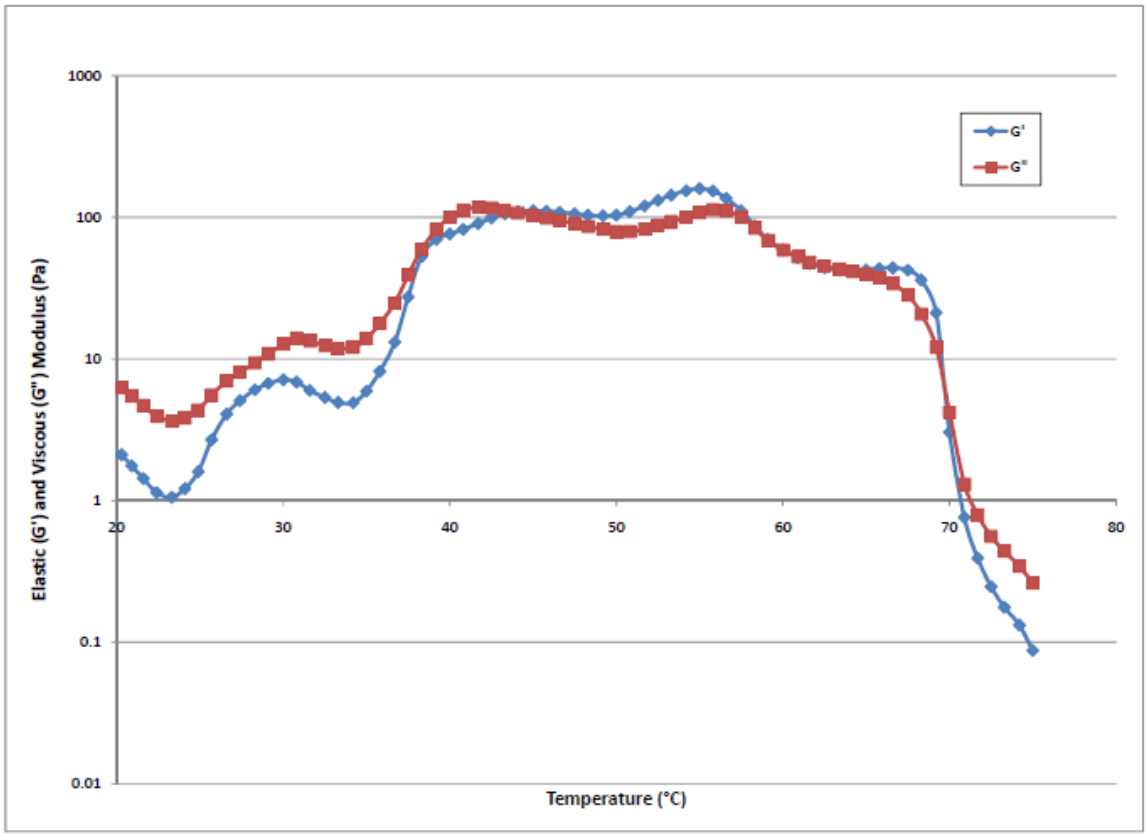

Figure 5.14 - Elastic and viscous modulus of 35% 550-2810-550 triblock material

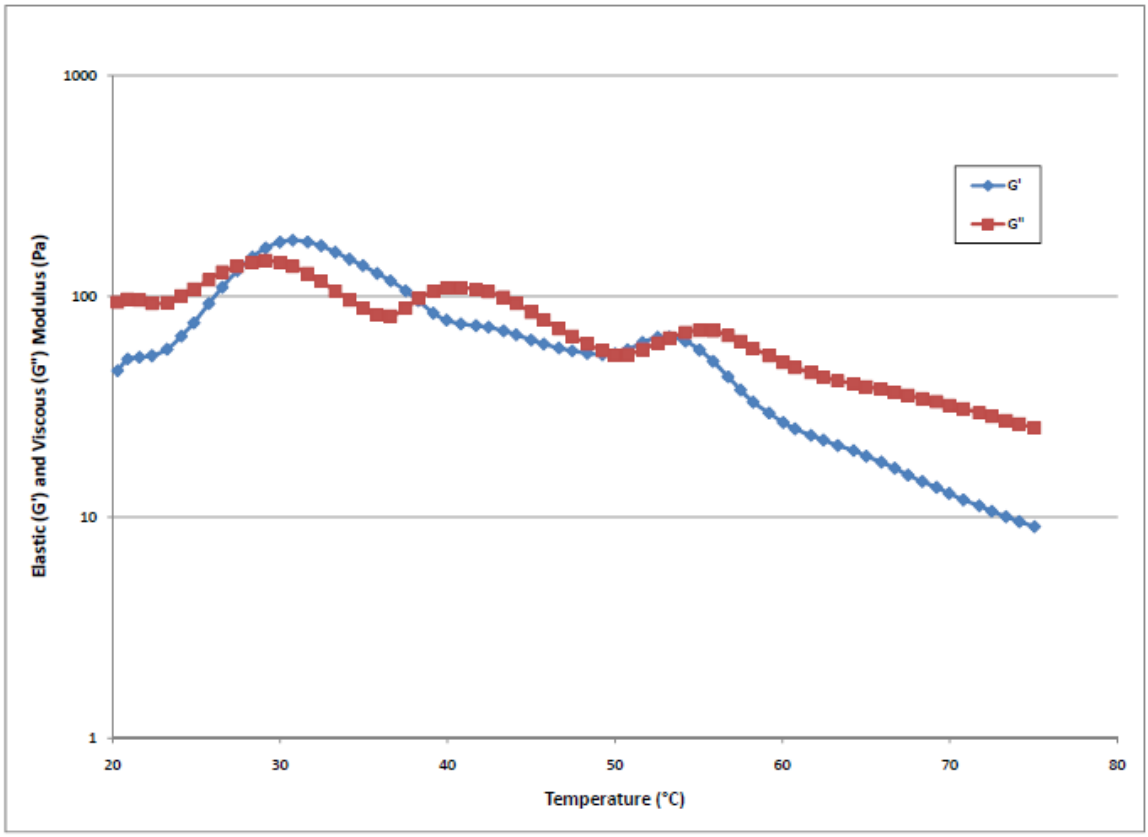

Figure 5.15 - Elastic and viscous modulus of 45% 550-2810-550 triblock material

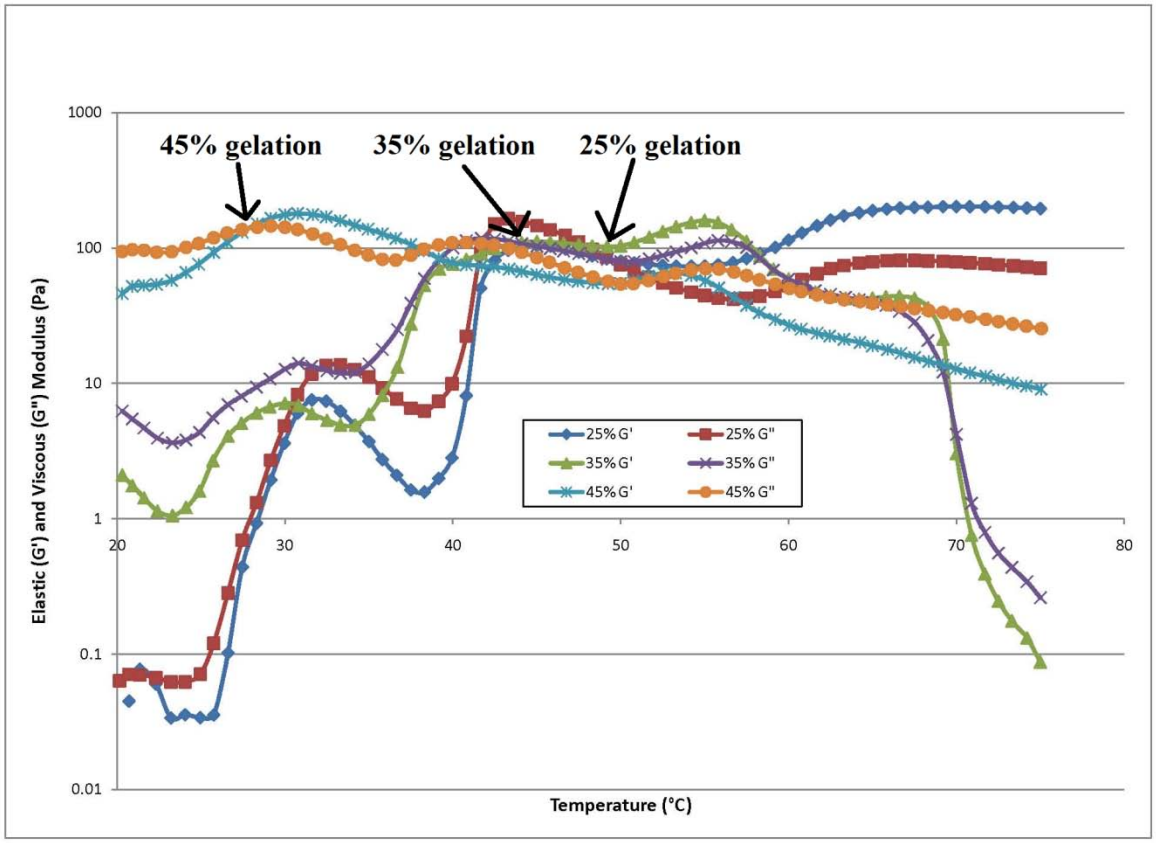

Figure 5.16 - Gelation point for 25%, 35%, and 45% 550-2810-550 triblock material

Table 5.3 - Maximum and minimum viscosity of 550-2810-550

550-2810-550 PEG-PLGA-PEG			
Concentration	Solution minimum Viscosity (cP)	Material maximum viscosity (cP)	Maximum viscosity temperature (°C)
25%	2.825	423	42.05
35%	8.908	8,299	33.7
45%	141	15,829.5	24.5

Table 5.4 – Maximum elastic modulus and corresponding temperature of 550-2810-550

550-2810-550 PEG-PLGA-PEG		
Concentration	Maximum elastic modulus temperature (°C)	Maximum elastic modulus (Pa)
25%	70.8	202
35%	55	159.6
45%	30.75	179.45

Chapter 6 : Increase mechanical properties and long-term stability of the gels using permanent crosslinks

The aim of the work described in this chapter is to increase the mechanical ability of PEG-PLGA-PEG to enable 3-D construction of scaffolds as well as alter the properties of the gelation to become irreversible. Due to the variety of PEG compounds and the fact that PEG is situated as an end compound in our triblock copolymer, it is possible to alter the type of PEG in order to facilitate the addition of additional crosslinks in our material. This variation to the PEG component as well as the ratio of a different type of PEG to PLGA is explored to attempt to increase the mechanical properties of the final gel and form an irreversible scaffold.

6.1 Introduction

PEG-PLGA-PEG triblock is PEG based, meaning the free end on either side of the polymer chain are PEG compounds. The type of PEG that has been used so far is a PEG methylether. Using PEG methylether in the triblock result in a free methyl group ($-CH_3$) on each end of the triblock (Figure 6.1). To be able to use Irgacure 2959, an acrylate end group ($-OOCH_3C=CH_2$) is needed. Irgacure 2959 works by being broken into free radicals by UV light. The free radicals that are created break apart carbon double bonds crosslinking different triblock copolymers and initiate a chain reaction, crosslinking any available polymer chains to create a network of polymers.

Usually, Irgacure 2959 is used with PEG diacrylate due to the fact that PEG diacrylate has an acrylate end group on both ends which allows for a high density of crosslinking between the PEG polymer (Figure 6.1) [25, 31, 42, 119]. PEG, as a general compound, is not very biodegradable even though it can be filtered out of the body by the kidneys and excreted, as long as its molecular weight is less than 10,000 Daltons. To be able to create a constant and reliable biomaterial in the body and use PEG, another type of material is needed to work together with the PEG [120]. For this reason, we needed to continue with our triblock copolymer.

PEG methylether is able to link with PLGA because it has an ester group (-OH) on one end. To be able to use Irgacure 2959, a type of PEG is needed that comprises of an ester end to bind with PLGA in the triblock polymerization reaction and an acrylate end group to join with other methacrylate moieties. PEG methacrylate allows for the bonding with PLGA and crosslinking with other PEG methacrylates using Irgacure 2959 as the photoinitiator (Figure 6.2). Using PEG methacrylate also creates a material that when crosslinked into a triblock with PLGA, has the same degradable properties as a PEG methylether triblock with PLGA. Since PEG compounds are generally not biodegradable, using the same type of biodegradable PLGA in this new material allows for the same biodegradable properties. Irgacure®2959 is soluble in DI water up to around 1% concentration as stated by the manufacturer, Ciba Specialty Chemicals. A final percentage of 0.03% Irgacure 2959 will be used since higher percentages are detrimental to the survival of cells as shown earlier [42]. The addition of Irgacure 2959 into a homogenous solution will create a thermosensitive and photocrosslinkable

hydrogel. After the printing of a certain amount of layers on a heated substrate, the scaffold can be briefly removed from the printer, while still in a warm environment, and placed under a 365nm UV light to create further crosslinking of the PEG-PLGA-PEG triblocks with each other, creating a non-reversible stiffer gel.

6.2 Materials and Methods

6.2.1 Materials

Polyethylene glycol methacryalate (PEGma) (Mn = 526 g/mol) (Sigma–Aldrich), DL-lactide (DLLA) (Aldrich), glycolide (GA) (Aldrich), anhydrous toluene (Sigma), and hexamethylene diisocynate (HMDI) (Sigma) were all used as received. All solvents and other chemicals are of analytical grade.

6.2.2 Synthesis of PEGma-PLGA-PEGma Polymer

The synthesis of PEGma-PLGA-PEGma is almost identical to the synthesis of PEG-PLGA-PEG. Using PEG methacrylate (Mw = 526) instead of mPEG, ring opening polymerization to form diblocks and coupling of the diblocks to form triblocks proceeded as stated in section 5.2.1. The material was rotoevaporated under vacuum for 30 minutes in a water bath at 85°C before being dissolved in dichloromethane and then precipitated in cold diethyl ether to remove any impurities. Again, the material was rotoevaporated and then was placed in a vacuum oven overnight to remove any residual solvents and finally stored at -20°C to prevent degradation of the PLGA.

To form a thermosensitive solution, DI water was added to the copolymer and stirred at 4°C until homogeneity was accomplished. To make the material photocrosslinkable, the material was weighed and 0.03% (w/w) of Irgacure 2959 was added. The material was stirred at 4°C for one hour in a dark environment to help prevent premature UV crosslinking.

6.2.3 Molecular Weight of PLGA

The molecular weight of the PLGA was varied to verify if it would affect the thermal gelation processes. A molar ratio of 78:22 for DLLA to GA in PLGA was used while the total molecular weights for the PLGA tested were 1404, 2810, and 5620. Because of the replacement of PEG, the polarity of the triblock was changed. The molecular weight of the PLGA was again varied to confirm any hydrophobic and hydrophilic issues.

6.2.4 Molecular Weight of PEGma

The molecular weight of the PLGAma could not be varied due to the insufficient supply of a variety of this material. Numerous chemical supply companies were contacted and only a PEGma of molecular weight 526 was produced for mass distribution. Higher and lower molecular weights of PEGma can be produced on a custom need to order basis but due to the cost of manufacturing, this option was eliminated for this work.

6.2.5 Rheology

6.2.5.1 Viscosity

The viscosity of aqueous solutions were measured as a function of temperature using a Brookfield DV-II+Pro Viscometer. The material was heated from 20°C to 75°C at a rate of 5°C per minute. A cone/plate set-up was used with a cone angle of 0.8° and gap distance of 0.013 mm.

6.2.5.2 Dynamic Mechanical Analysis

The solution to gel transition was investigated using a Texas Instrument AR 2000ex rheometer. The material was heated from 20°C to 75°C at a rate of 5°C per minute. Parallel plates having a diameter of 40 mm were used with a gap distance of 1 mm. The data was collected under controlled angular frequency (6.283 rad/s), oscillation stress (σ=0.7956 Pa), and strain (γ=0.216).

6.2.6 Photosensitivity

To test the photosensitivity of the triblock material, a UVP Blak-Ray B-100AP High Intensity UV lamp at 365nm wavelength was used. Material was pipetted onto a glass slide on a digitally controlled hotplate. The UV light was then positioned above the hotplate for 10 seconds increments (Figure 6.3). After 10 seconds, the UV light was moved away and the glass slide was tilted to verify if gelation had occurred. Once a material was visually considered a gel, the material was touched with a knife to test consistency. If when the knife touched the material and the material stuck to the knife,

gelation was not fully complete. Usually, once the tilt test was verified, the knife test also passed.

6.3 Results & Discussion

6.3.1 PEGma-PLGA-PEGma (526-2810-526)

Rheology was completed on 35% and 45% concentrations of 526-2810-526 PEGma-PLGA-PEGma triblock material in DI water. Compared to the elastic modulus of the previously tested PEG-PLGA-PEG (550-2810-550) material, this new material was not capable of supporting additional layer to build in 3-D (Table 6.1). The elastic modulus over a range of temperature of 35% concentration of 526-2810-526 was never greater than the viscous modulus (Figure 6.4). Because of this, the 35% concentration copolymer never became a gel. It remained in liquid form no matter the temperature. A 45% concentration was then tested to reveal that it too, did not gel at any temperature, G' was always less than G" (Figure 6.5). The viscosity of the 45% showed that there was a small increase in viscosity at 42°C but not a significant enough one for a material to gel (Figure 6.6). As the temperature continued to rise above 70°C, there was an increase in viscosity conveying that a lot of water in the material had been evaporated. These results show that a polymer triblock material made up of PEGma-PLGA-PEGma (526-2810-526) does not form tightly packed micelles as temperature increases and therefore does not gel. This is due to the non-polar quality of the acrylate end group of the PEG methacrylate. As temperature increased, the hydrophobic non-polar PLGA clumped together to avoid the water. The non-polar end groups collided with the somewhat non-polar PEG chains and interrupted the formation of micelles. To compensate for this type

of interaction, the molecular weight of the components were varied. Though not thermally sensitive, this material was capable of rapid gelation photocrosslinkably. After only 1 minute of UV irradiation, the material became stiff and was able to be peeled off of the glass slide, holding its shape even after removal from the glass slide.

6.3.2 PEGma-PLGA-PEGma with varied PLGA Mw

The molecular weight of the PLGA was varied in lieu of purchasing alternate molecular weights of PLGA due to monetary constraints and the simplicity of manually creating varied molecular weights of PLGA. A possible solution to help the formation of micelles was to increase the molecular weight of PLGA so that the similar non-polar acrylate end group on the PEG would be further away from the PLGA core. The opposite thought for a solution was to decrease the molecular weight of the PLGA so that there would be no attraction of the PLGA to the non-polar acrylate group.

6.3.2.1 PEGma-PLGA-PEGma (526-5620-526)

A batch of PEGma-PLGA-PEGma was created with a PLGA molecular weight of 5620 (526-5620-526) to create a copolymer with a higher molecular weight PLGA. Dissolution in water was unsuccessful due to the increase in hydrophobicity because of the increased PLGA content. As a result, the increase in PLGA molecular weight did not help the gelation of material since it could not dissolve in water.

6.3.2.2 PEGma-PLGA-PEGma (526-1404-526)

PEGma-PLGA-PEGma was created with a smaller PLGA molecular weight of 1404 (526-1404-526). This material was tested at concentrations of 25%, 35%, and 45% in DI water. The viscosity was tested to check for sharp increases which would indicate micelle formation. In general, the viscosity of the 25% concentration was consistent in the range of 20-30 cP through the temperature range from 20°C to 75°C (Figure 6.7). As temperature increased, the viscosity of the 35% concentration decreased (Figure 6.8). It reached a maximum of about 61 cP at low temperatures and then decreased to below 10 cP at temperatures above 60°C with a small increase at 70°C that is most likely due to water evaporation. Water evaporation is more visibly obvious with the 45% concentration (Figure 6.9). This material's viscosity is at its highest, 124.6 cP, at low temperatures, decreases steadily until 60°C and then increases due to water evaporation. All of the concentrations do not seem to form tightly packed micelles because they all did not have sharp increases in viscosity. The maximum viscosities for each are not close to the maximum viscosities of the PEG-PLGA-PEG (550-2810-550) material (Table 6.2). To fully verify, oscillation tests were completed to conclude if any of them gelled thermally. The elastic modulus of the 25% concentration did increase as temperature increased but so did the viscous modulus negating any possibility of gel formation (Figure 6.10). The elastic modulus, G', never crossed the viscous modulus, G", verifying that this material never gelled thermally. The viscous and elastic moduli of the 35% both hovered around 0.1 Pa for most of the temperature range (Figure 6.11). They fluctuated a couple times but at such low values that it could not be considered gelation. The viscous modulus became greater than the elastic modulus of the 45% concentration at around

62°C (Figure 6.12). As demonstrated in the viscosity tests of the 45% concentration, there was water evaporation which helped to account for the increase in viscous and elastic moduli and the point at which the elastic modulus was greater than the viscous modulus. The viscosity and oscillation tests showed that a PEGma-PLGA-PEGma triblock using PEGma of a molecular weight of 526 and PLGA of a molecular weight of 1404 cannot form a large network of micelles and therefore, not gel. All concentration s of this material experienced no problems gelling almost instantaneously under UV light though indicating that the thermal abilities of this triblock had been compromised by the altering of the PEG compound The material had the same consistency as the 526-2810-526 material after UV light irradiation. The change of molecular weight to PLGA had no effect on the material's photosensitivity.

6.3.3 Blend of PEG-PLGA-PEG and PEGma-PLGA-PEGma (550-2810-550/526-2810-526)

A material is needed that is stiff enough to keep its shape after printing to enable enough time for UV irradiation to crosslink the material permanently. PEGma-PLGA-PEGma is not able to become viscous enough with an increase in temperature while PEG-PLGA-PEG does not allow for further UV crosslinking. To combine the strengths of each material and hopefully eliminate any weaknesses, the materials were mixed in various ratios to create a material that becomes stiffer with an increase in temperature and also allows for further crosslinking with the use of the photoinitiator, Irgacure 2959.

6.3.3.1 50/50 Mix Ratio

A 50/50 ratio mix of PEG-PLGA-PEG and PEGma-PLGA-PEGma was first tested for viscosity as temperature was increased. A 50/50 ratio adding 0.03% w/w Irgacure 2959 was also tested for viscosity, 0.03% was used due to its potential toxicity to cells as mentioned before. Both of the materials were observed to have similar viscosities (Figure 6.13). The 50/50 mix without Irgacure 2959 did experience a rise in viscosity as temperatures rose past 60°C but that can be attributed to water evaporation. The 50/50 mix with 0.03% Irgacure 2959 added showed a brief increase in viscosity around 60°C but quickly leveled off. This brief increase in viscosity can be explained by crosslinking due to ambient light on the edges of the test plate preventing further evaporation of water at higher temperatures. As a liquid solution before gelation, the 50/50 mix had a viscosity 64 cP and reached a maximum viscosity of 76,790 cP at 33.7°C which is similar to the consistency of mustard (Tables 6.3 & 2.2). The elastic modulus of the 50/50 mix with and without Irgacure 2959 increased dramatically in the same temperature ranges as the viscosity increased, showing micelle formation occurred (Figure 6.14). Unfortunately, the material did not gel thermally but did become viscous enough to be able to hold its shape after micelle formation. Both the viscosity and elastic & viscous moduli plots show that a 50/50 mix with a 0.03% concentration of Irgacure 2959 has better mechanical properties and therefore might have been the proper material for 3-D printing. . However, after further testing made with a 0.03% concentration of Irgacure 2959 under a UV light, this material was never able to completely gel under UV light. After a total of five minutes of UV irradiation, the material still shifted on the glass slide while being

tilted. When an attempt was made to try and remove the material from the glass slide, the material fell apart.

6.3.3.2 35/65 Mix Ratio

A 35/65 ratio mix of PEG-PLGA-PEG and PEGma-PLGA-PEGma showed greater minimum viscosity than a 50/50 mix but also had a greater maximum viscosity (Table 6.3). The viscosity of a 35/65 mix in solution was around 218 cP and increased to 81,510 cP at a temperature of 37°C (Figure 6.15). As seen with the 50/50 mix, the 35/65 mix's elastic modulus increased in the same temperature range as when its viscosity increased (Figure 6.16). The material never technically gelled but the elastic modulus did increase close to the value of the viscous modulus and with such a high viscosity, it had some ability to hold its shape after being printed. This material became stiffer because it was photocrosslinkable, it took over 30 seconds for droplets to become stiff but unfortunately, it was still somewhat soft to the touch. The material could be lifted off the glass slide but was still fairly saturated with water and could not hold its shape

6.3.3.3 20/80 Mix Ratio

At a maximum viscosity of 122,836 cP, similar to sour cream and peanut butter, a 20/80 mix of PEG-PLGA-PEG and PEGma-PLGA-PEGma had the greatest viscosity of all mix ratios (Table 6.3). It also had the highest solution minimum viscosity of 228 cP (Figure 6.17). The 20/80 mix of material observed the closest maximum viscosity and maximum elastic modulus temperatures of 33.3°C and 33.98°C respectively. The material did not

technically gel when the elastic modulus was at its maximum but as the temperature increased, G' did become greater than G" (Figure 6.18). High elastic and viscous moduli data and the increase in viscosity at extreme high temperature are due to some water evaporation during testing. This material was able to gel fully under UV light in less than 1 minute. A comparison was made of the 20/80 gel to the 35/65 gel, after gelation, it is possible to view a 3-D structure with the 20/80 gel due to the quick photoresponsiveness of the material while the 35/65 gel has flattened and is no longer a 3-D structure because over time, the shape melted (Figure 6.19). To further test the 3-D building ability of the 20/80 material, a row of droplets were pipette onto a glass slide. A series of droplets on top of the old droplets were repeated after gelation of the previous droplet (Figure 6.20).. After 10 seconds of UV light irradiation for each round of droplets, another round of droplets was placed. As shown in the final gelation pictures, the material is capable of holding its shape and building vertically. To also demonstrate the shape holding aspects of this material, some of the droplets were peeled back off of the glass slide.

6.3.3.4 10/90 Mix Ratio

As the % of PEG-PLGA-PEG decreased below 20 to only 10%, the materials ability to become viscous decreased greatly. A 10/90 ratio mix of PEG-PLGA-PEG and PEGma-PLGA-PEGma had a solution viscosity of 12.4 cP and a maximum viscosity of only 50,210 cP (Figure 6.21). The viscosity and elastic and viscous moduli show the same strange reaction to increased temperature as an unmixed PEGma-PLGA-PEGma material; they continue to increase (Figure 6.22). The elastic and viscous moduli are an order of magnitude lower than any other mix materials signifying that this material does

not possess any thermal abilities (Table 6.3). This material gelled photocrosslinkably because of the large amount of PEGma-PLGA-PEGma polymer; there were many sites where Irgacure can form additional crosslinks. For a material to posses both thermal and photosensitivity, the percentage of PEG-PLGA-PEG needs to be higher than 10% of the polymers concentration. This higher percentage will allow micelle formation helping to create a sol-to-gel transition temperature.

6.4 Conclusions

A triblock polymer material consisting of only PEGma-PLGA-PEGma cannot thermally form a material that is capable of holding its shape over time. Varying the molecular weight of PLGA does not significantly affect the final thermal or photocrosslinkable gelation of the material. Through regulation of the ratio of the materials, a combination of PEG-PLGA-PEG and PEGma-PLGA-PEGma material with good thermal properties capable of increasing material properties high enough to allow for its shape to hold over time has been developed.

A 20/80 mix of PEG-PLGA-PEG and PEGma-PLGA-PEGma possess the highest maximum viscosity and maximum elastic modulus, 122,836 cP and 93.9 Pa respectively of all mixed triblock polymer materials investigated (Figures 6.23 & 6.24). The measured elastic modulus of human liver, using ultrasonic techniques, was 430 ± 81.7 Pa and 640 ± 80 Pa under 5% strain (Table 6.4) [121-122]. A different technique was used to measure the elastic modulus of the liver than the technique in this work but the comparison shows that our material possesses mechanical properties in the range of

human liver tissue. A material that satisfies all requirements for use in a SFF printer has been found; a mix of PEG-PLGA-PEG and PEGma-PLGA-PEGma material dissolved in water is a low-viscous solution before being printed, has a short solution to gel transition time, and is an irreversible mechanically stiff material that allows for vertical building.

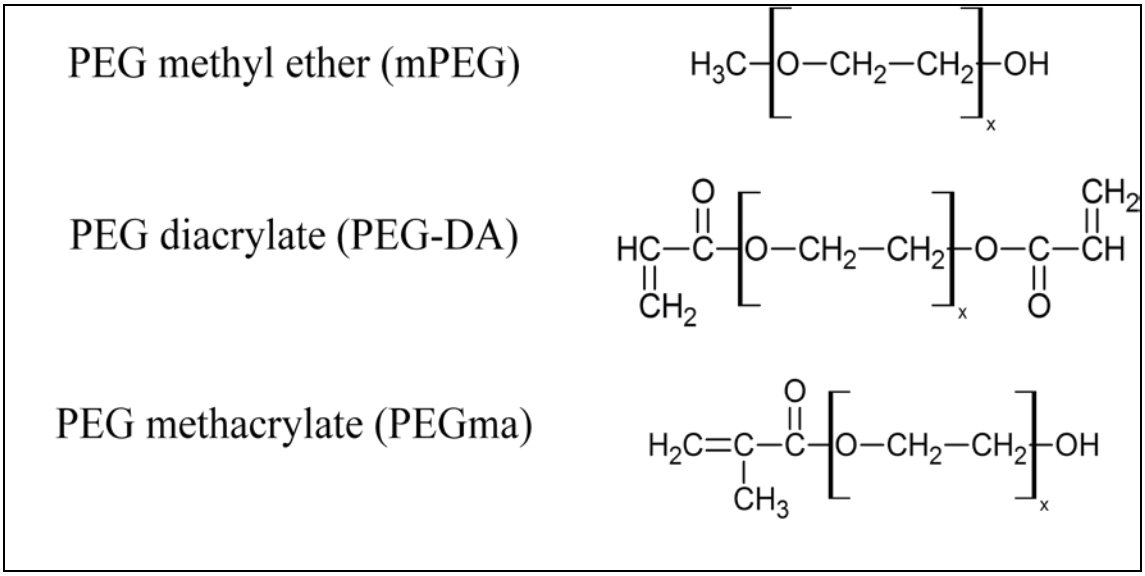

Figure 6.1 - Various chemical structure of PEG

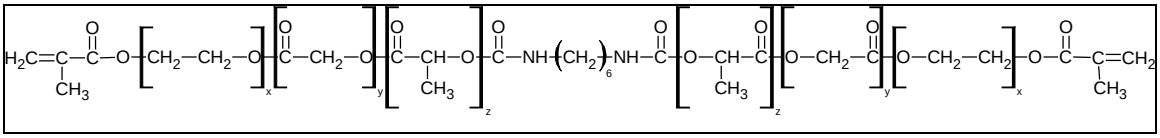

Figure 6.2 - Chemical structure of PEGma-PLGA-PEGma

Table 6.1 - Comparison of maximum elastic modulus

Concentration	Maximum Elastic Modulus (Pa)		
	PEG-PLGA-PEG (550-2810-550)	PEGma-PLGA-PEGma (526-2810-526)	PEGma-PLGA-PEGma (526-1404-526)
35%	159.6	0.1966	0.501
45%	179.45	7.68975	3.4315

Table 6.2 - Comparison of maximum viscosities

Concentration	Maximum Viscosity (cP)	
	PEG-PLGA-PEG (550-2810-550)	PEGma-PLGA-PEGma (526-1404-526)
25%	423	40.37
35%	8,299	60.765
45%	15,829.50	124.585

Figure 6.3 - UV Light set-up

Table 6.3 - Comparison of mixed polymers - (PEG-PLGA-PEG/PEGma-PLGA-PEGma)

Mix of PEG-PLGA-PEG and PEGma-PLGA-PEGma (550-2810-550/526-2810-526) with 0.03% Irgacure 2959					
Mix Ratio	Solution Minimum Viscosity (cP)	Material Maximum Viscosity (cP)	Maximum Viscosity Temperature (°C)	Maximum Elastic Modulus (Pa)	Maximum Elastic Modulus Temperature (°C)
50/50	64	76,790	33.7	34.3	35.75
35/65	217.75	81,510	37	63.745	40
20/80	228.435	122,836.10	33.3	93.888	33.98
10/90	12.39	50,210	75	7.701	75

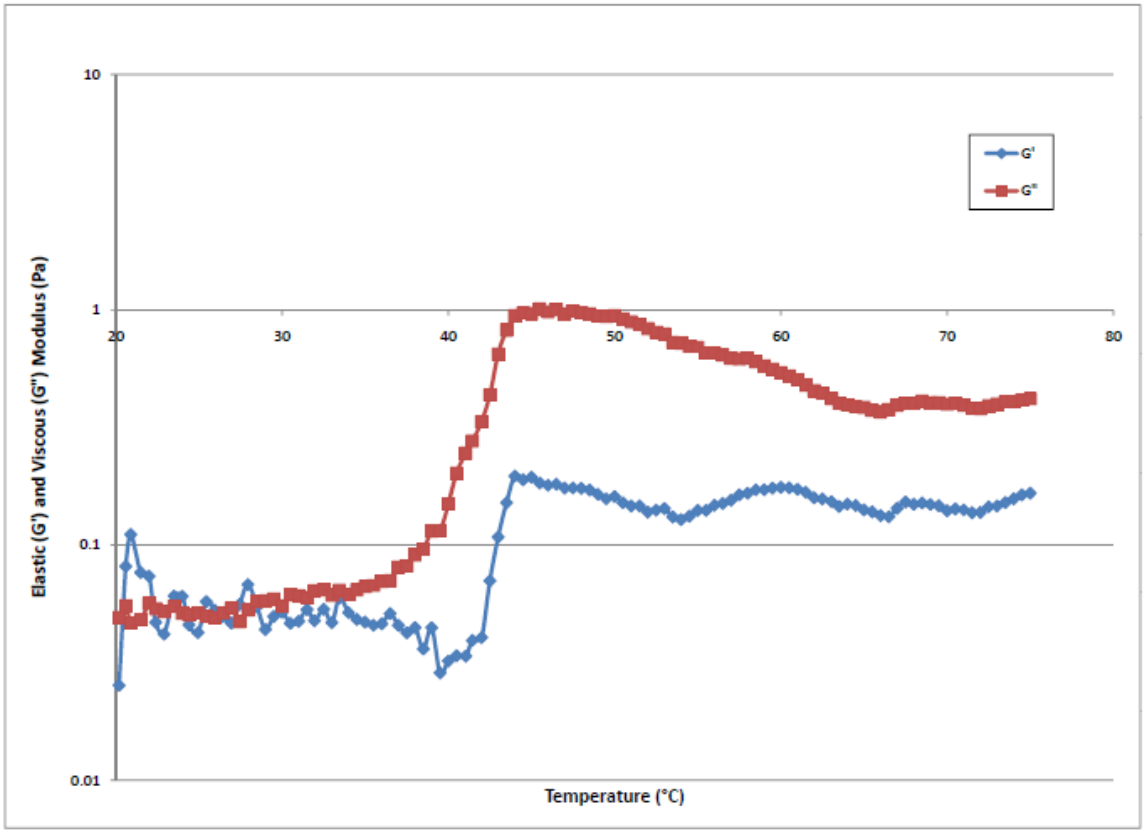

Figure 6.4 - Elastic and viscous modulus of 35% 526-2810-526 triblock material

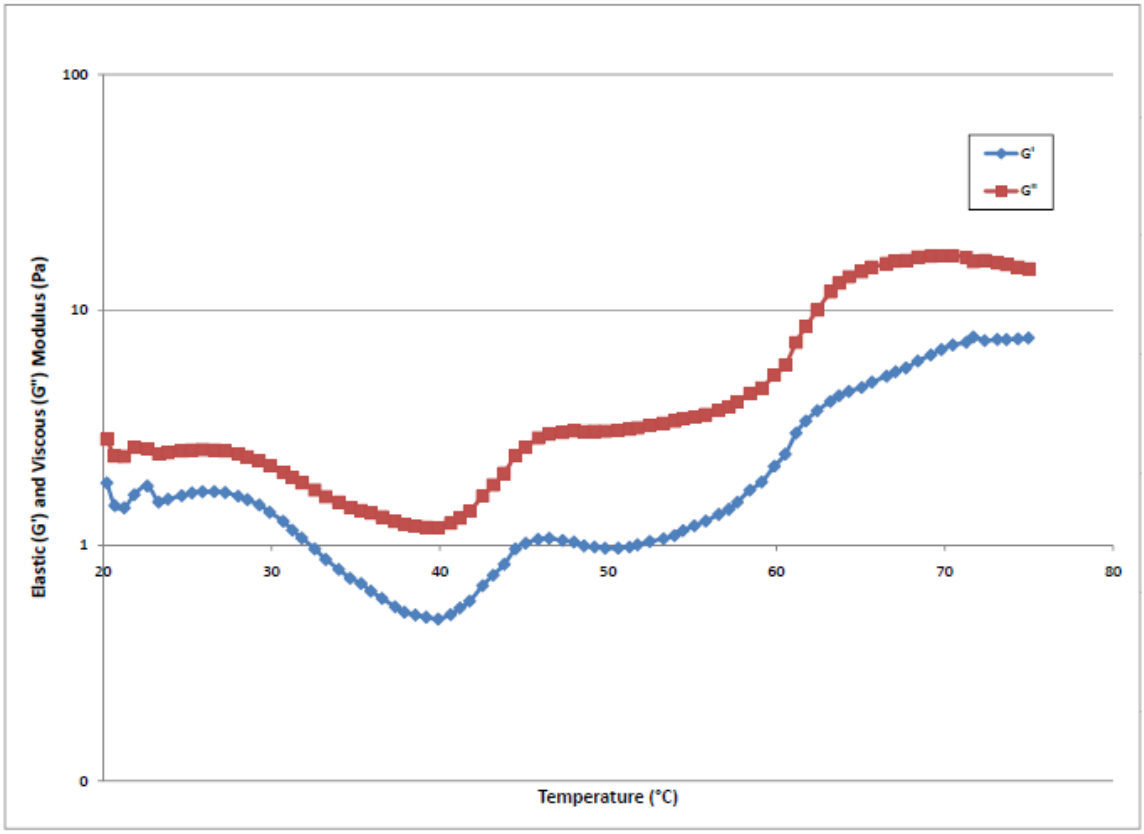

Figure 6.5 - Elastic and viscous modulus of 45% 526-2810-526 triblock material

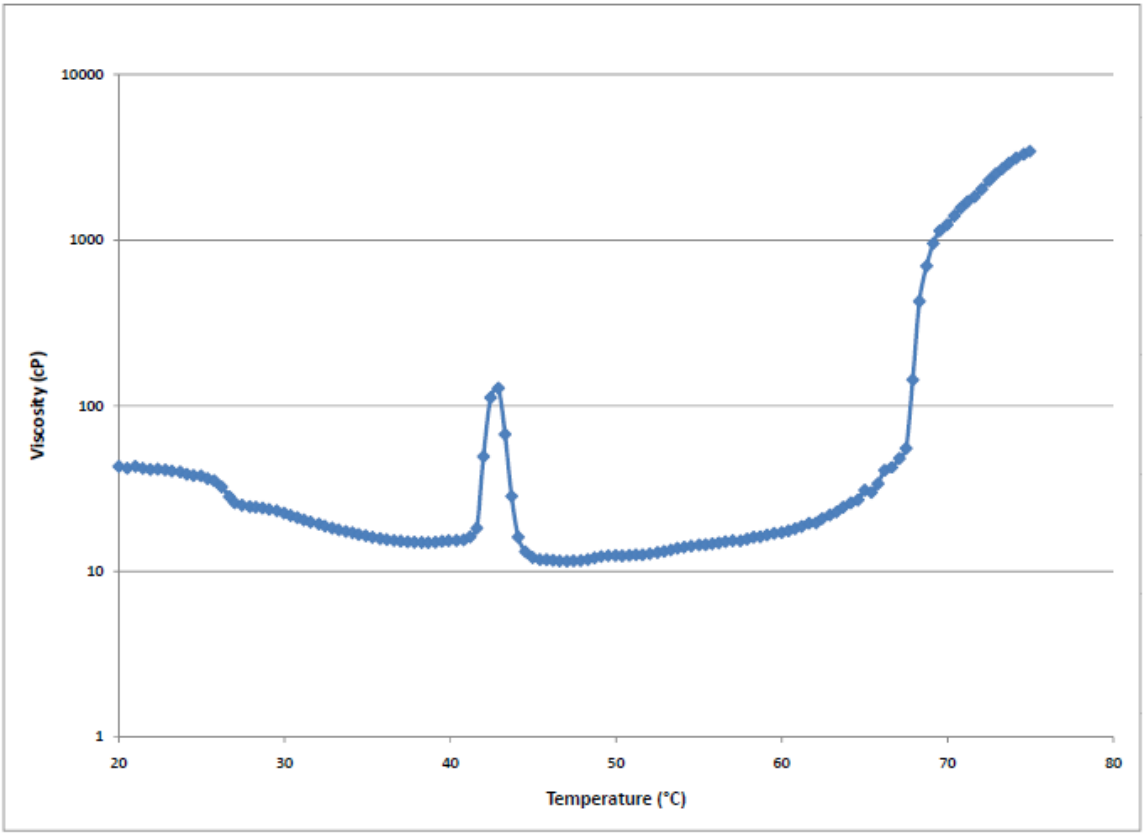

Figure 6.6 - Viscosity of 45% 526-2810-526 triblock material

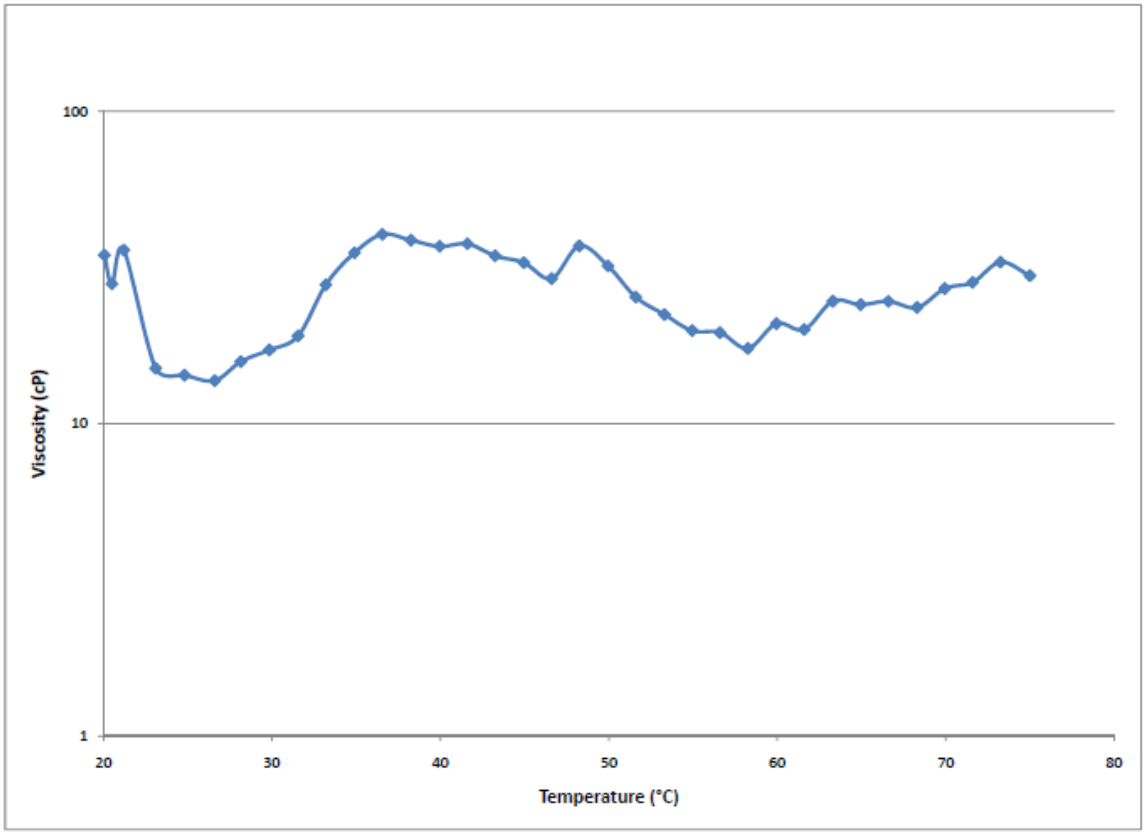

Figure 6.7 - Viscosity of 25% 526-1405-526 triblock material

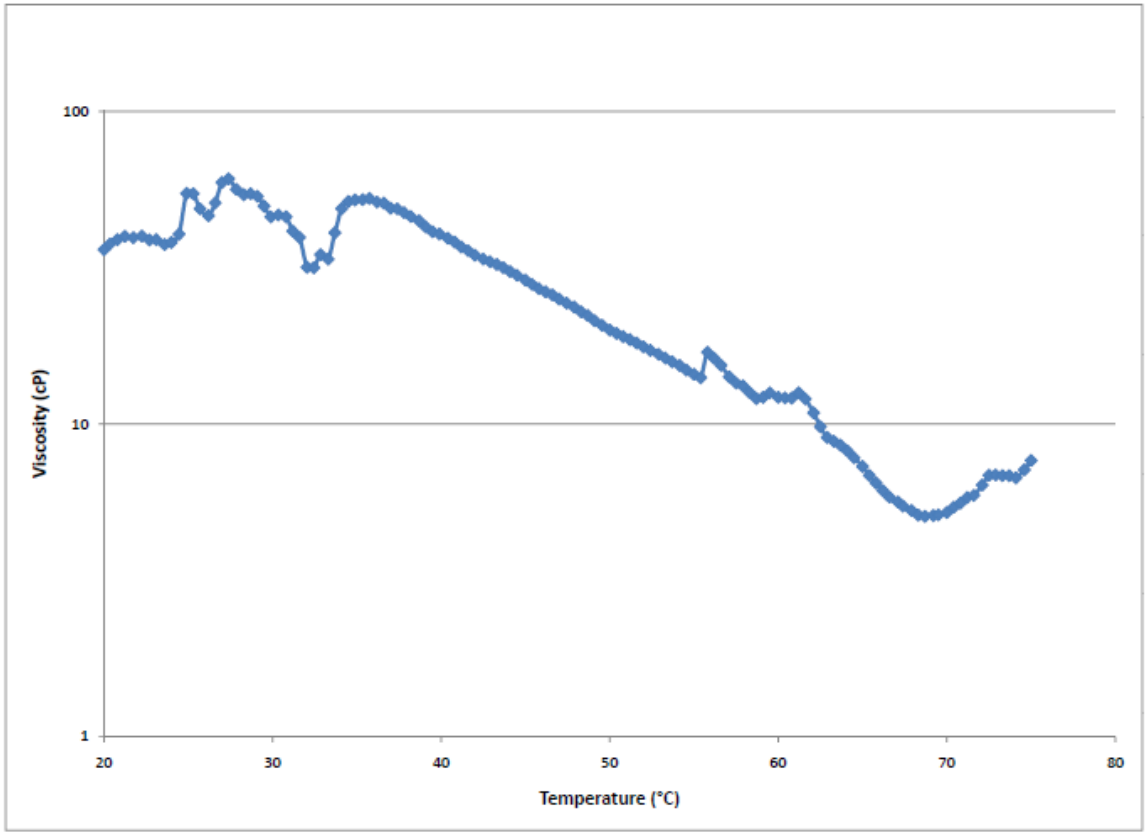

Figure 6.8 - Viscosity of 35% 526-1405-526 triblock material

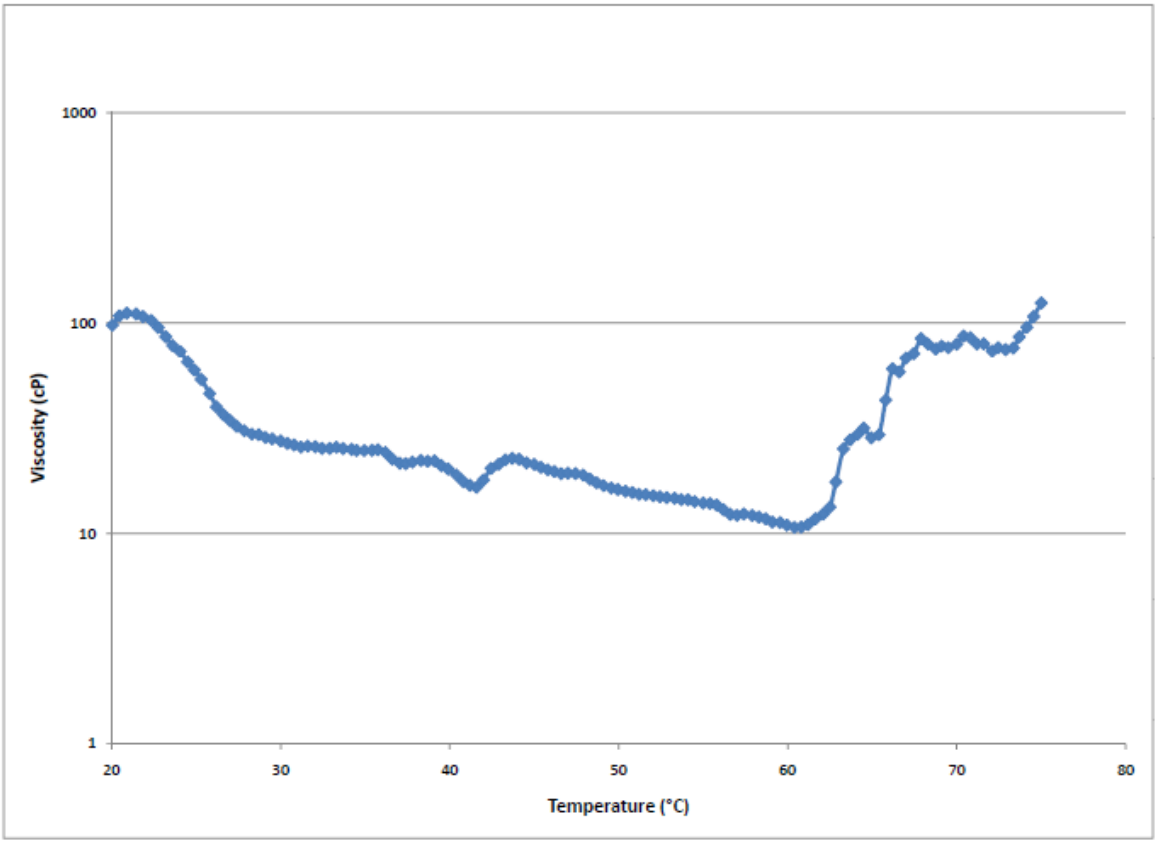

Figure 6.9 - Viscosity of 45% 526-1405-526 triblock material

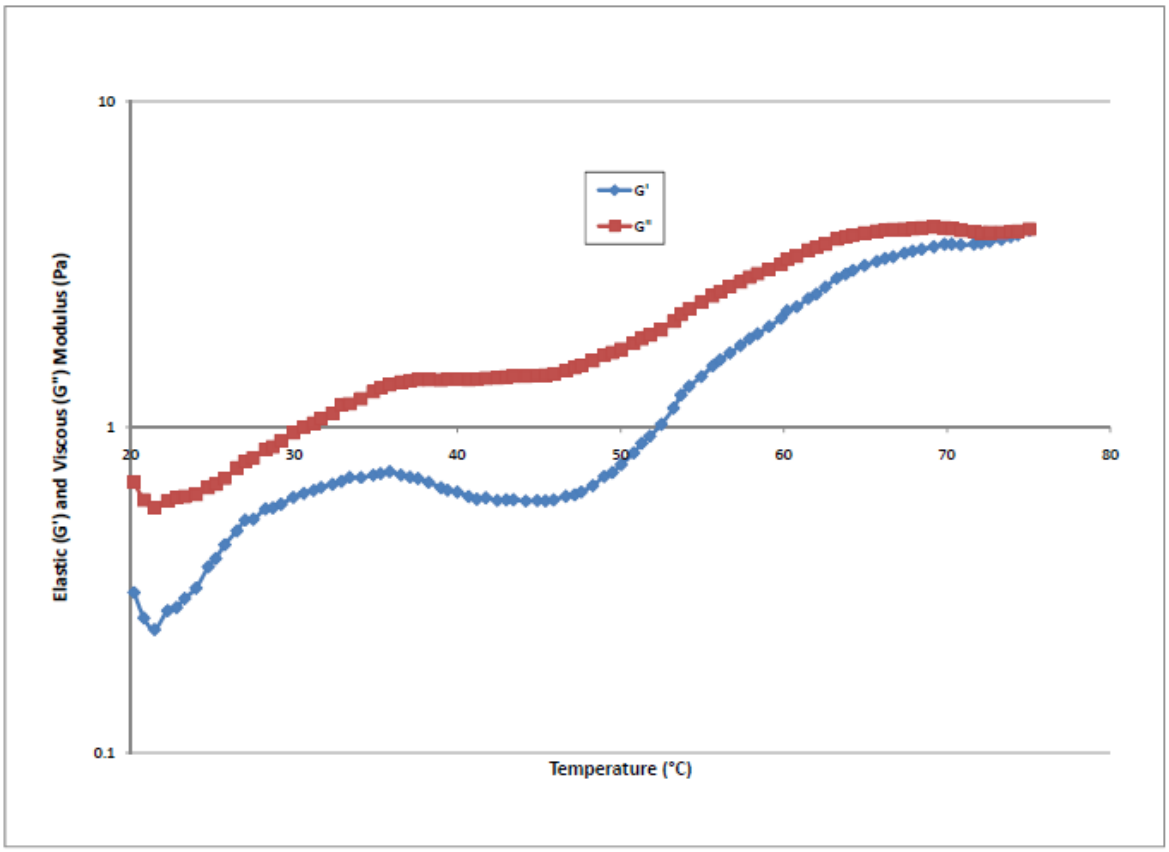

Figure 6.10 - Elastic and viscous modulus of 25% 526-1404-526 triblock material

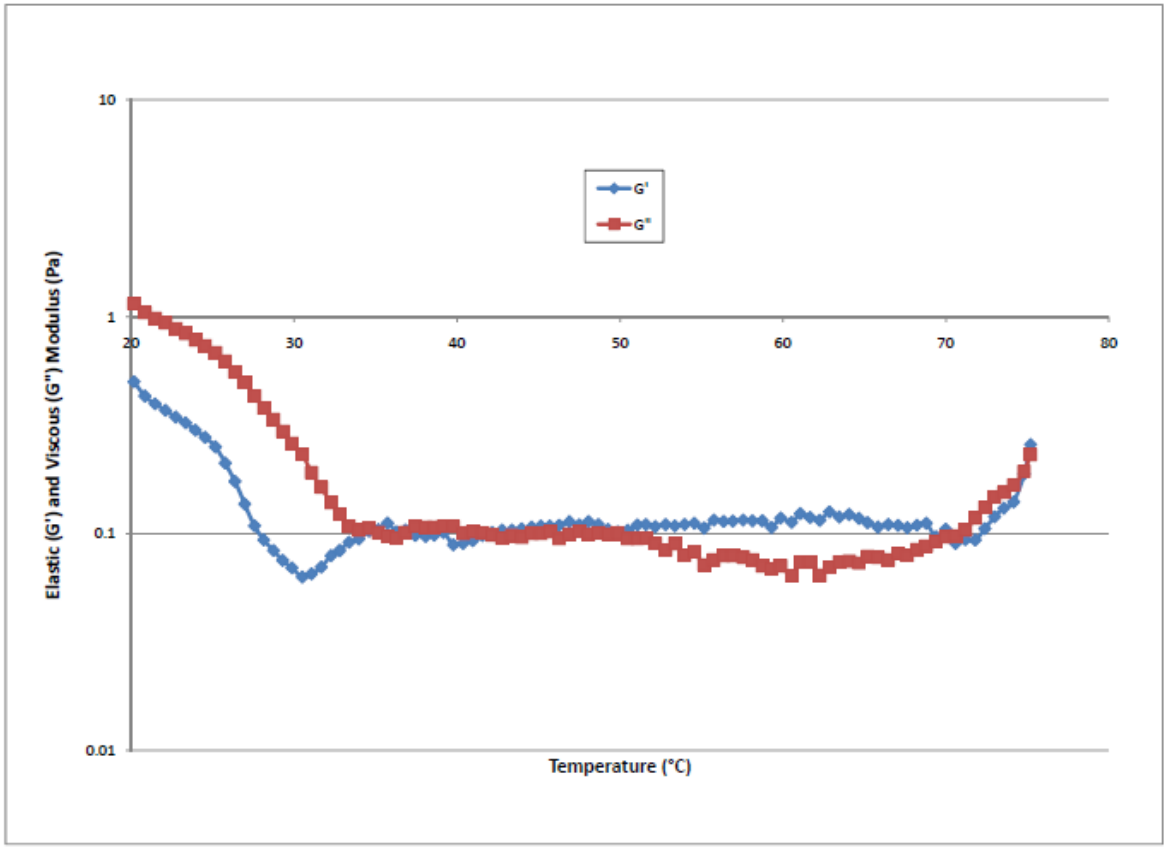

Figure 6.11 - Elastic and viscous modulus of 35% 526-1404-526 triblock material

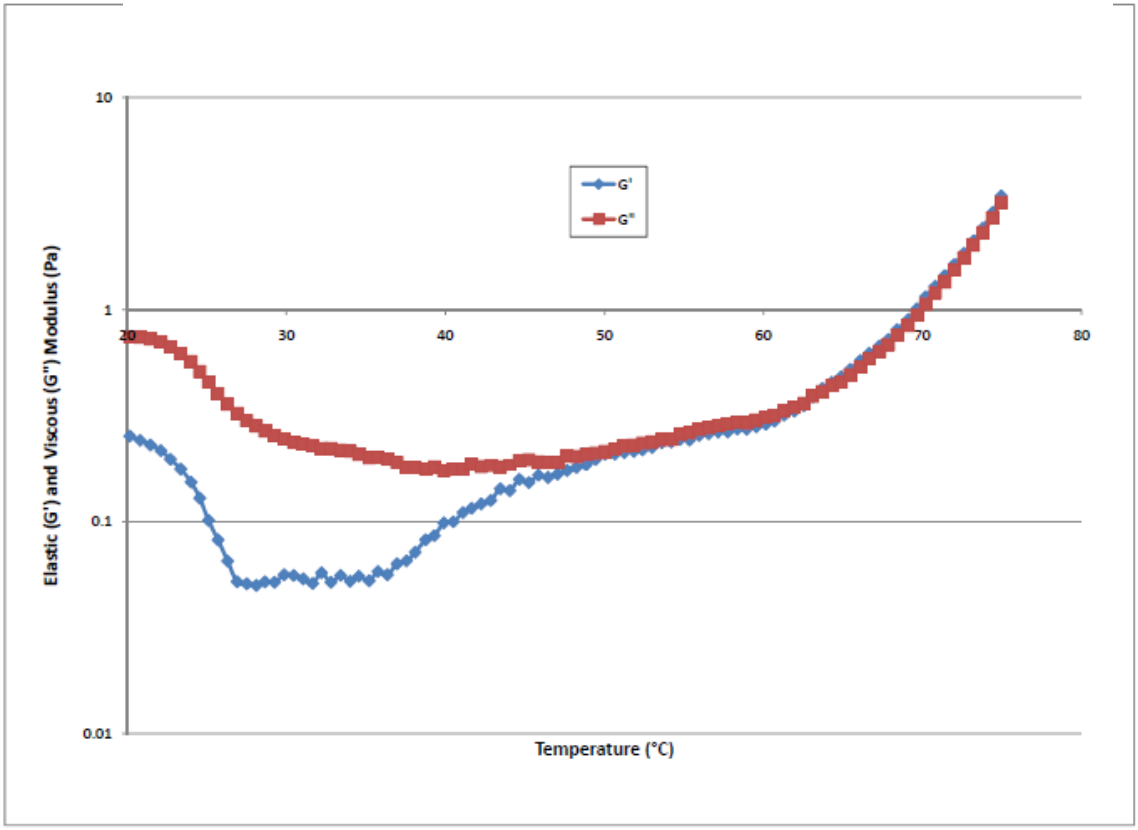

Figure 6.12 - Elastic and viscous modulus of 45% 526-1404-526 triblock material

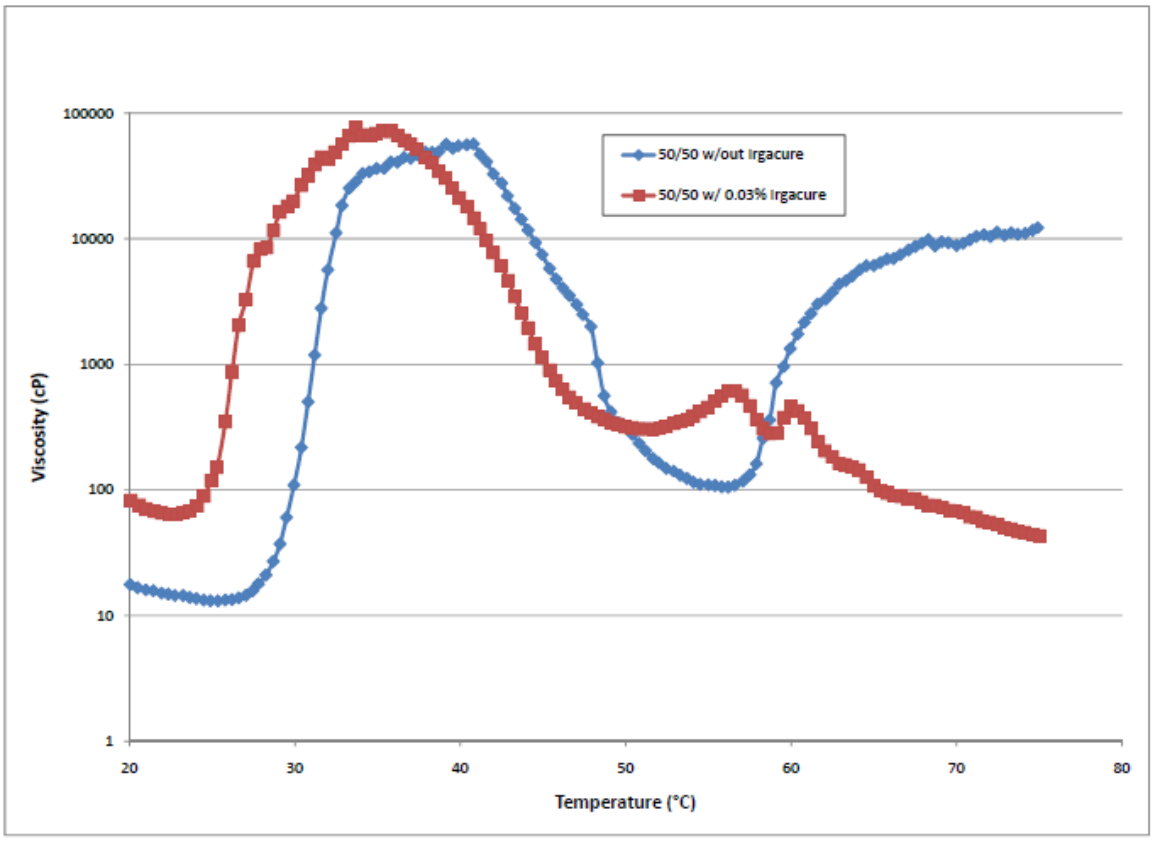

Figure 6.13 - Viscosity of 45% concentration of 50/50 mix of 550-2810-550 and 526-1404-526 triblock material with and without 0.03% Irgacure

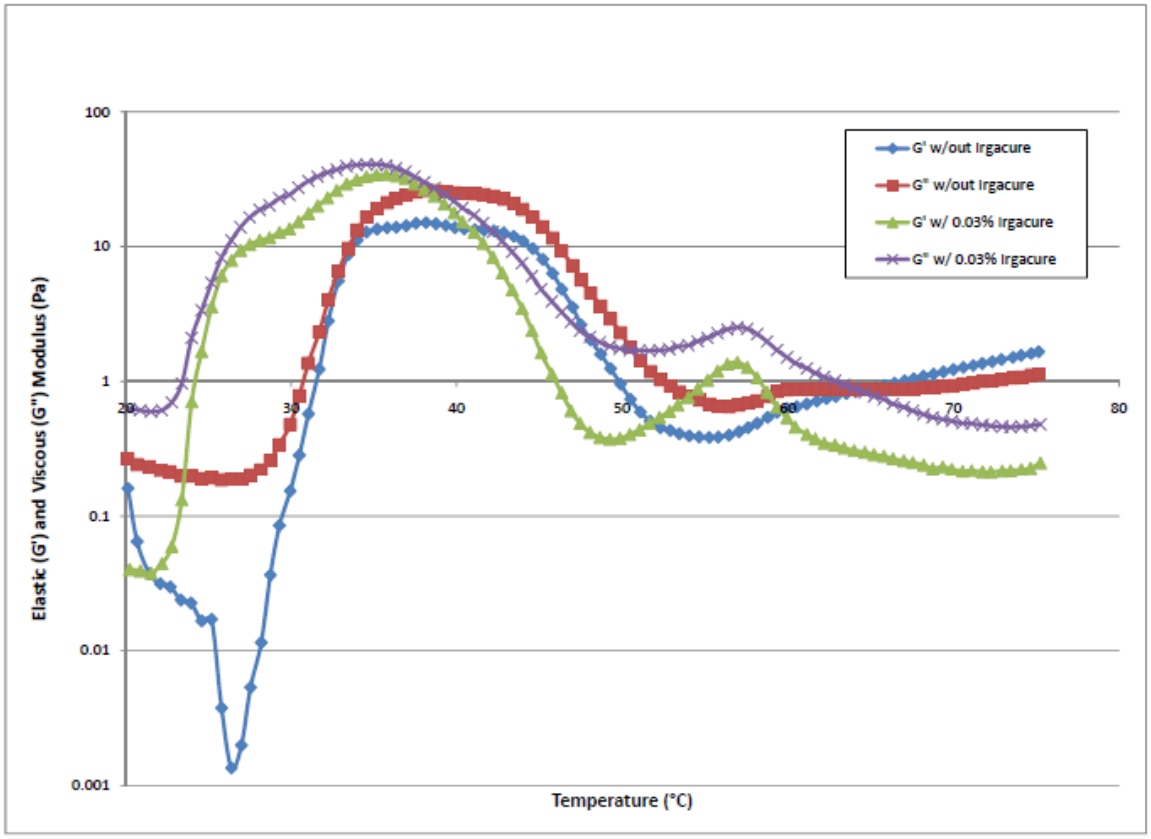

Figure 6.14 - Elastic and viscous modulus of 45% concentration of 50/50 mix of 550-2810-550 and 526-1404-526 triblock material with and without 0.03% Irgacure

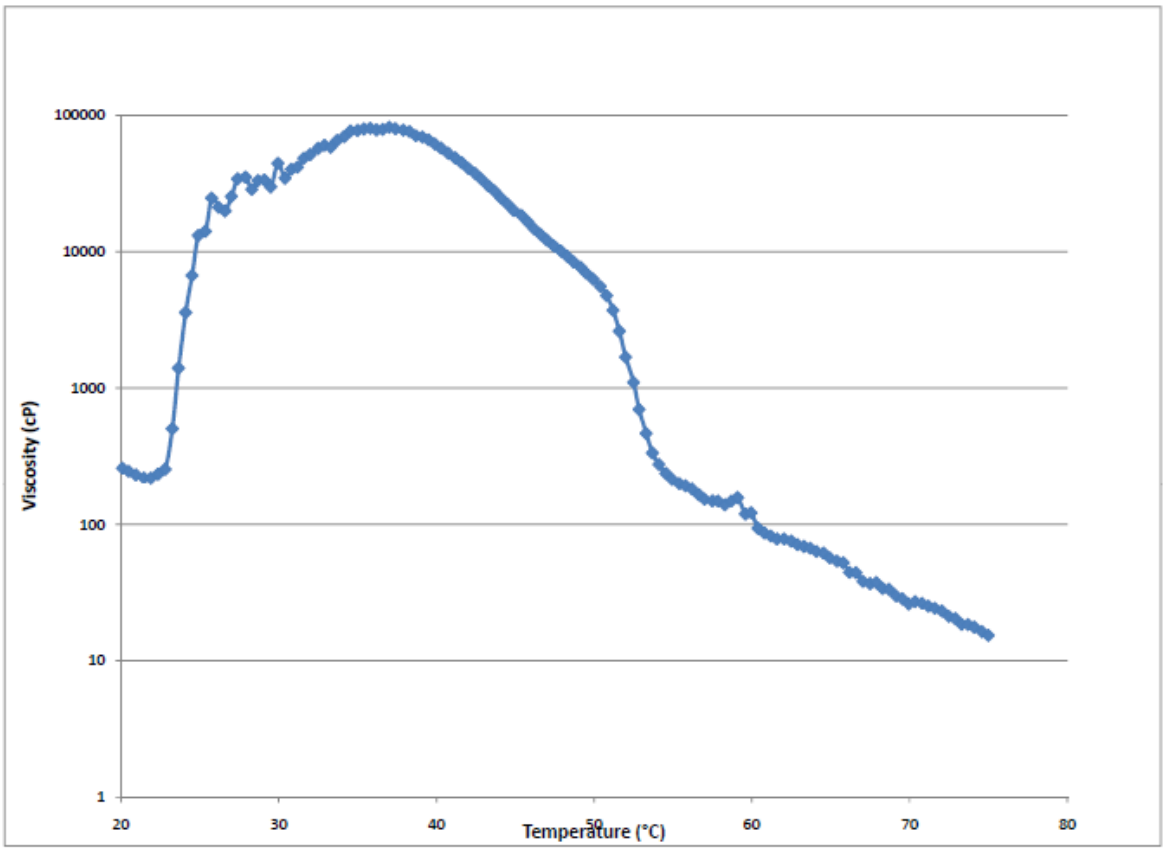

Figure 6.15 - Viscosity of 45% concentration of 35/65 mix of 550-2810-550 and 526-1404-526 triblock material with 0.03% Irgacure

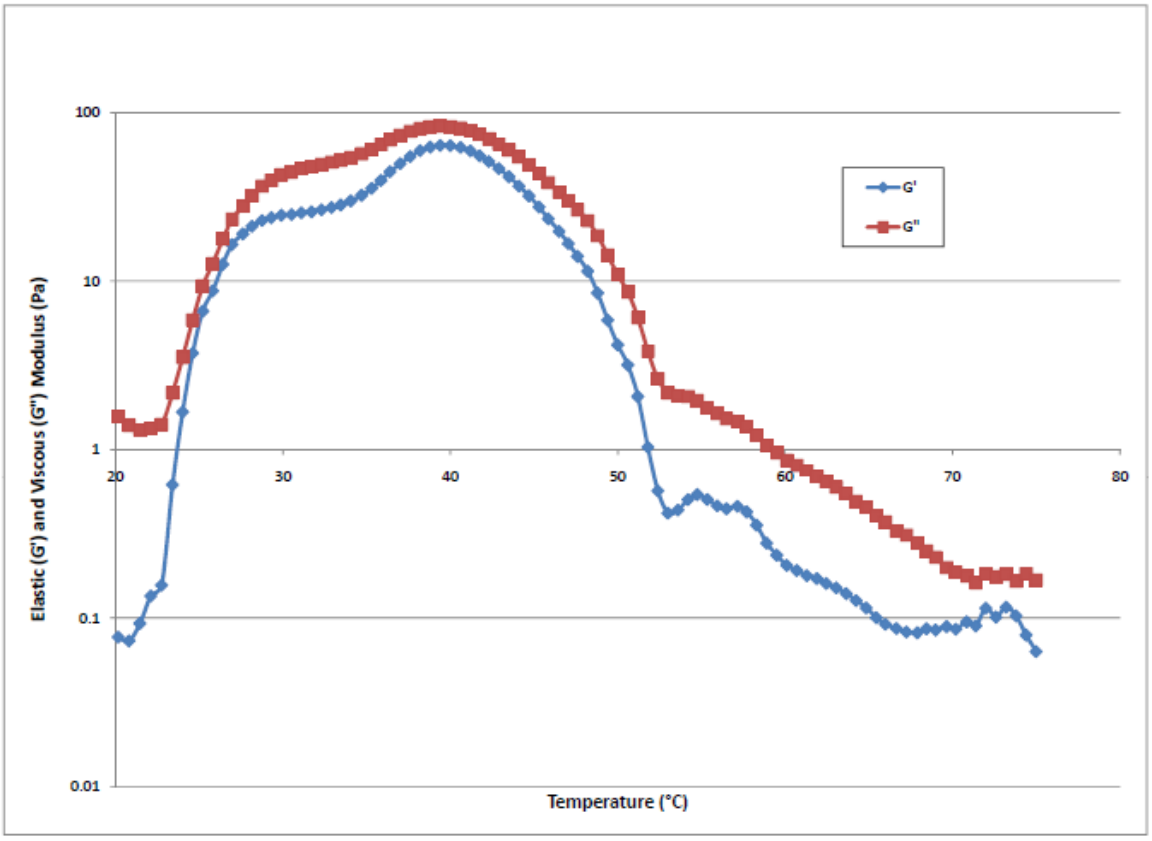

Figure 6.16 - Elastic and viscous modulus of 45% concentration of 35/65 mix of 550-2810-550 and 526-1404-526 triblock material with 0.03% Irgacure

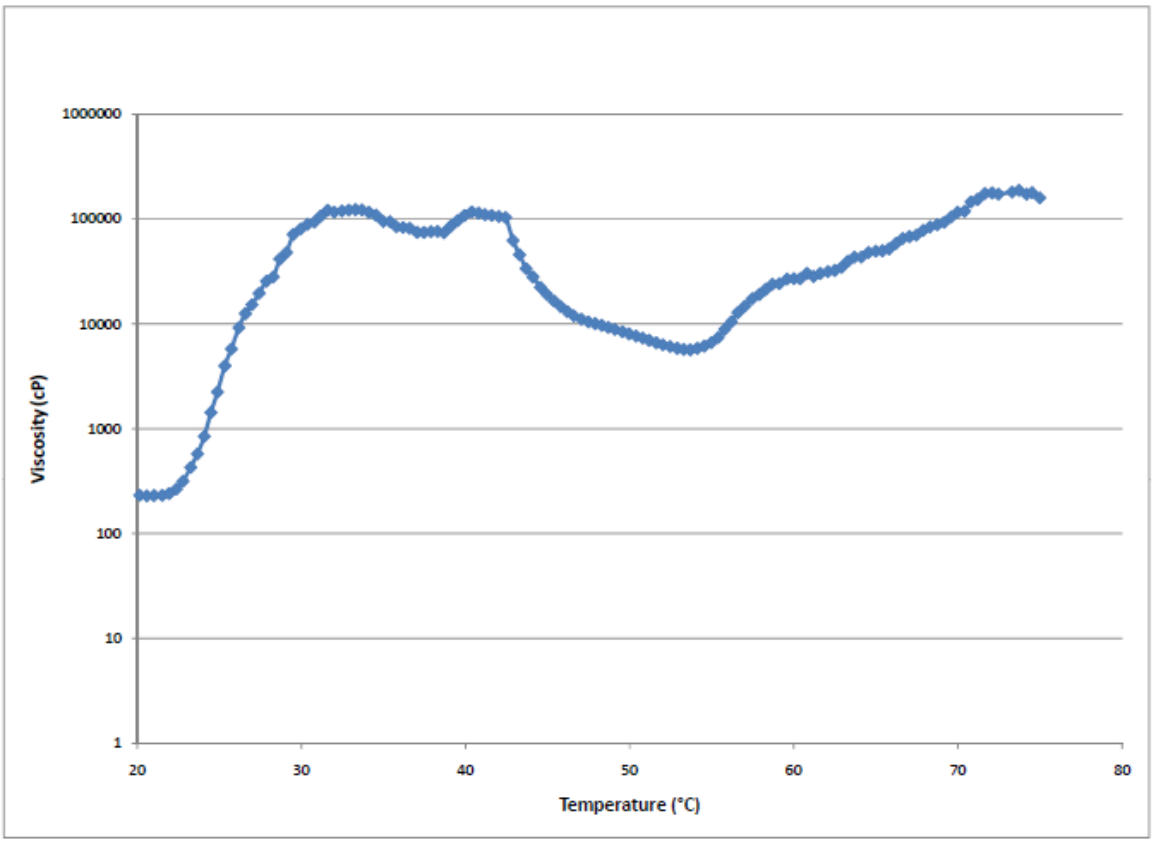

Figure 6.17 - Viscosity of 45% concentration of 20/80 mix of 550-2810-550 and 526-1404-526 triblock material with 0.03% Irgacure

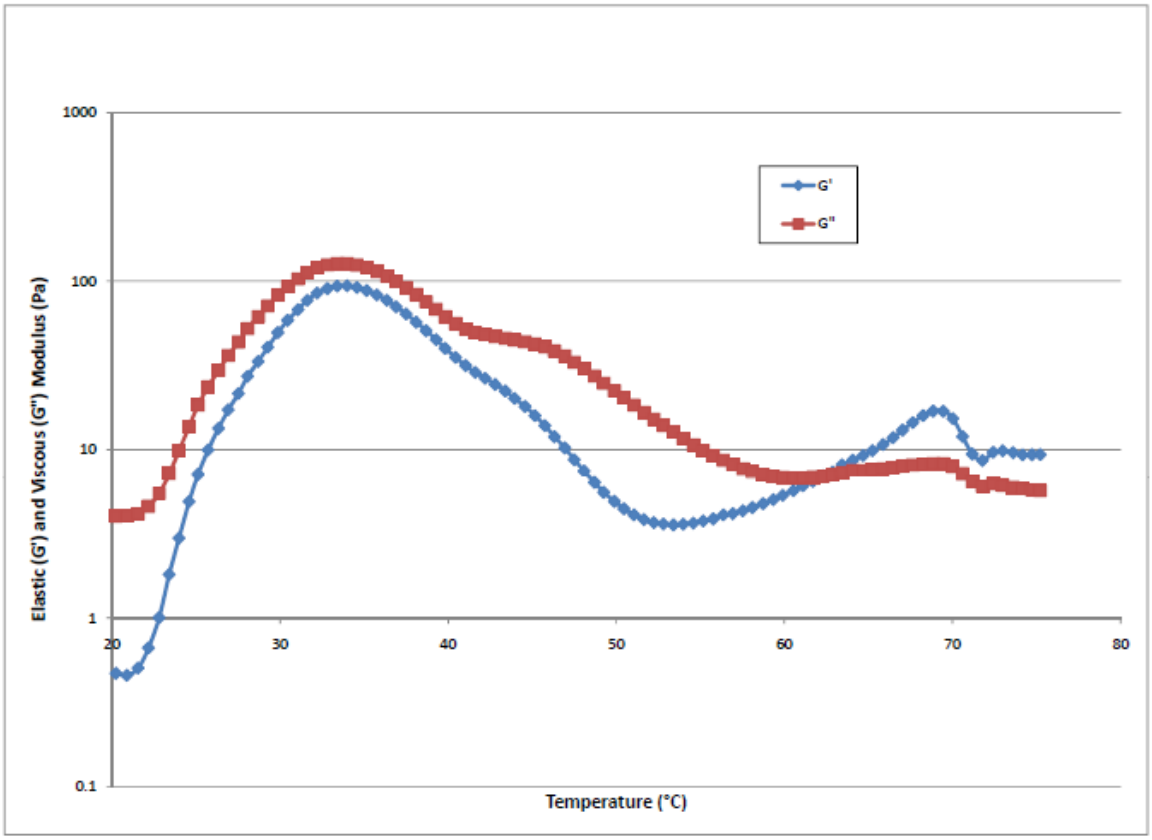

Figure 6.18 - Elastic and viscous modulus of 45% concentration of 20/80 mix of 550-2810-550 and 526-1404-526 triblock material with 0.03% Irgacure

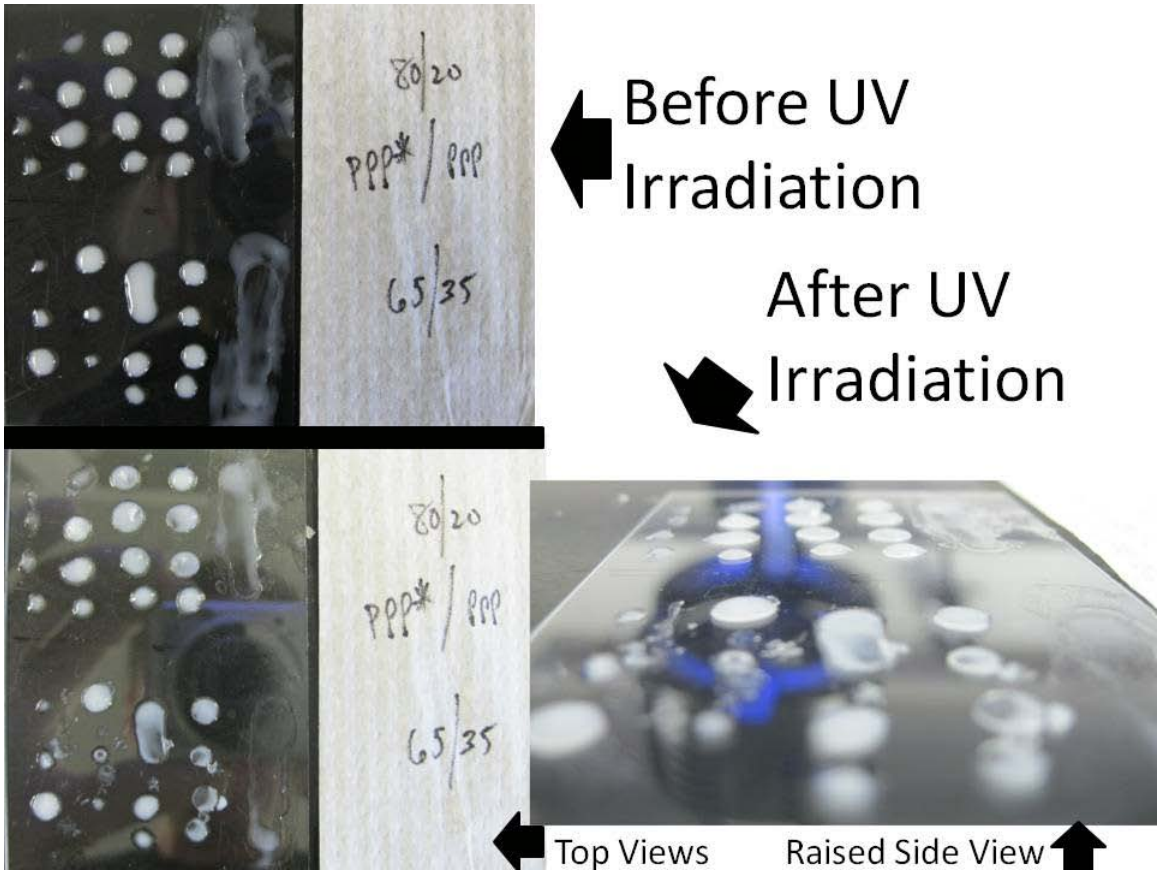

Figure 6.19 - Comparison of 20/80 mix to 35/65 mix triblock copolymer material

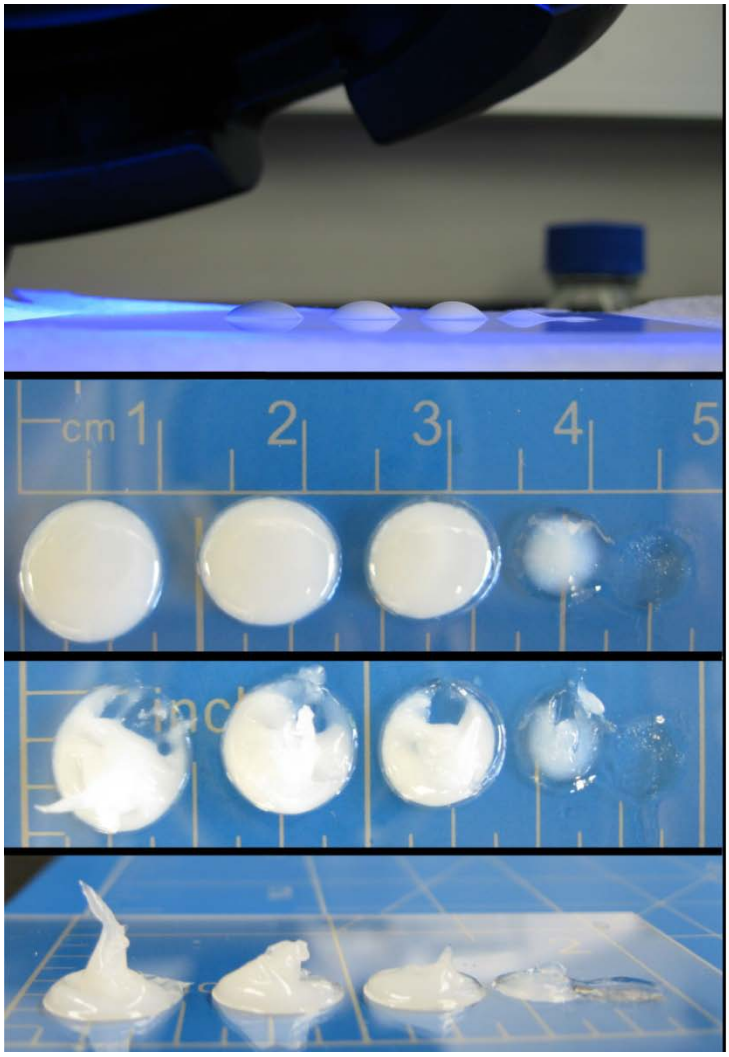

Figure 6.20 - 20/80 mix triblock copolymer material gelation

The material on the far left was a grouping of 5 droplets. Down the row, 4 droplets, 3, 2, and finally the droplet on the far right comprises of only one droplet.

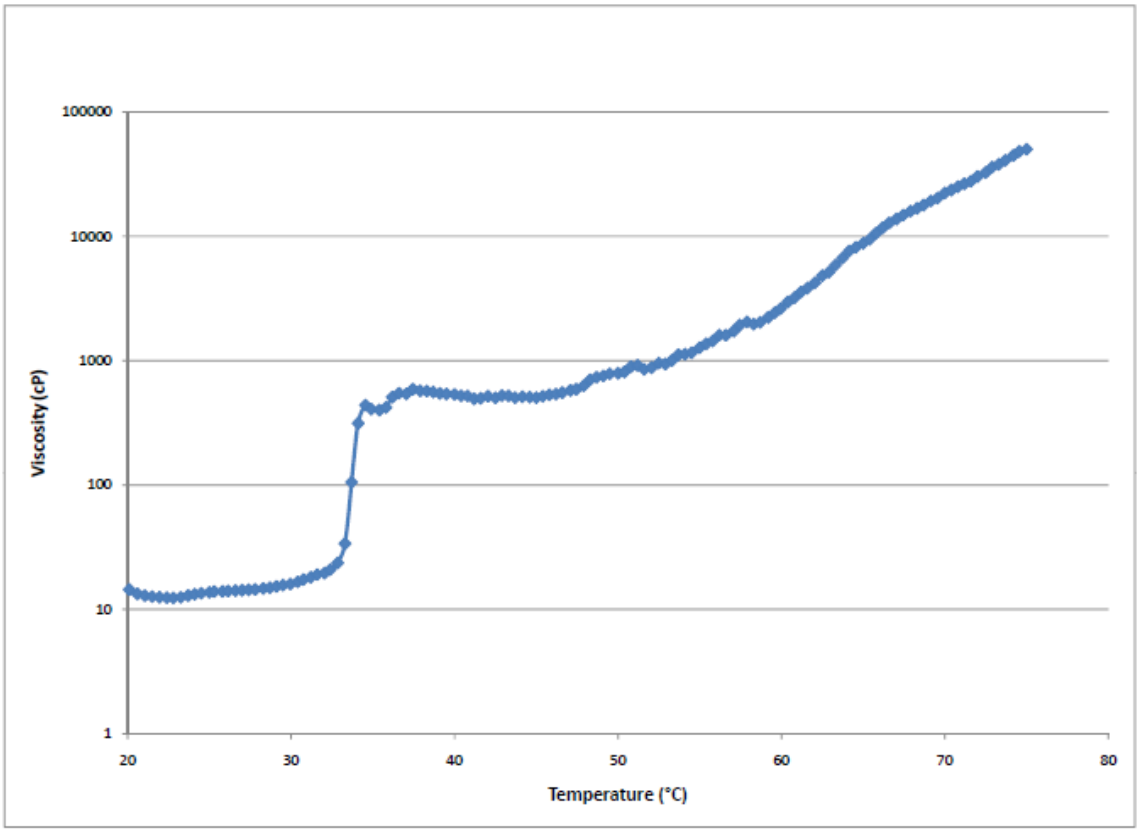

Figure 6.21 - Viscosity of 45% concentration of 10/90 mix of 550-2810-550 and 526-1404-526 triblock material with 0.03% Irgacure

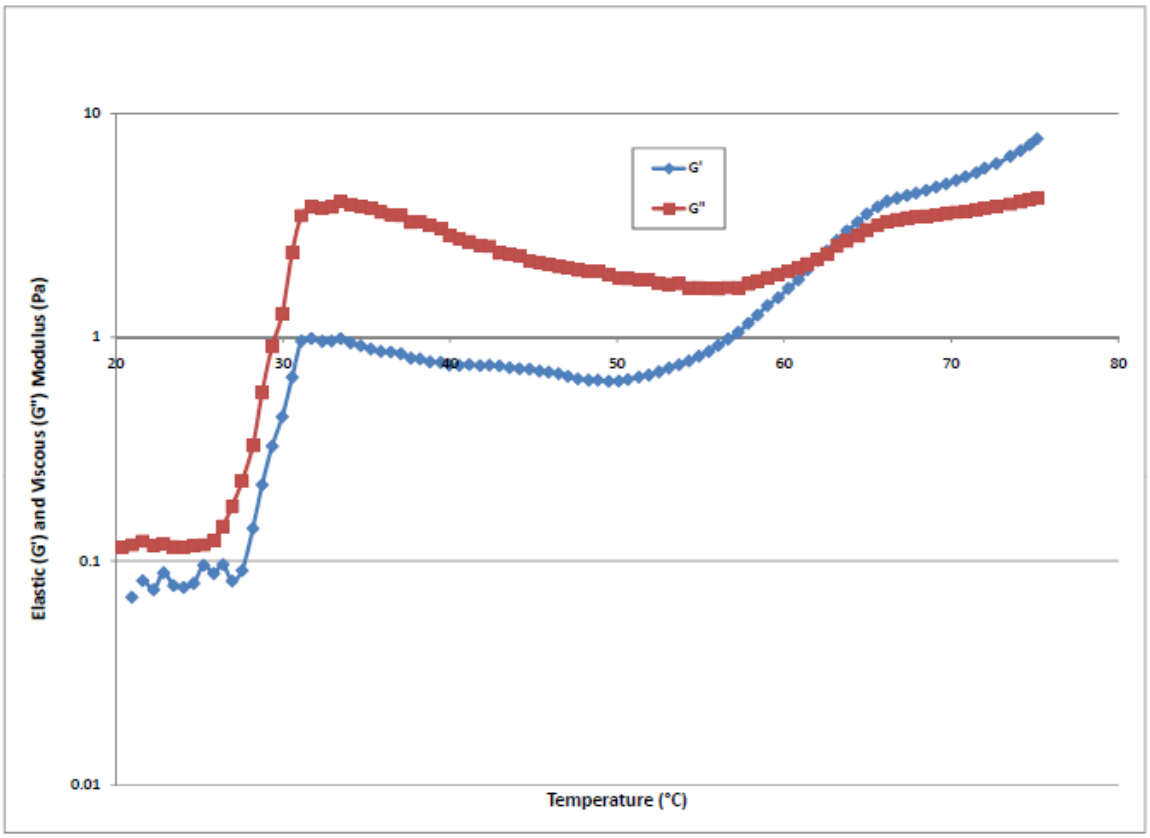

Figure 6.22 - Elastic and viscous modulus of 45% concentration of 10/90 mix of 550-2810-550 and 526-1404-526 triblock material with 0.03% Irgacure

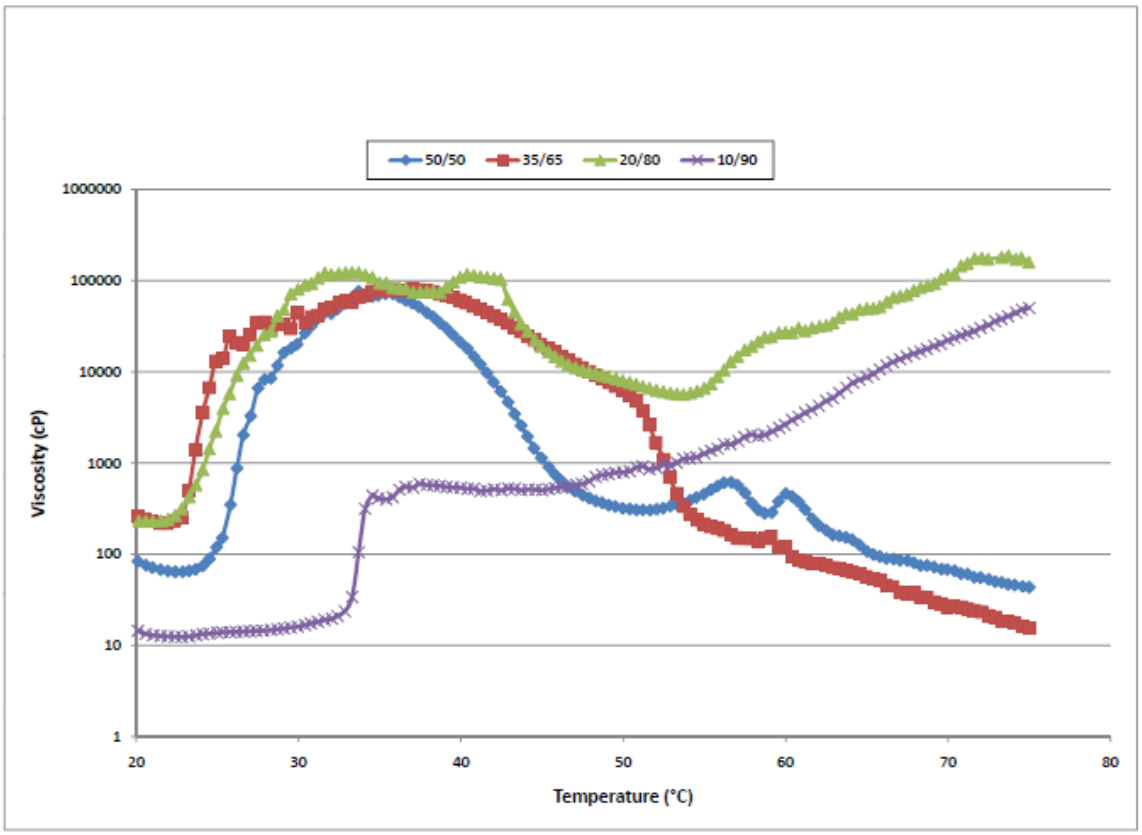

Figure 6.23 - Comparison of viscosity for all mixes of 550-2810-550 and 526-2810-526

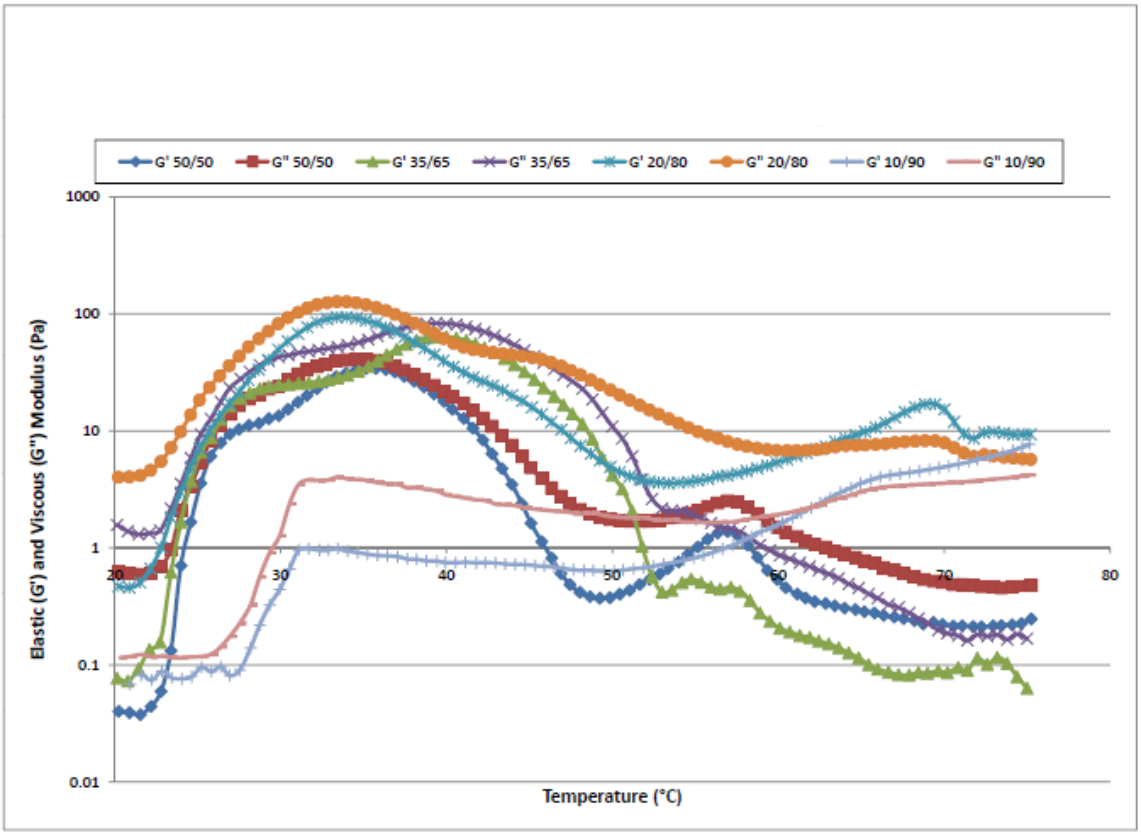

Figure 6.24 - Comparison of gelation characteristics for all mixes of 550-2810-550 and 526-2810-526

Table 6.4 - Elastic modulus comparison to measured liver tissue

Sample	Avg. Elastic Modulus (Pa)	Reference
20:80 Blend PPP:PPP	285.75 ± 63.2	
Liver	430 ± 81.7*	Chen, Ultrasonics 1996
Liver (Under 5% Strain)	640 ± 80*	Yeh, Ultrasound in Med. and Bio. 2002

***-** Measured using Ultrasonic technique

Chapter 7 : Assess the feasibility of the biomaterial for 3-Dimensional tissue scaffold printing

The aim of the work described in this chapter is to test the optimized biomaterial in a SFF printer. All of the necessary requirements have been met by the material and actual application tests are needed to verify application purposes. The tests will be completed using a 3-D printer developed in the Biomedical Design and Manufacturing Lab at Drexel University.

7.1 Introduction

A newly developed 3-D SFF printing system was created for this project to fabricate 3-D scaffolds for tissue engineering applications. Briefly, the SFF system is a three-axis printing machine capable of moving a 3-axis arm and delivery printing nozzles in the X, Y, and Z axis separately and/or simultaneously. This configuration provides the flexibility and control that enables the SFF system to create complex 3-D objects. The system includes multiple dispensing print heads with nozzles (Figure 7.1). Actuators and a solenoid driver were installed with a pneumatic microvalve to provide actuation speeds. A multi-valve controller was utilized to control the extrusion of two pneumatic nozzles independently or simultaneously. Two precise air pressure regulators and two digital gauges were implemented to provide precise pressure force to the printing material reservoirs and pneumatic nozzles. Two digital temperature controllers were utilized to maintain the temperature of the printing nozzles and the syringe barrels. A hotplate with horizontal stage was selected to provide a balanced and heated substrate for printing

(Figure 7.2).

7.2 Methods and Materials

For feasibility studies, a printer designed and built by the Biomedical Design and Manufacturing Lab at Drexel University was used. A schematic of the setup is shown in Figure 7.1 with an actual picture of the system shown in Figure 7.2.

7.2.1 Material Printing

7.2.1.1 2-D Printing

The printer abilities needed to be confirmed before printing structures to prevent clogging and damage to any parts of the printer. The variables that were significant to the printing process were frequency, printing speed (feed rate), valve pressure, material reservoir pressure, voltage, step time, needle temperature, and substrate temperature. To prevent damage to the printer, all values were initially tested in their respective low ranges of values. All of these variables effect the extrusion method of the material out of the printing nozzle. The method has a large affect on the consistency of the material being printing. There are three common modes of extrusion deposition: droplet, continuous, and contact (Figure 7.3). Each mode was tested to find the most efficient method of printing the material.

Once a set of variables were found to consistently print the material, 2-D circle shapes of 20mm diameter were printed on a heated substrate. After printing , the circles were placed under a UV flood light to photocrosslink the material. The resulting layers were examined to verify full gelation. The final layer height of the gelled material was also necessary to acquire for z-axis height in 3-D printing. Once a set layer height was determined, it can be programmed in to the software so that the printer automatically increments the z-axis movement for each layer.

7.2.1.2 3-D Printing

Following the successful printing of individual layers, two different 3-D designs were created for modeling with our material, the Drexel D and a 3 tiered round birthday cake (Figure 7.4). The models were printed 5 layers at a time with breaks for UV light irradiation.

7.2.2 Software

The software procedure of the printing process is shown in Figure 7.5. First, a 3-D model is created using CAD system, then Modelworks slicing software is used to carve a STL 3-D model into a 2-D contour ".SLC" file. The developed MATLAB script is implemented to read the ".SLC" files and integrate the model coordinates and the printing path into CCStudio. In this control scheme, MATLAB is always the host software that reads the slice files and sends command signals to control the motion of the three arms and to direct the nozzle controller for printing.

A MATLAB based GUI integration interface has been developed to minimize the operating procedures for users (Figure 7.6). Users are able to enter ".STL" file names to print and create a separate file that combines multiple files into one seamless file. Each ".STL" file needs a tool number which corresponds to the material and the printing nozzle. To use this software, we first needed to utilize a CAD program to create a heterogeneous structure which has two distinct models which are then individually saved in binary ".STL" format files. For now, this prototype software is only designed for identifying two materials and for use with one or two nozzles. The system has the capabilities to add up to six materials for six independent printing nozzles but is currently only optimized for up to two. The user friendly integrated software can also be modified to recognize six models as a heterogeneous structure.

By sequentially clicking the steps on the integrated software, ".STL" files are sliced into ".APT" language files and then the two ".APT" files are automatically combined into a single ".APT" file. Automatic modification functions are applied to alter commands and add a transition code between each layer of each ".APT" file database. After the modification, a complete ".APT" file has been created and is ready for simulation or printing purpose.

7.2.3 Hardware

The mechanical moving system consists of three servomotors and three linear digital optical encoders with a precision of 0.5 μm used in conjunction with the Texas

Instruments DSP (Digital Signal Processor) microprocessor. A 741MD-SS needle microvalve (Figure 7.7) was used as the printing nozzle for the PEG-PLGA-PEG/PEGma-PLGA-PEGma mix material. The dimensions of this microvalve include a total length of 127.5mm, outside diameter of 26.7mm, and various needle inner diameters of 100, 150, 200, 250, 330, and 410 μm. The pneumatic microvalve has an adjustable needle stroke with a unique calibration feature that allows the user to maintain an exact deposit size of low to high viscosity fluids with exceptional control. Air pressure retracts the piston and needle, lifting the needle off the seat inside the dispensing tip, and permitting fluid flow through the tip. Once the cycle is complete, air pressure is exhausted, which will cause the piston spring to return the needle back to its original position, subsequently stopping fluid flow. The stainless steel shutoff needle is seated in the hub of the dispensing tip rather than the valve body. This design minimizes dead fluid volume by having fluid cutoff occur as close as possible to the dispensing orifice. The pneumatic microvalve can work by continuous extrusion or droplet deposition according to the printing frequency and back pressure setting. In order to obtain smooth 3-D microstructures, continuous extrusion was adopted as a printing method to form the structure. Due to the fact that our printer was using pneumatic microvalves, we were able to preheat the material to help initiate micelle formation by heating the barrel and syringe tip. A 120 cm long heating tape was used to maintain constant temperature by wrapping the syringe barrel. The printing nozzle was also enclosed by a heating barrel to keep constant temperature. Two thermocouples (OMEGA) were placed between the heating tape and the syringe and between the microvalve and the heating barrel to monitor temperature.

Disposable needle tips are long stainless steel tubes which can be very easily clogged by high viscosity material. A custom made copper tip with inner diameter of 250μm was designed to replace the disposable needle tip (Figure 7.8). The copper tip helps keeps the solution at the same temperature as the microvalve. A valve actuator was installed on the pneumatic microvalve to provide actuation speeds as short as 5 milliseconds, and cycle rates as high as 600 per minute. A commercially available 10cc polypropylene syringe barrel with piston was used as the material container to deliver the solution. The syringe barrel was connected with compressed air to provide back pressure to thrust the material into the chamber of the valve. The intensity of the pressure was totally dependent on the property of the material used.

7.3 Results & Discussion

7.3.4 2-D Printing

Before demonstrating 3-D printing, printing of simple designs in 2-D was needed to verify that the printer could handle the material. The 20/80 mix of PEG-PLGA-PEG and PEGma-PLGA-PEGma was printed and was capable of precisely printing a circle. This simple design was used in order to adjust the settings of the printer to be able to handle the material. UV light distance, frequency, and air pressure to the reservoirs and needles were necessary to vary to find the optimal value so that the printing material was able to easily flow out of the tip of the nozzle on command. The final settings for the printer can be found in Table 7.1. Frequency was found to be an important variable in printing our material. It had a great effect on the extrusion method we chose. Figure 7.9 shows

attempts of the continuous and contact extrusion modes. The continuous extrusion deposition mode allowed for the most consistent diameter of line while printing our material. Using any other mode caused clumping of the material on the substrate. To be able to print precise architecture, a consistent printing line is needed so we decided to use variables that allowed us to print the material continuously. The frequency was initially tested at 4 Hz but was found through steps of 2 Hz that 8 Hz provided the optimal flow of material for printing. Substrate temperature was optimized to 35°C in previous work but the addition of heat to the needle helped to decrease the solidification time of the material. Because we used a pneumatic valve, we were able to handle higher viscosity. The addition of a heated needle increased solution viscosity but since we were able to handle it, the decrease in solidification time helped printing time. The material was never static in the printing needle so a needle temperature of 35°C initiated the micelle formation in the material before actually being printed. We used a default value for printing speed, valve pressure, and voltage of 100 cm/min, 75psi, and 0-5V square wave respectively to help decrease variables. To prevent random large air pockets in the print material tubes, it was found after testing reservoir pressures of zero to 3 psi, a value of 0.1 psi worked best. Finally, step time of the material affected flow of the material and contributed to the width of the material line being printed. Two different needle tips were tested at time intervals ranging from 40-80ms. To form the most consistent thinnest line, it was concluded that the 150μm needle at a time interval of 70ms would be the best choice. Unfortunately, with a thinner needle tip, there was no consistency in line width.

Shapes of circles were printed using the best variables followed by photocrosslinking (Figure 7.10). The circles were designed to be a diameter of 20mm. The printer was designed to print the exact design and not to account for printed material width. Printing precise circles with consistent diameters allowed the progression of printing to move to 3-D structures.

7.3.5 3-D Printing

Initial printing in 3-D proved to be difficult due to the fact that a droplet of material could not fully gel on top of the previous layer. The sequentially printed layer tended to fall off the sides of the previous layer. This created a structure that was not the height of two fully gelled droplets as well as a structure that was larger at the base than one gelled droplet. This effect was called the pyramid effect because if one droplet was placed on top of another over and over again, a pyramid, instead of a pillar, would be formed. To compensate for this effect, the distance of the UV light was varied and kept at maximum intensity on the newly printed droplets. A minimum height of 15cm was possible due to space needed by the movement of the printing arm in the X and Y directions.

Two designs for 3-D printing were used, a Drexel D and 3 tiered birthday cake. The Drexel D design consists of a 2-D drawing printed over and over again; multiple layers combined to create a 3-D structure. The Drexel D structure is a total of 20 layers of printing, the height and overall look of the structure is shown in Figure 7.11. The cake design consists of three levels; each level is a solid circle repeated 10 times followed by

the next level which is another solid circle but with a smaller diameter. This cake design was used to represent the full 3-D structure capabilities of this material. Overall views and a side view is provided in Figure 7.12. The pyramid effect is visible in the side view of the 3 tiered cake structure. Due to the pyramid effect, the edges posses a low slope that leads to the substrate, the edges of the cake are not as clean as originally intended. This effect is mostly just visible on top of the substrate, the top two tiers of the cake have crisper edges. The spread of material in the bottom layer was tracked and found to slow after 7 hours (Figure 7.12D). This effect is believed to be due to the low surface contact angle of the printing substrate as well as the total time printing. Because of the size of the design, the whole build took over 2 days. The material was left out printing for the duration of the printing allowing for additional factor to contribute to the final shape of the structure.

7.4 Conclusions

Printing variables were tested in order to find an optimal extrusion deposition mode for printing a 20/80 mix of PEG-PLGA-PEG / PEGma-PLGA-PEGma material. Custom nozzle tips were manufactured to help aid in continuous deposition since this type of mode would work best with the equipment and setup we built . 2-D circle designs were printed to further optimize the variables to allow for 3-D printing. A 3-D Drexel D and 3 tiered birthday cake were printed to prove the 3-D capabilities of the material. A pyramid effect was observed in both designs by the material that was initially printed onto the substrate; the angle between the material and substrate, contact angle, was very large.

Once layers of material were allowed to photocrosslink, the subsequent layers did not exhibit this pyramid effect.

A 3-D structure was possible with our SFF printer using a 20/80 mix of PEG-PLGA-PEG / PEGma-PLGA-PEGma material. Printing time was decreased with the use of a heated nozzle as well as UV irradiation after every 10 layers of material. The final Drexel D and birthday cake structures were able to retain their shape even after printing and removal from the substrate. To acquire more precise structures, a longer printing time would be needed to allow for increased UV irradiation breaks. This additional time would allow for the quicker transition of material to an irreversible material, preventing any further deformation of the printed structure.

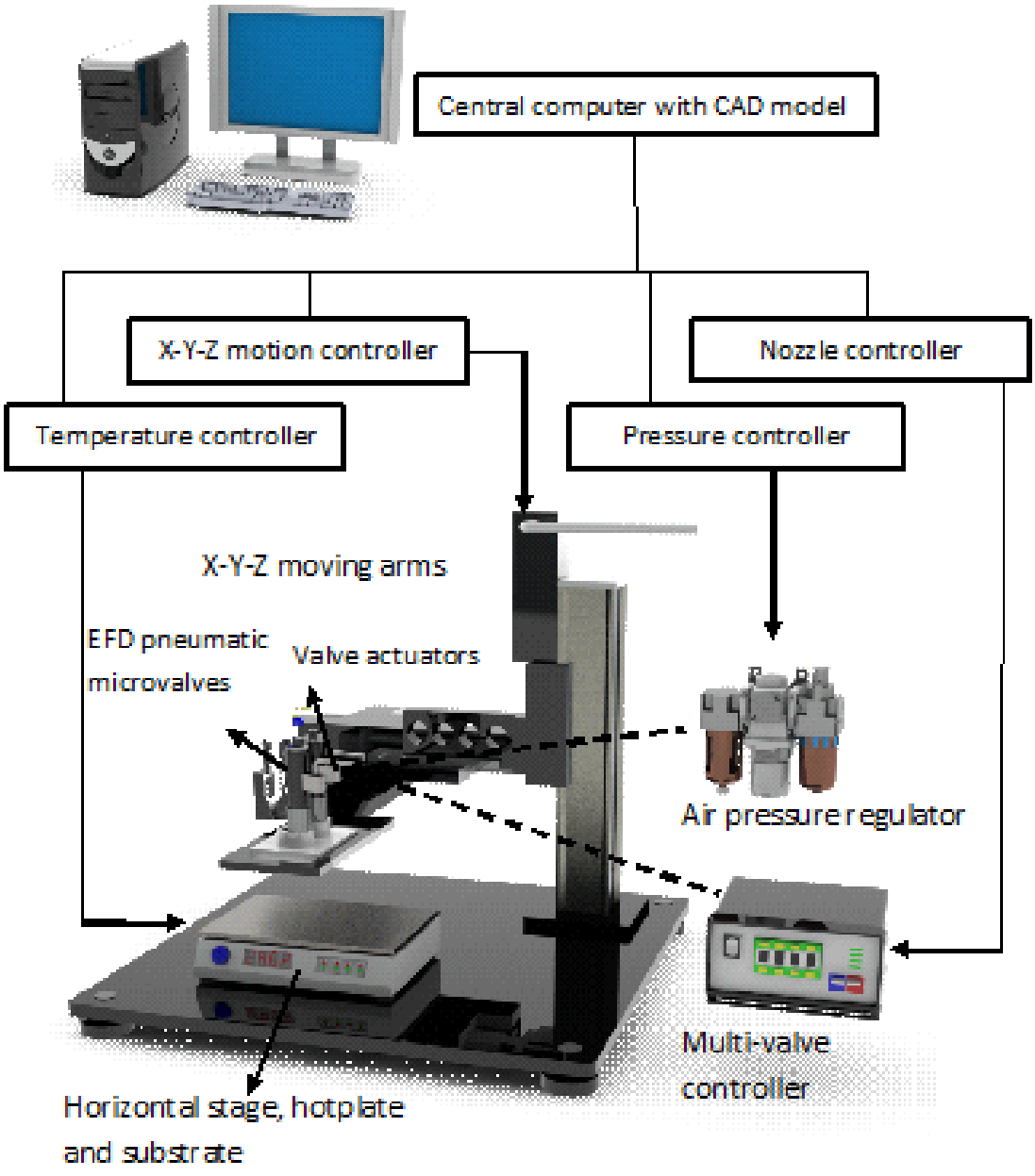

Figure 7.1 - Schematic of 3-D Printer

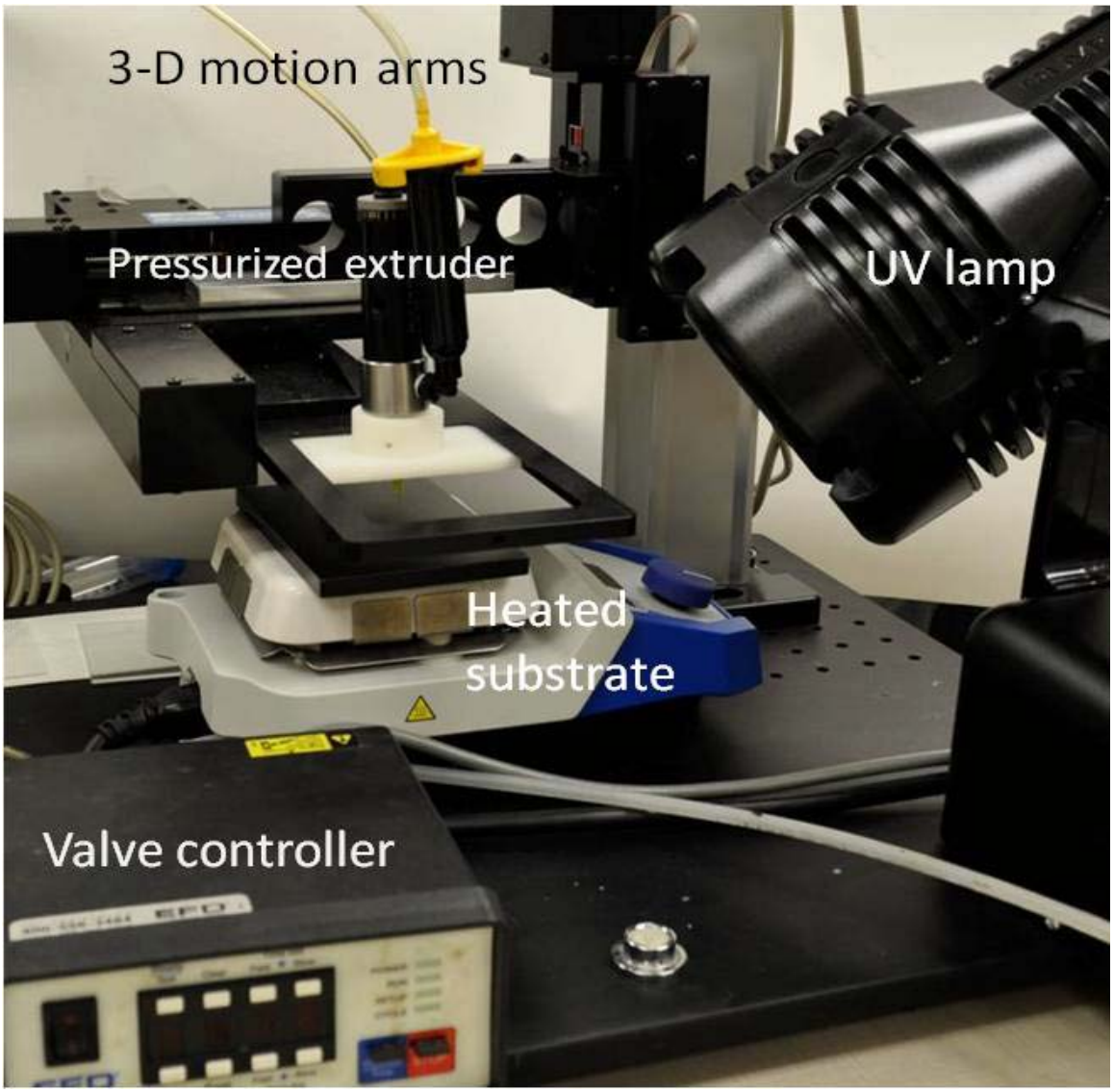

Figure 7.2 - Actual 3-D Printer Set-up

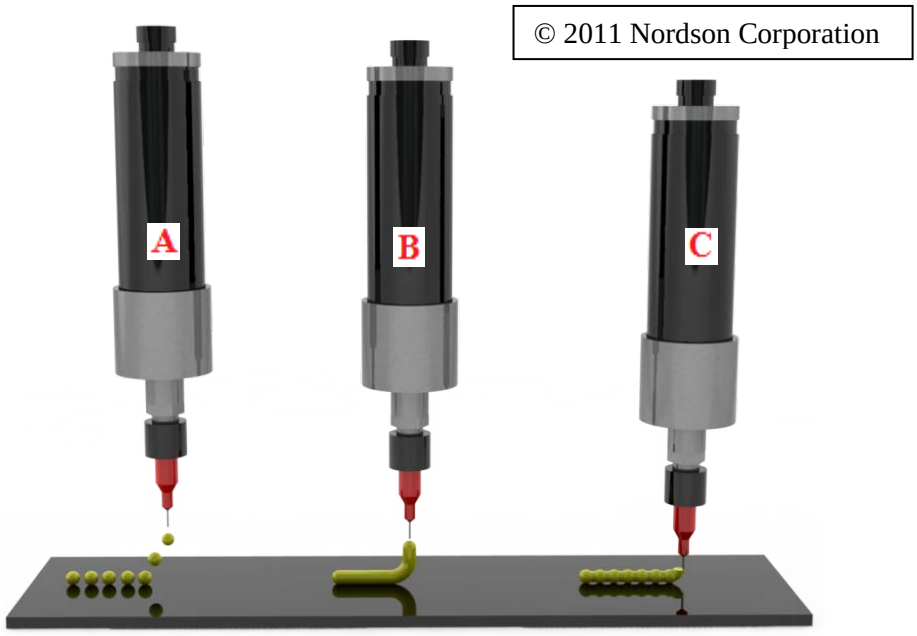

Figure 7.3 - Extrusion method deposition modes: A) droplet mode, B) continuous mode, and C) contact mode

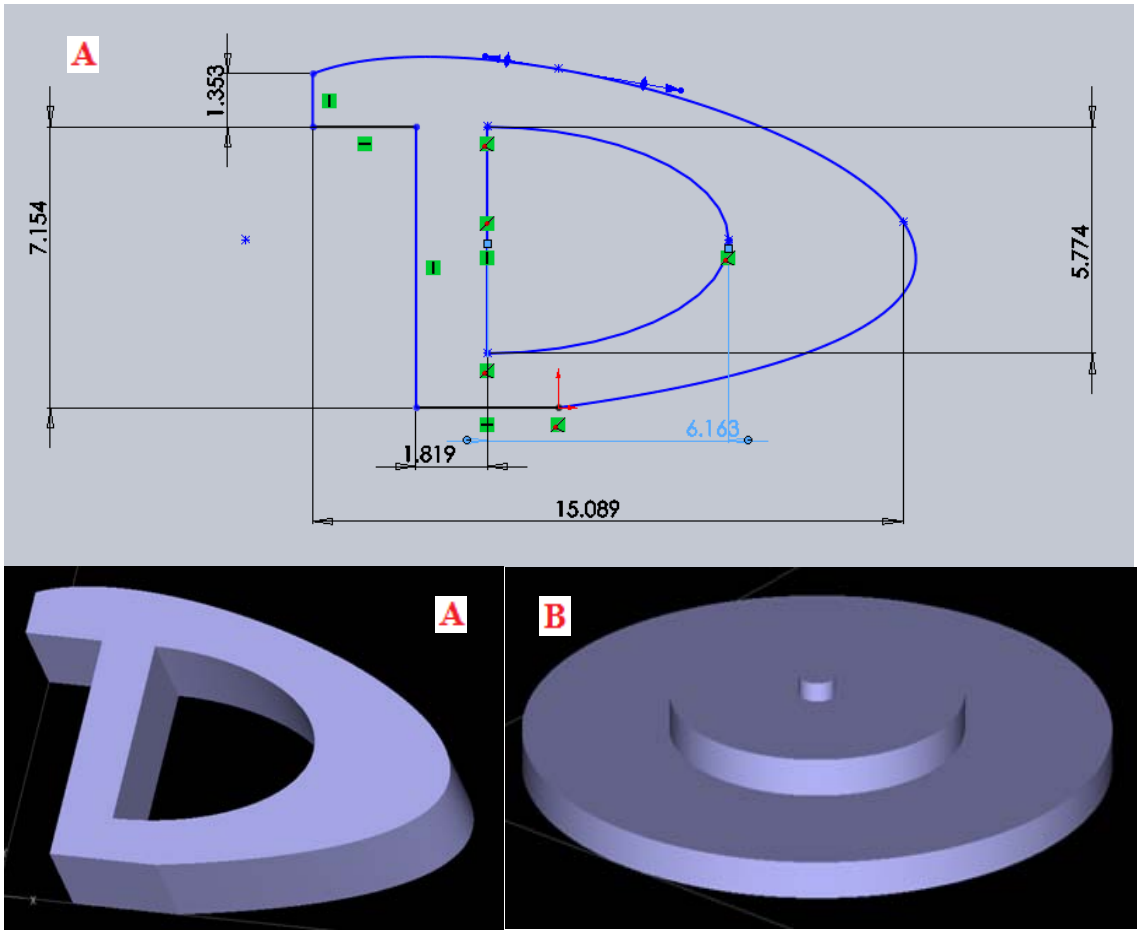

Figure 7.4 - 3-D structure designs: A) Drexel D, B) 3 tiered birthday cake

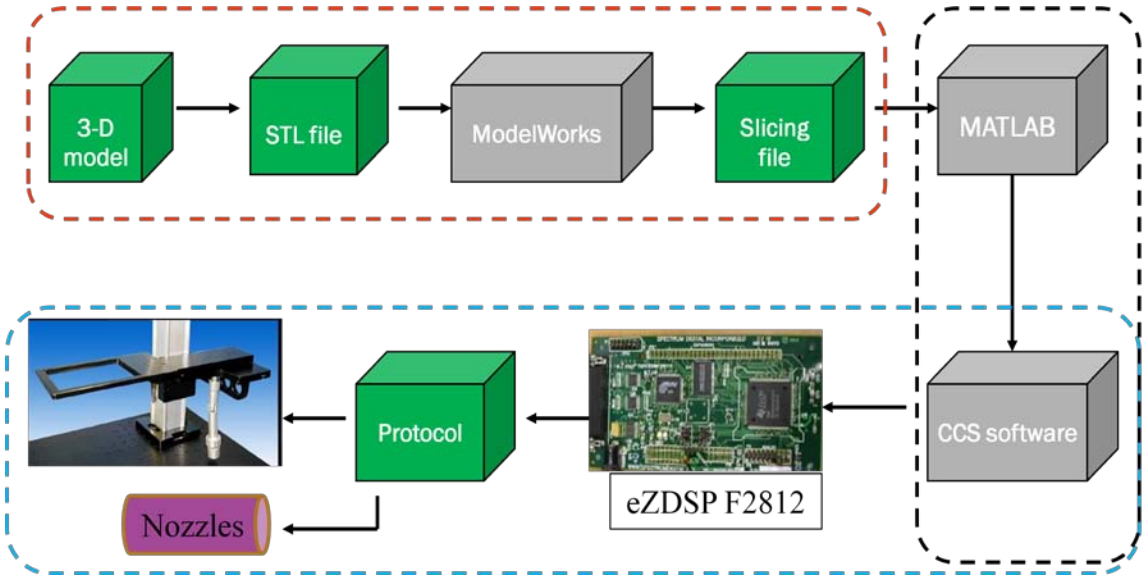

Figure 7.5 - Schematic of the Software Printing Process

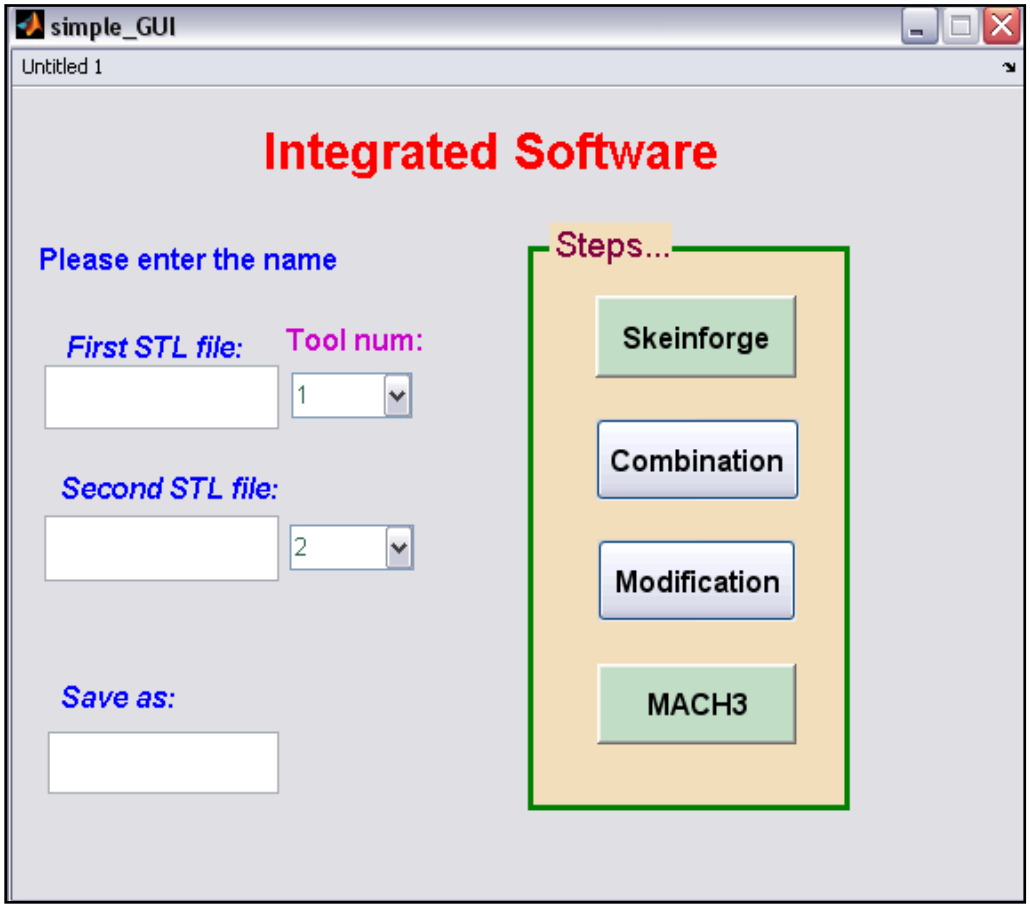

Figure 7.6 - Integrated Software for 3-D Printing Preparation

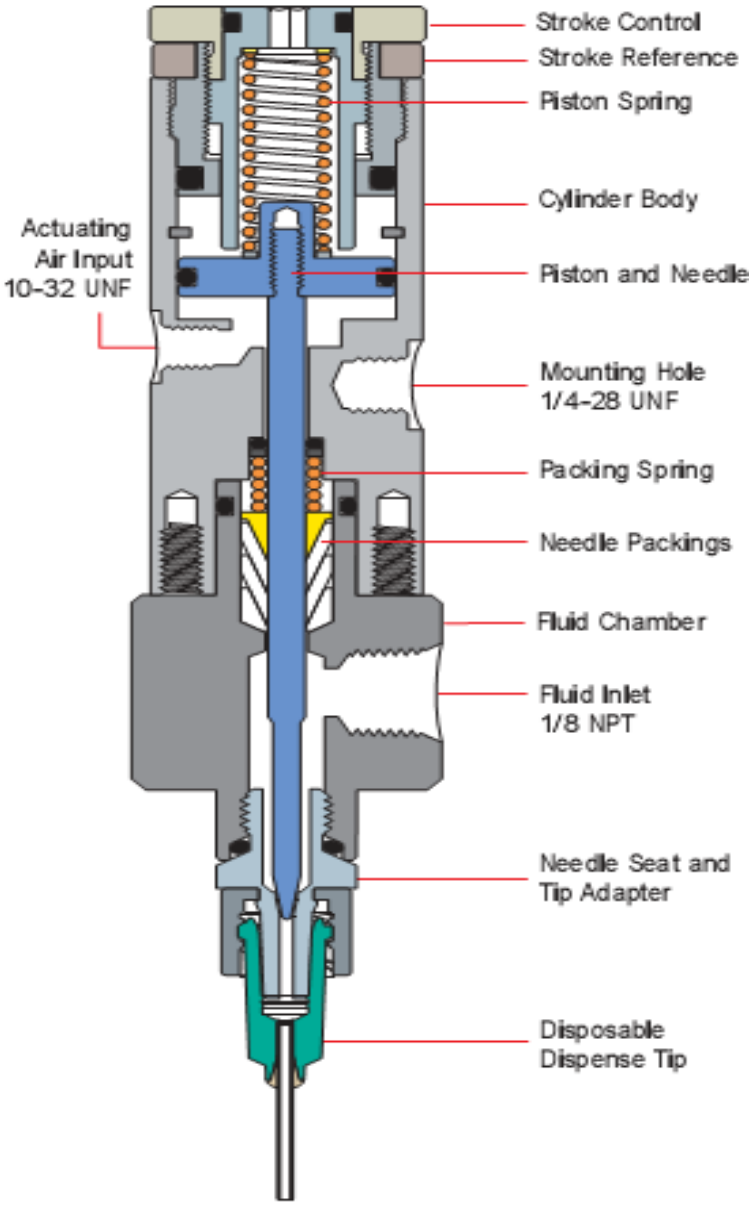

Figure 7.7 - Schematic of 741MD-SS Needle Microvalve [123]

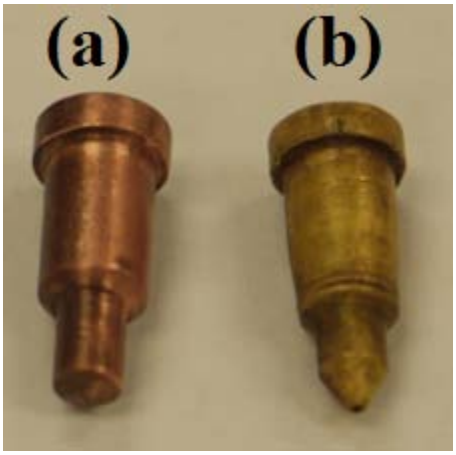

Figure 7.8 - Custom Copper Needle Tips of Inner Diameters (a) 250 µm and (b) 500 µm

Table 7.1 - SFF printer variables tested and final values

Variable	Tested Values	Final Value
Frequency	4, 6, and 8 Hz	8 Hz
Printing Speed (feed rate)		100 cm/min
Valve Pressure		75 psi
Material Reservoir Pressure	0-3 psi	0.1 psi
Voltage		Square Wave 5/0 V
Step Time	40-80 ms w/ 100 um needle 40-80 ms w/ 150 um needle	70 ms w/ 150 um needle
Needle Temperature		35° C
Substrate Temperature		35° C

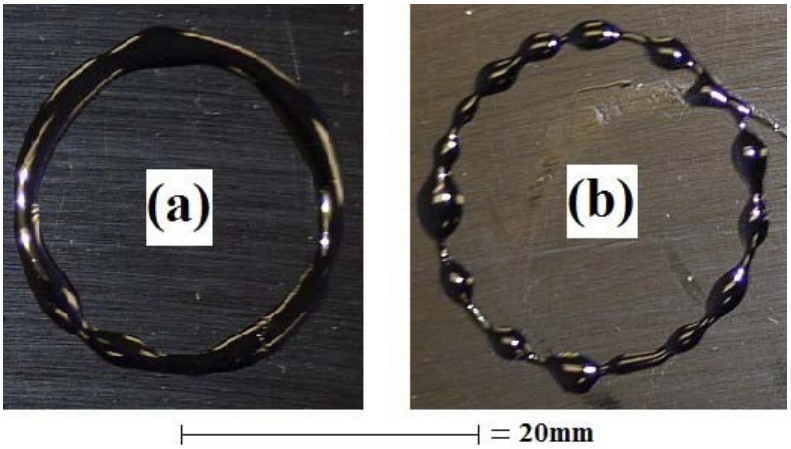

Figure 7.9 - 2-D printed circles: (a) Continuous and (b) Contact. Width of line = 1mm

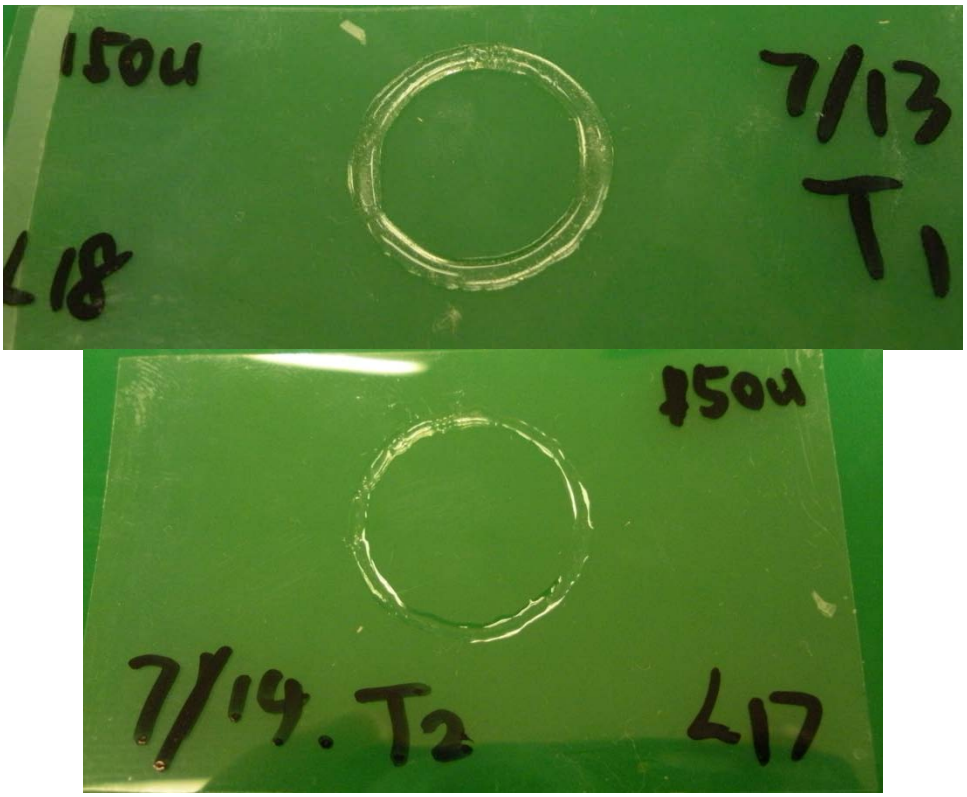

Figure 7.10 - Final printing variables confirmed. ID =19mm OD = 21mm

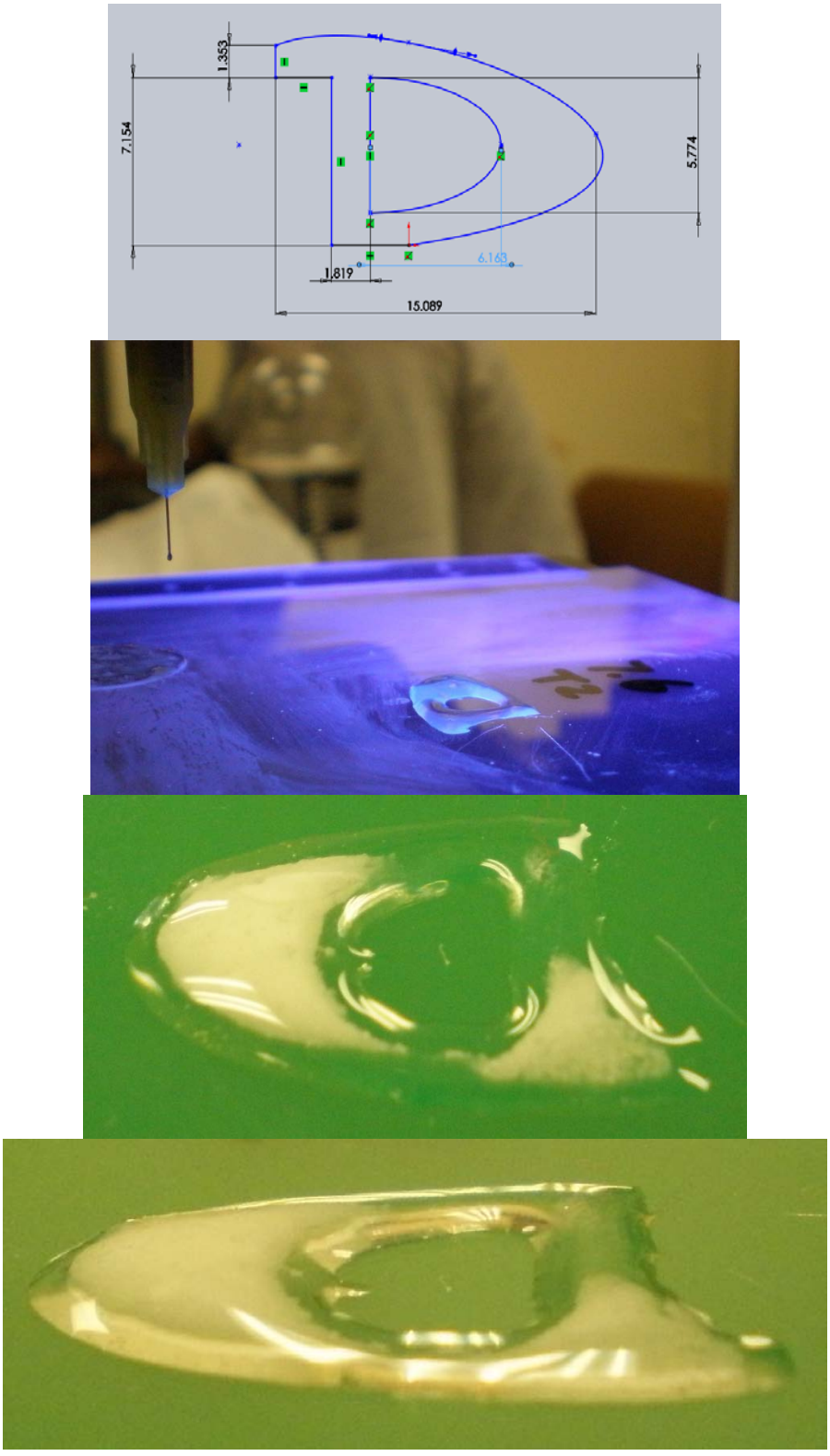

Figure 7.11 - 3-D Drexel D structure (10 layers)

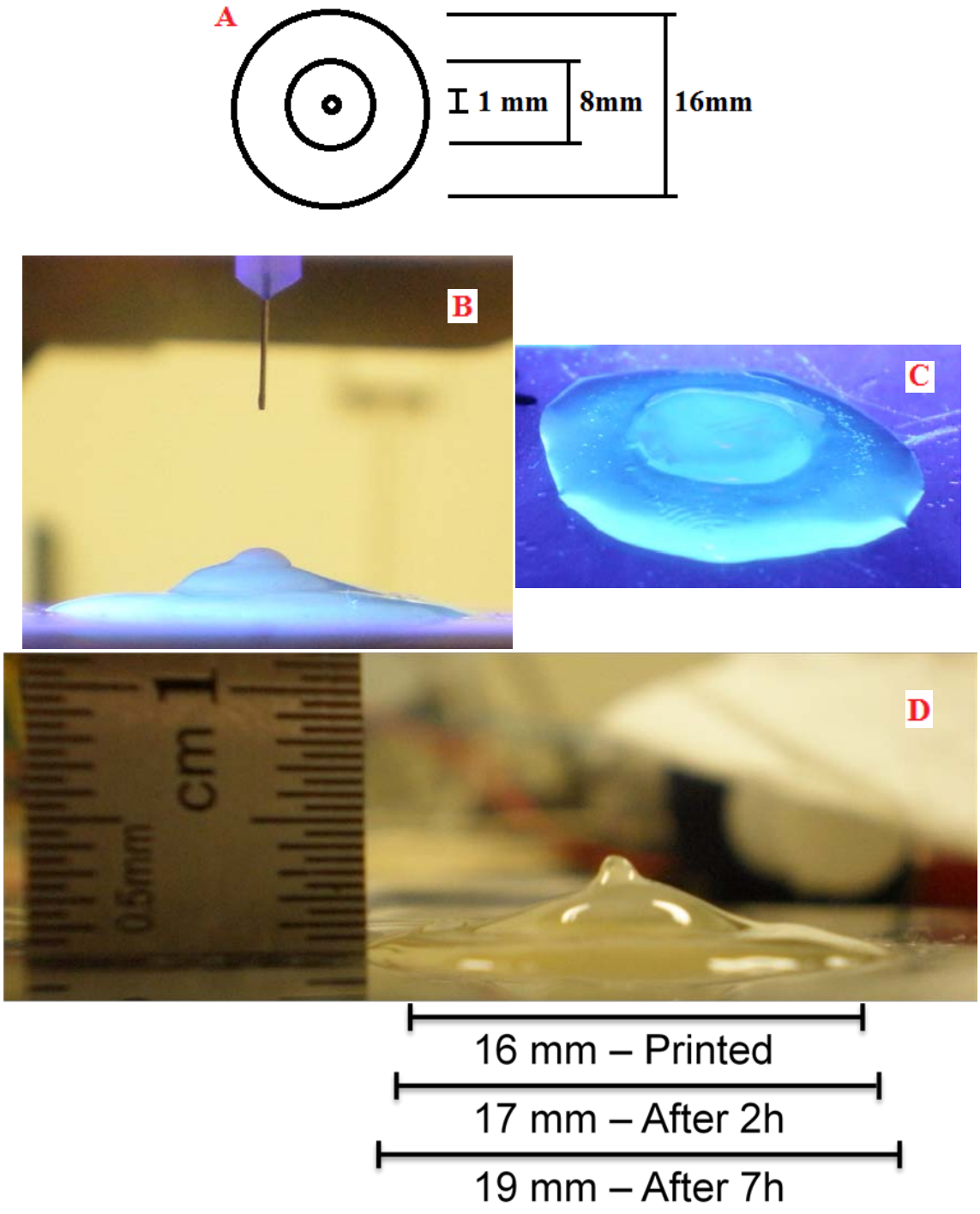

Figure 7.12 - 3-D Three tiered birthday cake: A) program dimensions, B)side view of printed structure, C) isometric view of printed structure, and D) time duration spread effect during printing

Chapter 8 : Conclusions and Recommendations for Future Work

8.1 Conclusions

A novel material has been developed that is capable of being used in numerous types of solid freeform fabrication printers to print 3-dimensional scaffolds for soft tissue. Bio-printing materials that have been or are currently being used for building scaffolds were researched and were unacceptable for use in our multiple SFF printers. A 20/80 mix of low molecular weight PEG-PLGA-PEG and low molecular weight PEGma-PLGA-PEGma triblock copolymer dissolved in DI water produced a material that is of low viscosity to allow for easy movement through SFF printers. This biocompatible and degradable material possesses a two stage gelation process. It is a non-viscous 228 cP solution at 20°C and quickly transitions to a 122,836 cP material with an increase in temperature to 33°C. To increase the material properties further and create a network of irreversible crosslinks, irradiation of UV light is needed. This material accomplishes all necessary requirements for it to be applicable for SFF printers: 1) low viscous solution before printing, 2) no mixing is needed to form a homogenous gel, 3) has a short solution to gel transition time, 4) mechanically strong material to allow for vertical building, and 5) irreversible gel to prevent deformation of the final printed structure. This is the only biomaterial available that is capable of meeting the conditions previously mentioned. There are no other previously reported synthesized materials like this PEGma-PLGA-PEGma triblock polymer.

Chitosan and other naturally derived materials were investigated for use as a common material in SFF printers. But, their inability to be a non-viscous solution, gel rapidly, or gel without complicated or time consuming steps does not allow for simple use with multiple printers. A photocrosslinkable material permits quick gelation and eliminated the need for multiple print heads since it does not need another crosslinking material. The challenges with photocrosslinkable material was the UV light irradiation source and the ability of a droplet of material to hold its shape after printing before gelation. Thermosenstive materials were able to gel rapidly allowing for material to hold its shape after printing but, unlike photocrosslinkable material, reversible. To be able to create a thermosensitive material with the mechanical properties to allow for 3-dimensional building, a high viscous initial material was needed after printing and before irradiation. A combination of thermosensitive and photocrosslinkable material met every need for SFF printing.

The thermosensitive material, PEG-PLGA-PEG, was examined as well as the mechanism of gelation and the effect of altering the molecular weights of the PEG and PLGA. PEG-PLGA-PEG, dissolved in water, becomes a gel as temperature increases past its sol-to-gel transition point because of the formation of micelles in the material. PLGA is hydrophobic and is the driving force of micelle formation. As temperature increases, the PLGA parts of the copolymer chains clump together with the PEG compounds interacting with the water because of its hydrophilicity. The micelles continue to grow as temperature increases. At a temperature point, PEG becomes as hydrophobic as the PLGA and the micelles break apart reverting back to a liquid solution.

The synthesis of the triblock had to be established with additional steps needed for purification. These additional steps eliminated any pH problems as well as helping viscosity problems since extra solvents in the final materials were preventing full gelation. By increasing the molecular weight of the PEG, the viscosity of the initial solution increased without any effect on the final gel. A very high molecular weight of PEG did not dissolve in water, it tended to clump together and solidify while in water. The increase in molecular weight of PLGA had a similar effect as PEG. A higher molecular weight of PLGA created a solution of higher viscosity. Too high of molecular weight of PLGA created a material that was too hydrophobic to be soluble in water (Figure 8.1). Viscosity tests using a viscometer revealed that as the concentration of triblock polymer increased in water, the viscosity of the initial solution increased as well as the maximum material viscosity. It was interesting to note that the temperatures at which gelation occurred decreased as the concentration increased. Oscillatory tests completed on a rheometer show that the maximum elastic modulus, G', which correlates to the mechanical properties as a gel, are similar at maximum viscosities. The 45% concentration of triblock showed the greatest viscosity of 15,830 cP. This viscosity is comparable to the viscosity of chocolate syrup, which is unable to hold its shape and therefore unable to be used as a 3-D building material.

To help increase the mechanical properties and long term stability of the gel, Irgacure 2959, a photoinitiator was added to the triblock. Irgcaure 2959 works by breaking double

bonds between carbon molecules, stabilizing that bond, and then repeating. Irgacure 2959 breaks apart into free radicals once it is initiated by UV light irradiation. The free radicals are what break apart the carbon double bonds because they are less stable than single carbon bonds. The radicals start a chain reaction of breaking apart carbon double bonds and securing other available free carbons to form a network of crosslinks. PEG-PLGA-PEG does not have any available carbon double bonds for Irgacure to break so a different type of PEG was needed since the PEG was the outside component of the triblock with an available free end. PEG methacrylate was substituted for the original PEG methyl ether. The synthesis of this polymer to create a PEGma-PLGA-PEGma tiblock polymer was the same as the PEG-PLGA-PEG material. This new material was investigated to see if it was capable of gelation thermally and photocrosslinkablely. Thermally, PEGma-PLGA-PEGma (526-2810-526) was unable to gel or even increase its viscosity. The polarity of the new acrylate group at the end of the PEGma interferes with micelle formation because it is somewhat hydrophobic, too similar to the hydrophobicity of the PLGA. The length of the triblock chain affects the formation of micelles so the PLGA molecular weight was varied. Results were similar to the results of varying PLGA molecular weight in PEG-PLGA-PEG. As the molecular weight increased, so did the viscosity until the material became so hydrophobic because of the PLGA that it was unable to dissolve in water. Viscosity tests of the PEGma-PLGA-PEGma triblock with PLGA molecular weights of 2810 and 1404 showed that the viscosities of various concentrations were much lower than the viscosities of the original PEG-PLGA-PEG material. Oscillation tests proved that this new material does not gel. The elastic modulus was orders of magnitude below that of PEG-PLGA-PEG. Thermally, this

material is unable to gel, but in contrast, the material was visibly able to crosslink with UV irradiation. With no thermosensitivity and some photocrosslinkability, the material was not mechanically strong enough to be able to be built vertically.

A material that was a combination of PEG-PLGA-PEG and PEGma-PLGA-PEGma gelled thermally and possessed the ability to crosslink with UV light. Four different types of mixes of PEG-PLGA-PEG/PEGma-PLGA-PEGma were prepared and compared: 50/50, 35/65, 20/80, and 10/90. A final polymer concentration of 45% was used since this % consistently had the best material properties as shown in previous tests. As the ratio increased from 50/50 to 20/80, the material became more viscous thermally and stiffer as a UV crosslinked material. Above 20/80, the 10/90 material's properties declined and looked similar to the properties of PEGma-PLGA-PEGma material. The 20/80 mix was found to have the highest maximum viscosity of 122,836 cP which is comparable to sour cream and peanut butter and also have the highest elastic modulus. The elastic modulus was reached at the lowest temperature, helping to prevent evaporation of the water content. After micelle formation, the 50/50, 35/65, and 20/80 mixes of materials are able to hold shape allowing for UV irradiation to create permanent crosslink and increase the mechanical properties of the material. The 20/80 mix had the highest solution viscosity, 228 cP, but the value is still within the range of viscosity that most SFF printers are capable of handling. The 20/80 mix also had the highest elastic modulus as a gel, 93.9 Pa, of all materials tested. Thermally, the material did not technically form a gel since the elastic modulus was never greater than the viscous modulus but the material was stiff enough to be able to hold its shape before UV

irradiation. This material retained the best photosensitivity of all mixed triblock polymer materials; it gelled the quickest and was able to hold its shape and even hold a shape it was molded into.

A 20/80 mix of low molecular weight PEG-PLGA-PEG and low molecular weight PEGma-PLGA-PEGma, gelled with the help of temperature and UV irradiation, is capable of 3-D building. This material mixed with DI water forms a material that has low viscosity as a solution at low temperature and is capable of drastically increasing viscosity and mechanical properties at a temperature of 33°C. This material is capable of holding its 3-D shape in order for UV irradiation to further increase the mechanical properties and form an irreversible network of crosslinks to confirm that the structure of the material will be permanent before degradation of the materials occur.

8.2 Recommendations

This work has exciting implications for the use of PEG-PLGA-PEG and PEGma-PLGA-PEGma as building materials in solid freeform technology for soft tissue scaffolds. Future work should include biotesting of this material and fine tuning the properties to be able to maximize the viscosity thermally as well as UV irradiation time. This would allow for the incorporation of cells and growth factor into the printing process. Other applications of the building materials have been shown to be compatible with cell proliferation and viability but the combination of PEG, PLGA, and PEGma needs to be verified for compatibility with various cell types. Study of the type of tissue being

replaced would benefit the integration of the gels with the surrounding tissue, architecture of the printed scaffold as well as placement of cells, growth factor, or any type of drug in the scaffold. Once the material properties of the tissue being replaced are similar to that tissue as well as any cells or other material being compatible with that tissue, optimization of the scaffold can continue in vitro and eventually proceed to pre-clinical trials.

An optimization of the printer would also be very beneficial to the process of creating these scaffolds. A UV light capable of emitting enough intensity so that instant crosslinking occurs would allow for much quicker operation of printing. UV flood lights do not allow for enough intensity for instantaneous crosslinking and UV focused light systems require the light source be place within ½ inch to the material for maximum intensity [124]. Greater than ½ inch distance from the light source to the material causes a loss of more than 80% of intensity. A separate enclosure of the printing substrate and printing area from the nozzle and material reservoir would allow for temperature controlled chambers. This would help to keep material a consistent viscosity for transport. This would also allow for better properties for printed material, helping to keep the droplet shapes and printed architecture to allow for less use of the UV light. Instead of UV irradiation after every one or two layers, it could be used every three or four so that larger structures could be build and less UV light would be needed.

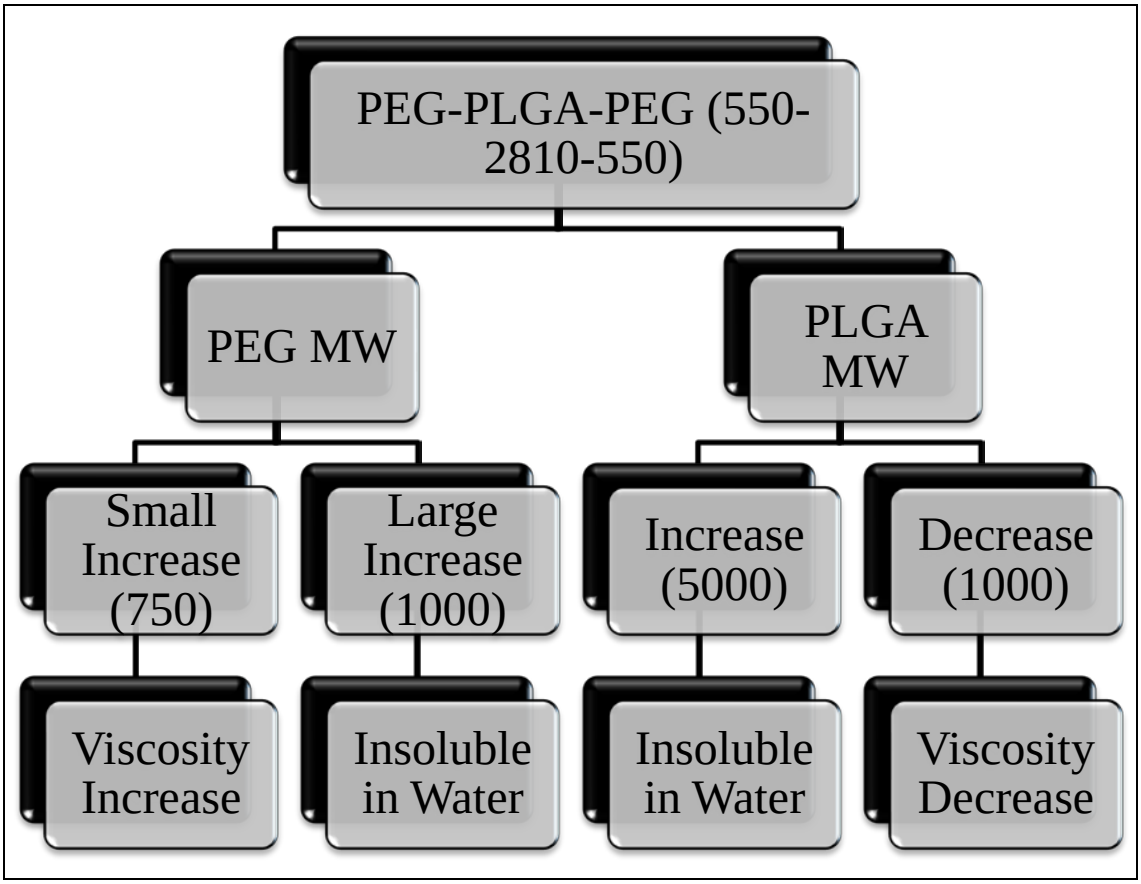

Figure 8.1 - Schematic of how PEG and PLGA molecular weight (MW) affect solution viscosity

References

1. Langer, R. and J.P. Vacanti, *Tissue Engineering.* Science, 1993. **260**(5110): p. 920-926.

2. Yang, S., et al., *The Design of Scaffolds for Use in Tissue Engineering. Part I. Traditional Factors.* Tissue Engineering, 2001. **7**(6): p. 679-689.

3. Patrick, C.W.J., *Adipose tissue engineering: The future of breast and soft tissue reconstruction following tumor resection.* Seminars in Surgical Oncology, 2000. **19**(3): p. 302-311.

4. Naito, Y., et al., *Successful clinical application of tissue-engineered graft for extracardiac Fontan operation.* J Thorac Cardiovasc Surg, 2003. **125**(2): p. 419-420.

5. Landers, R., et al., *Fabrication of soft tissue engineering scaffolds by means of rapid prototyping techniques.* Journal of Materials Science, 2002. **37**(15): p. 3107-3116.

6. Boland, T., et al., *Cell and organ printing 2: Fusion of cell aggregates in three-dimensional gels.* The Anatomical Record Part A: Discoveries in Molecular, Cellular, and Evolutionary Biology, 2003. **272A**(2): p. 497-502.

7. Williams, D., *Benefit and risk in tissue engineering.* Materials Today, 2004. **7**(5): p. 24-29.

8. Orsi, S., D. Guarnieri, and P. Netti, *Design of novel 3D gene activated PEG scaffolds with ordered pore structure.* Journal of Materials Science: Materials in Medicine.

9. Serrano, M.C., E.J. Chung, and G.A. Ameer, *Advances and Applications of Biodegradable Elastomers in Regenerative Medicine.* Advanced Functional Materials, 2010. **20**(2): p. 192-208.

10. Griffith, L.G. and G. Naughton, *Tissue engineering--current challenges and expanding opportunities.* Science, 2002. **295**: p. 1009-1014.

11. Hodde, J., *Naturally Occurring Scaffolds for Soft Tissue Repair and Regeneration.* Tissue Engineering, 2002. **8**(2): p. 295-308.

12. Zhou, J., et al., *Electrowetting-based multi-microfluidics array printing of high resolution tissue construct with embedded cells and growth factors.* Virtual and Physical Prototyping, 2007. **2**(4): p. 217 - 223.

13. Sun, W. *Computer Aided Tissue Engineering*. [cited 2011; Available from: http://www.gvu.gatech.edu/~jarek/spm/Sun.html.

14. Sun, W. and e. al., *Computer-aided tissue engineering: overview, scope and challenges.* Biotechnology Application in Biochemistry, 2004. **39**: p. 29-47.

15. Hoffman, A.S., *Hydrogels for Biomedical Applications.* Annals of the New York Academy of Sciences, 2001. **944**(BIOARTIFICIAL ORGANS III: TISSUE SOURCING, IMMUNOISOLATION, AND CLINICAL TRIALS): p. 62-73.

16. Campoccia, D., et al., *Semisynthetic resorbable materials from hyaluronan esterification.* Biomaterials, 1998. **19**(23): p. 2101-2127.

17. Prestwich, G.D., et al., *Controlled chemical modification of hyaluronic acid: synthesis, applications, and biodegradation of hydrazide derivatives.* Journal of Controlled Release, 1998. **53**(1-3): p. 93-103.

18. Drury, J.L. and D.J. Mooney, *Hydrogels for tissue engineering: scaffold design variables and applications.* Biomaterials, 2003. **24**(24): p. 4337-4351.

19. MIRSADRAEE, S., et al., *Development and Characterization of an Acellular Human Pericardial Matrix for Tissue Engineering.* Tissue Engineering, 2006. **12**(4): p. 763-773.

20. Elder, B.D., S.V. Eleswarapu, and K.A. Athanasiou, *Extraction techniques for the decellularization of tissue engineered articular cartilage constructs.* Biomaterials, 2009. **30**(22): p. 3749-3756.

21. Wilson, W.C.J. and T. Boland, *Cell and organ printing 1: Protein and cell printers.* The Anatomical Record Part A: Discoveries in Molecular, Cellular, and Evolutionary Biology, 2003. **272A**(2): p. 491-496.

22. Barron, J., D. Krizman, and B. Ringeisen, *Laser Printing of Single Cells: Statistical Analysis, Cell Viability, and Stress.* Annals of Biomedical Engineering, 2005. **33**(2): p. 121-130.

23. Hutmacher, D.W., *Scaffolds in tissue engineering bone and cartilage.* Biomaterials, 2000. **21**(24): p. 2529-2543.

24. Liu Tsang, V. and S.N. Bhatia, *Three-dimensional tissue fabrication.* Advanced Drug Delivery Reviews, 2004. **56**(11): p. 1635-1647.

25. Williams, C.G., et al., *Variable cytocompatibility of six cell lines with photoinitiators used for polymerizing hydrogels and cell encapsulation.* Biomaterials, 2005. **26**(11): p. 1211-1218.

26. Williams, J.M., et al., *Bone tissue engineering using polycaprolactone scaffolds fabricated via selective laser sintering.* Biomaterials, 2005. **26**(23): p. 4817-4827.

27. Fang, Z., B. Starly, and W. Sun, *Computer-aided characterization for effective mechanical properties of porous tissue scaffolds.* Computer-Aided Design, 2005. **37**(1): p. 65-72.

28. Wu, B.M., et al., *Solid free-form fabrication of drug delivery devices.* Journal of Controlled Release, 1996. **40**(1-2): p. 77-87.

29. Griffith, L.G. and G. Naughton, *Tissue Engineering--Current Challenges and Expanding Opportunities.* Science, 2002. **295**(5557): p. 1009-1014.

30. Griffith, L.G., et al., *In Vitro Organogenesis of Liver Tissuea.* Annals of the New York Academy of Sciences, 1997. **831**(1): p. 382-397.

31. Amsden, B.G., et al., *Methacrylated Glycol Chitosan as a Photopolymerizable Biomaterial.* Biomacromolecules, 2007. **8**(12): p. 3758-3766.

32. Bryant, S.J., C.R. Nuttelman, and K.S. Anseth, *Cytocompatibility of UV and visible light photoinitiating systems on cultured NIH/3T3 fibroblasts in vitro.* Journal of Biomaterials Science, Polymer Edition, 2000. **11**: p. 439-457.

33. Dikovsky, D., H. Bianco-Peled, and D. Seliktar, *The effect of structural alterations of PEG-fibrinogen hydrogel scaffolds on 3-D cellular morphology and cellular migration.* Biomaterials, 2006. **27**(8): p. 1496-1506.

34. Monro, T.M., et al., *Observation of Self-Trapping of Light in a Self-Written Channel in a Photosensitive Glass.* Physical Review Letters, 1998. **80**(18): p. 4072.

35. Theodorakopoulos, C., V. Zafiropulos, and J.J. Boon, *A Final Report on the Oxidation and Composition Gradients of Aged Painting Varnishes Studied with Pulsed UV Laser Ablation*, in *Lasers in the Conservation of Artworks*, J. Nimmrichter, W. Kautek, and M. Schreiner, Editors. 2007, Springer Berlin Heidelberg. p. 249-256.

36. Appelt, B.K., *Characterizing photoresists by thermal analysis.* Polymer Engineering & Science, 1983. **23**(3): p. 125-128.

37. Goto, K., et al., *Simple differential Giemsa staining of sister chromatids after treatment with photosensitive dyes and exposure to light and the mechanism of staining.* Chromosoma, 1975. **53**(3): p. 223-230.

38. Obara, K., et al., *Photocrosslinkable chitosan hydrogel containing fibroblast growth factor-2 stimulates wound healing in healing-impaired db/db mice.* Biomaterials, 2003. **24**(20): p. 3437-3444.

39. Ishihara, M., et al., *Photocrosslinkable chitosan as a dressing for wound occlusion and accelerator in healing process.* Biomaterials, 2002. **23**(3): p. 833-840.

40. Benfarhi, S., et al., *Synthesis of clay nanocomposite materials by light-induced crosslinking polymerization.* European Polymer Journal, 2004. **40**(3): p. 493-501.

41. Xin, A.X., C. Gaydos, and J.J. Mao, *In vitro Degradation Behavior of Photopolymerized PEG Hydrogels as Tissue Engineering Scaffold.* Engineering in Medicine and Biology

Society, 2006. EMBS '06. 28th Annual International Conference of the IEEE, 2006: p. 2091-2093.

42. Sabnis, A., et al., *Cytocompatibility Studies of an in situ Photopolymerized Thermoresponsive Hydrogel Nanoparticle System using Human Aortic Smooth Muscle Cells.* Journal of Biomedical Materials Research, Part A, 2010. **91**(1): p. 52-59.

43. Mi, F.-L., H.-W. Sung, and S.-S. Shyu, *Synthesis and characterization of a novel chitosan-based network prepared using naturally occurring crosslinker.* Journal of Polymer Science Part A: Polymer Chemistry, 2000. **38**(15): p. 2804-2814.

44. Mi, F.-L., et al., *Synthesis and characterization of biodegradable TPP/genipin co-crosslinked chitosan gel beads.* Polymer, 2003. **44**(21): p. 6521-6530.

45. Liu, V.A. and S.N. Bhatia, *Three-Dimensional Photopatterning of Hydrogels Containing Living Cells.* Biomedical Microdevices, 2002. **4**(4): p. 257-266.

46. Ono, K., et al., *Photocrosslinkable chitosan as a biological adhesive.* Journal of Biomedical Materials Research, 2000. **49**(2): p. 289-295.

47. Bryant, S.J. and K.S. Anseth, *Controlling the spatial distribution of ECM components in degradable PEG hydrogels for tissue engineering cartilage.* Journal of Biomedical Materials Research Part A, 2003. **64A**(1): p. 70-79.

48. Alhadlaq, A., et al., *Adult Stem Cell Driven Genesis of Human-Shaped Articular Condyle.* Annals of Biomedical Engineering, 2004. **32**(7): p. 911-923.

49. Spiller, K.L., S.A. Maher, and A.M. Lowman, *Hydrogels for the Repair of Articular Cartilage Defects.* Tissue Engineering Part B: Reviews. **0**(0): p. null.

50. Ifkovits, J.L. and J.A. Burdick, *Review: Photopolymerizable and Degradable Biomaterials for Tissue Engineering Applications.* Tissue Engineering, 2007. **13**(10): p. 2369-2385.

51. Bhattarai, N., J. Gunn, and M. Zhang, *Chitosan-based hydrogels for controlled, localized drug delivery.* Advanced Drug Delivery Reviews, 2010. **62**(1): p. 83-99.

52. Bhattarai, N., et al., *PEG-grafted chitosan as an injectable thermosensitive hydrogel for sustained protein release.* Journal of Controlled Release, 2005. **103**(3): p. 609-624.

53. Zhang, X.-Z., D.-Q. Wu, and C.-C. Chu, *Synthesis, characterization and controlled drug release of thermosensitive IPN-PNIPAAm hydrogels.* Biomaterials, 2004. **25**(17): p. 3793-3805.

54. Jeong, B., Y.H. Bae, and S.W. Kim, *Thermoreversible Gelation of PEG−PLGA−PEG Triblock Copolymer Aqueous Solutions.* Macromolecules, 1999. **32**(21): p. 7064-7069.

55. Jeong, B., et al., *Biodegradable block copolymers as injectable drug-delivery systems.* Nature, 1997. **388**(6645): p. 860-862.

56. Jeong, B. and A. Gutowska, *Lessons from nature: stimuli-responsive polymers and their biomedical applications.* Trends in Biotechnology, 2002. **20**(7): p. 305-311.

57. Jeong, B., Y. Han Bae, and S. Wan Kim, *Biodegradable thermosensitive micelles of PEG-PLGA-PEG triblock copolymers.* Colloids and Surfaces B: Biointerfaces, 1999. **16**(1-4): p. 185-193.

58. Jeong, B., et al., *Thermogelling Biodegradable Polymers with Hydrophilic Backbones: PEG-g-PLGA.* Macromolecules, 2000. **33**(22): p. 8317-8322.

59. Jeong, B., S.W. Kim, and Y.H. Bae, *Thermosensitive sol-gel reversible hydrogels.* Advanced Drug Delivery Reviews, 2002. **54**(1): p. 37-51.

60. Arnott, S., et al., *The agarose double helix and its function in agarose gel structure.* Journal of Molecular Biology, 1974. **90**(2): p. 269-272.

61. Rees, D.A. and E.J. Welsh, *Secondary and Tertiary Structure of Polysaccharides in Solutions and Gels.* Angewandte Chemie International Edition in English, 1977. **16**(4): p. 214-224.

62. Merriam-Webster, *Merriam-Webster's Collegiate® Dictionary, 11th Edition*. 2011, Franklin Publishers: Springfield, MA.

63. Brookfield, E.L., *MORE SOLUTIONS TO STICKY PROBLEMS*, I. Brookfield Engineering Labs., Editor. 2005: Middleboro, MA.

64. DIMA, D.T. *Viscosity Comparison*. [cited 2011 7/12]; Available from: http://www.dimadt.com/index.php/technicalinformation/.

65. Starly, B., et al., *Internal architecture design and freeform fabrication of tissue replacement structures.* Computer-Aided Design, 2006. **38**(2): p. 115-124.

66. Li, M.G., X.Y. Tian, and X.B. Chen, *A brief review of dispensing-based rapid prototyping techniques in tissue scaffold fabrication: role of modeling on scaffold properties prediction.* Biofabrication, 2009. **1**(3): p. 032001.

67. Sen, A.K. and J. Darabi, *Droplet ejection performance of a monolithic thermal inkjet print head.* Journal of Micromechanics and Microengineering, 2007. **17**(8): p. 1420.

68. Sun, J., et al., *Comparison of micro-dispensing performance between micro-valve and piezoelectric printhead.* Microsystem Technologies, 2009. **15**(9): p. 1437-1448.

69. Amirzadeh Goghari, A. and S. Chandra, *Producing droplets smaller than the nozzle diameter by using a pneumatic drop-on-demand droplet generator.* Experiments in Fluids, 2008. **44**(1): p. 105-114.

70. Hoffman, A.S., *Hydrogels for biomedical applications.* Advanced Drug Delivery Reviews, 2002. **54**(1): p. 3-12.

71. Berger, J., et al., *Structure and interactions in covalently and ionically crosslinked chitosan hydrogels for biomedical applications.* European Journal of Pharmaceutics and Biopharmaceutics, 2004. **57**(1): p. 19-34.

72. Chen, H., et al., *Genipin Cross-Linked Alginate-Chitosan Microcapsules: Membrane Characterization and Optimization of Cross-Linking Reaction.* Biomacromolecules, 2006. **7**(7): p. 2091-2098.

73. Kim, S., et al., *Chitosan/gelatin-based films crosslinked by proanthocyanidin.* Journal of Biomedical Materials Research Part B: Applied Biomaterials, 2005. **75B**(2): p. 442-450.

74. Jin, J., M. Song, and D.J. Hourston, *Novel Chitosan-Based Films Cross-Linked by Genipin with Improved Physical Properties.* Biomacromolecules, 2003. **5**(1): p. 162-168.

75. Patel, V.R. and M.M. Amiji, *Preparation and Characterization of Freeze-dried Chitosan-Poly(Ethylene Oxide) Hydrogels for Site-Specific Antibiotic Delivery in the Stomach.* Pharmaceutical Research, 1996. **13**(4): p. 588-593.

76. Koyano, T., et al., *Attachment and growth of cultured fibroblast cells on PVA/chitosan-blended hydrogels.* Journal of Biomedical Materials Research, 1998. **39**(3): p. 486-490.

77. Berger, J., et al., *Structure and interactions in chitosan hydrogels formed by complexation or aggregation for biomedical applications.* European Journal of Pharmaceutics and Biopharmaceutics, 2004. **57**(1): p. 35-52.

78. Qu, X., A. Wirsén, and A.C. Albertsson, *Novel pH-sensitive chitosan hydrogels: swelling behavior and states of water.* Polymer, 2000. **41**(12): p. 4589-4598.

79. Gang, Z., et al., *The study of tri-phasic interactions in nano-hydroxyapatite/konjac glucomannan/chitosan composite.* Journal of Materials Science, 2007. **42**(8): p. 2591-2597.

80. Shantha, K.L. and D.R.K. Harding, *Preparation and in-vitro evaluation of poly[N-vinyl-2-pyrrolidone-polyethylene glycol diacrylate]-chitosan interpolymeric pH-responsive hydrogels for oral drug delivery.* International Journal of Pharmaceutics, 2000. **207**(1-2): p. 65-70.

81. Lin, Y.-H., et al., *Physically crosslinked alginate/N,O-carboxymethyl chitosan hydrogels with calcium for oral delivery of protein drugs.* Biomaterials, 2005. **26**(14): p. 2105-2113.

82. Chen, S.-C., et al., *A novel pH-sensitive hydrogel composed of N,O-carboxymethyl chitosan and alginate cross-linked by genipin for protein drug delivery.* Journal of Controlled Release, 2004. **96**(2): p. 285-300.

83. Eiselt, P., et al., *Porous carriers for biomedical applications based on alginate hydrogels.* Biomaterials, 2000. **21**(19): p. 1921-1927.

84. Kuo, C.K. and P.X. Ma, *Ionically crosslinked alginate hydrogels as scaffolds for tissue engineering: Part 1. Structure, gelation rate and mechanical properties.* Biomaterials, 2001. **22**(6): p. 511-521.

85. Coutinho, D.F., et al., *Modified Gellan Gum hydrogels with tunable physical and mechanical properties.* Biomaterials, 2010. **31**(29): p. 7494-7502.

86. Ma, L., et al., *Collagen/chitosan porous scaffolds with improved biostability for skin tissue engineering.* Biomaterials, 2003. **24**: p. 4833-4841.

87. Kim, S.B., et al., *The characteristics of a hydroxyapatite-chitosan-PMMA bone cement.* Biomaterials, 2004. **25**: p. 5715-5723.

88. Adekogbe, I. and A. Ghanem, *Fabrication and characterization of DTBP-crosslinked chitosan scaffolds for skin tissue engineering.* Biomaterials, 2005. **26**: p. 7241-7250.

89. Li, Z., et al., *Preparation and in vitro investigation of chitosan/nano-hydroxyapatite composite used as bone substitute materials.* Journal of materials science: materials, 2005. **16**: p. 213 - 219.

90. Yin, Y., et al., *Preparation and characterization of macroporous chitosan-gelatin/b-tricalcium phosphate composite scaffolds for bone tissue engineering.* J Biomed Mater Res A. , 2003. **67**: p. 844-855.

91. Wu, Y.-C., et al., *Bone tissue engineering evaluation based on rat calvaria stromal cells cultured on modified PLGA scaffolds.* Biomaterials, 2006. **27**: p. 896-904.

92. Csaba, N., M. Köping-Höggård, and M.J. Alonso, *Ionically crosslinked chitosan/tripolyphosphate nanoparticles for oligonucleotide and plasmid DNA delivery.* International Journal of Pharmaceutics, 2009. **382**(1-2): p. 205-214.

93. Bhumkar, D. and V. Pokharkar, *Studies on effect of pH on cross-linking of chitosan with sodium tripolyphosphate: A technical note.* AAPS PharmSciTech, 2006. **7**(2): p. E138-E143.

94. Hwang, J.K. and H.H. Shin, *Rheological Properties of Chitosan Solutions.* Korea-Australia Rheology Journal, 2000. **12**(3/4): p. 175-179.

95. Kumbar, S.G., K.S. Soppimath, and T.M. Aminabhavi, *Synthesis and characterization of polyacrylamide-grafted chitosan hydrogel microspheres for the controlled release of indomethacin.* Journal of Applied Polymer Science, 2003. **87**(9): p. 1525-1536.

96. Deem, R. and S. Targan, *Evidence of a dynamic role of the target cell membrane during the early stages of the natural killer cell lethal hit.* The Journal of Immunology, 1984. **133**(1): p. 72-77.

97. Mwale, F., et al., *Biological Evaluation of Chitosan Salts Cross-Linked to Genipin as a Cell Scaffold for Disk Tissue Engineering.* TISSUE ENGINEERING, 2005. **11**(1/2): p. 130-141.

98. Mi, F.-L., et al., *In vivo biocompatibility and degradability of a novel injectable-chitosan-based implant.* Biomaterials, 2002. **23**(1): p. 181-191.

99. Di Martino, A., M. Sittinger, and M.V. Risbud, *Chitosan: A versatile biopolymer for orthopaedic tissue-engineering.* Biomaterials, 2005. **26**(30): p. 5983-5990.

100. Noble, L., et al., *A non-covalently cross-linked chitosan based hydrogel.* International Journal of Pharmaceutics, 1999. **192**(2): p. 173-182.

101. Mwale, F., et al., *Biological Evaluation of Chitosan Salts Cross-Linked to Genipin as a Cell Scaffold for Disk Tissue Engineering.* Tissue Engineering, 2005. **11**: p. 130-140.

102. Mi, F.-L., et al., *In vivo biocompatibility and degradability of a novel injectable-chitosan-based implant.* Biomaterials, 2002. **23**: p. 181-191.

103. Dureja, H., A.K. Tiwary, and S. Gupta, *Simulation of skin permeability in chitosan membranes.* International Journal of Pharmaceutics, 2001. **213**(1-2): p. 193-198.

104. Fujita, M., et al., *Inhibition of vascular prosthetic graft infection using a photocrosslinkable chitosan hydrogel.* Journal of Surgical Research, 2004. **121**(1): p. 135-140.

105. Vernengo, J., et al., *Evaluation of novel injectable hydrogels for nucleus pulposus replacement.* Journal of Biomedical Materials Research Part B: Applied Biomaterials, 2008. **84B**(1): p. 64-69.

106. Hirokawa, Y. and T. Tanaka, *Volume phase transition in a non-ionic gel.* AIP Conference Proceedings, 1984. **107**(1): p. 203-208.

107. Dubovik, A.S., et al., *Studies of the Thermal Volume Transition of Poly(N-isopropylacrylamide) Hydrogels by High-Sensitivity Differential Scanning Microcalorimetry. 2. Thermodynamic Functions.* Macromolecules, 2000. **33**(23): p. 8685-8692.

108. Ebara, M., et al., *Introducing Reactive Carboxyl Side Chains Retains Phase Transition Temperature Sensitivity in N-Isopropylacrylamide Copolymer Gels.* Macromolecules, 2000. **33**(22): p. 8312-8316.

109. Schmaljohann, D., et al., *Thermo-Responsive PNiPAAm-g-PEG Films for Controlled Cell Detachment.* Biomacromolecules, 2003. **4**(6): p. 1733-1739.

110. Jeong, B., Y.H. Bae, and S.W. Kim, *Drug release from biodegradable injectable thermosensitive hydrogel of PEG-PLGA-PEG triblock copolymers.* Journal of Controlled Release, 2000. **63**(1-2): p. 155-163.

111. Kenley, R.A., et al., *Poly(lactide-co-glycolide) decomposition kinetics in vivo and in vitro.* Macromolecules, 1987. **20**(10): p. 2398-2403.

112. Mi, F.-L., et al., *Kinetic study of chitosan-tripolyphosphate complex reaction and acid-resistive properties of the chitosan-tripolyphosphate gel beads prepared by in-liquid curing method.* Journal of Polymer Science Part B: Polymer Physics, 1999. **37**(14): p. 1551-1564.

113. Shu, X.Z. and K.J. Zhu, *A novel approach to prepare tripolyphosphate/chitosan complex beads for controlled release drug delivery.* International Journal of Pharmaceutics, 2000. **201**(1): p. 51-58.

114. Desai, K.G.H. and H.J. Park, *Preparation and characterization of drug-loaded chitosan-tripolyphosphate microspheres by spray drying.* Drug Development Research, 2005. **64**(2): p. 114-128.

115. Mezger, T.G., *The Rheology Handbook: For users of rotational and oscillatory rheometers*. 2002, Hannover, Germany: Vencentz Verlog.

116. Noguchi, T., et al., *Involvement of Cyclins in Cell Proliferation and Their Clinical Implications in Soft Tissue Smooth Muscle Tumors.* Am J Pathol, 2000. **156**(6): p. 2135-2147.

117. Cannizzarro, S.M. and R. Langer, *Biomaterials, Syntheticand Engineering Strategies*. Biomimetic Materials and Design, Biointerfacial Strategies, Tissue Engineering, and Targeted Drug Delivery, ed. A.K. Dillow and A.M. Lowman. 2002, New York: Marcel Dekker, Inc.

118. Karmen, A., F. Wróblewski, and J.S. LaDue, *TRANSAMINASE ACTIVITY IN HUMAN BLOOD.* The Journal of Clinical Investigation, 1955. **34**(1): p. 126-133.

119. Dai, X., et al., *Free radical polymerization of poly(ethylene glycol) diacrylate macromers: Impact of macromer hydrophobicity and initiator chemistry on polymerization efficiency.* Acta Biomaterialia. **In Press, Corrected Proof**.

120. Abuchowski, A., et al., *Alteration of immunological properties of bovine serum albumin by covalent attachment of polyethylene glycol.* Journal of Biological Chemistry, 1977. **252**(11): p. 3578-81.

121. Chen, E.J., et al., *Young's modulus measurements of soft tissues with application to elasticity imaging.* Ultrasonics, Ferroelectrics and Frequency Control, IEEE Transactions on, 1996. **43**(1): p. 191-194.

122. Yeh, W.-C., et al., *Elastic modulus measurements of human liver and correlation with pathology.* Ultrasound in Medicine & Biology, 2002. **28**(4): p. 467-474.

123. Nordson, E. *741MD-SS Needle Microvalve*. 2011 [cited 2011; Available from: http://www.nordson.com.

124. Dymax, C. *Guide to Selecting and Using DYMAX UV LIGHT CURING SYSTEMS*. 2010 [cited 2010 July 15]; Available from: http://www.dymax.com/pdf/literature/lit010a_guide_to_uv_light_curing_systems.pdf.

Vita

Chris Geisler

Education

- Ph.D., February 2012, Biomaterials and Biomechanics,
  Mechanical Engineering and Mechanics, Drexel University, Philadelphia, PA, USA
- M.S., June 2009,
  Mechanical Engineering and Mechanics, Drexel University, Philadelphia, PA, USA
- B.S., ***Honors, Concentration: Design and Manufacturing,*** June 2007,
  Mechanical Engineering and Mechanics, Drexel University, Philadelphia, PA, USA

Publications & Presentations

C.Geisler, H. Li, D.M. Wootton, P.I. Lelkes, J.G. Zhou. "Thermosensitive / Photocrosslinkable Hydrogel for Soft Tissue Scaffold Printing," ASME 2011 International Manufacturing Science and Engineering Conference, Oregon State University, Corvallis, OR, June 2011.

H. Li, **C.Geisler**, D.M. Wootton, J.G. Zhou. "A New Flexible and Multi-Purpose System Design for 3-Dimensional Printing," ASME 2010 International Manufacturing Science and Engineering Conference, Erie, PA, Oct. 2010.

C.Geisler, H. Li, D.M. Wootton, P.I. Lelkes, J.G. Zhou. "Soft Biomaterial Study for 3-D Tissue Scaffold Printing," ASME 2010 International Manufacturing Science and Engineering Conference, Erie, PA, Oct. 2010.

C.Geisler, H. Li, D.M. Wootton, P.I. Lelkes, J.G. Zhou. "Thermosensitive / Photocrosslinkable Hydrogel for Soft Tissue Scaffold Printing," ASME 2011 International Manufacturing Science and Engineering Conference, Oregon State University, Corvallis, OR, June 2011.

C.Geisler, H. Li, D.M. Wootton, P.I. Lelkes, J.G. Zhou. "Soft Biomaterial Study for 3-D Tissue Scaffold Printing," ASME 2010 International Manufacturing Science and Engineering Conference, Erie, PA, Oct. 2010.

C. Geisler, D.M. Wootton, P.I. Lelkes, R. Fair, J.G. Zhou. "Material Study for Electrowetting-based Multi-microfluidics Array Printing of High Resolution Tissue Construct with Embedded Cells and Growth Factors." ASME 2010 First Global Congress on NanoEngineering for Medicine and Biology, Houston, Texas, February 2010.

C. Geisler, L. Lu, D.M. Wootton, P. Lelkes, R. Fair, J. Zhou. "Electrowetting-based Multi-Microfluidics Array Printing of High Resolution Tissue Construct with Embedded Cells and Growth Factors." The 8th International Conference on Frontiers of Design and Manufacturing, Tianjin, China, September 2008.